AD_____

Award Number: DAMD17-03-1-0051

TITLE: Superoxide dismutase and transcription factor sox9 as mediators of tumor suppression by mac25 (IGFBP-rp1) in prostate cancer cells

PRINCIPAL INVESTIGATOR: Stephen R. Plymate, M.D.

CONTRACTING ORGANIZATION: University of Washington
Seattle, WA 98195

REPORT DATE: October 2006

TYPE OF REPORT: Final

PREPARED FOR: U.S. Army Medical Research and Materiel Command
Fort Detrick, Maryland 21702-5012

REPORT DOCUMENTATION PAGE

Form Approved
OMB No. 0704-0188

1. REPORT DATE *(DD-MM-YYYY)*	**2. REPORT TYPE**	**3. DATES COVERED** *(From - To)*
01/10/06	Final	1 Apr 2005 – 30 Sep 2006

4. TITLE AND SUBTITLE

Superoxide dismutase and transcription factor sox9 as mediators of tumor suppression by mac25 (IGFBP-rp1) in prostate cancer cells

5a. CONTRACT NUMBER

5b. GRANT NUMBER
DAMD17-03-1-0051

5c. PROGRAM ELEMENT NUMBER

6. AUTHOR(S)
Stephen R. Plymate, M.D.

E-Mail: splymate@u.washington.edu

5d. PROJECT NUMBER

5e. TASK NUMBER

5f. WORK UNIT NUMBER

7. PERFORMING ORGANIZATION NAME(S) AND ADDRESS(ES)

University of Washington
Seattle, WA 98195

8. PERFORMING ORGANIZATION REPORT NUMBER

9. SPONSORING / MONITORING AGENCY NAME(S) AND ADDRESS(ES)
U.S. Army Medical Research and Materiel Command
Fort Detrick, Maryland 21702-5012

10. SPONSOR/MONITOR'S ACRONYM(S)

11. SPONSOR/MONITOR'S REPORT NUMBER(S)

12. DISTRIBUTION / AVAILABILITY STATEMENT
Approved for Public Release; Distribution Unlimited

13. SUPPLEMENTARY NOTES

14. ABSTRACT: The most significant conclusion that is going to be derived from the work on this proposal is the relationship of tumor cell contribution to the extra cellular environment and tumor growth. This was unexpected when we started this proposal and this work has not been completed. However, based on the findings generated in this DOD proposal Dr. Plymate has received a 5yr NCI/NIH U54 Program Project to further develop these interactions.

15. SUBJECT TERMS
No subject terms provided

16. SECURITY CLASSIFICATION OF:			**17. LIMITATION OF ABSTRACT**	**18. NUMBER OF PAGES**	**19a. NAME OF RESPONSIBLE PERSON**
a. REPORT	**b. ABSTRACT**	**c. THIS PAGE**			USAMRMC
U	U	U	UU	52	**19b. TELEPHONE NUMBER** *(include area code)*

Table of Contents

Introduction: Prostate cancer is largely incurable once it has metastasized to other organs and progressed to a state of androgen independence, and metastatic cells frequently cease to express the AR. Paradoxically, although castration and removal of circulating androgens is one treatment for prostate cancer at initial diagnosis, re-expression of the AR in cultured cancer cells strongly inhibits their growth and tumorigenicity. The research proposed here will determine the ability of sod2 and sox9 to effectively carry out the tumor suppressive function of mac25 and to what extent sod2 and sox9 are also regulated by the AR. If mac25 and AR actions are similar, then mac25 could be visualized as a substitute in metatstatic cells and an effective control mechanism for androgen-independent disease. Experiments with gene transfection address the extent of sod2 and sox9 induction by both mac25 and the AR, the individual anti-tumor activity of each protein, and the identification of other genes which may be up-regulated by mac25. The system will be manipulated by artificial expression of individual proteins in cell cultures as well as blocking cellular synthesis of individual proteins with antisense DNA. The consequences of these manipulations will be assessed by laboratory assays to determine rates of cell proliferation, the ability to grow in conditions which favor tumor cells, the occurrence of programmed cell death, production of specific gene products, production of molecules which inhibit progression of cells through the cell cycle (cell division), and the initiation of signaling from the IGF cell surface receptor.

Task 1: Determine if either SOD-2 or sox9 is necessary and/or sufficient for effective tumor suppression by mac25.

a) Measure levels of sod2 and sox9 expression in mac25 by Western and Northern blotting (Months 1-3)
b) Perform in vivo and in vitro tumor cell growth assays, and apoptosis assays, using cell lines transfected with sod, sox, or mac25 (Months 3-12)
c) Develop antisense oligonucleotide technique with sod2 and sox9, confirm inhibition of expression, and perform bioassays as described in 1b in the presence either sod or sox antisense. (Months 6-12)

* Results of Task 1 are in the attached paper - Drivdahl R, Tennant MK, Sprenger CT, Nelson PS, Plymate SR 2004 Transcription Factor SOX9 Regulation of Prostate Cancer Growth. Oncogene. 3;23(26):4584-93

Task 2:Analyze the effects of both SOD-2 and sox9 on specific proteins and activities of cell cycle and apoptotic pathways known to be regulated by mac25. This will determine if any or all of these activities are mimicked by SOX9 or SOD-2 alone, or if expression of both genes is required. If only one is required, this would indicate that its induction is an early event in a cascade initiated by mac25.

a) Determine expression of specified cell cycle proteins, and perform flow cytometry, in M12/sod2 and M12/sox9. Repeat in presence of antisense oligos in cases where both sod2 and sox9 are upregulated. (Months 12-18)
b) Clone sod2 and sox9 in adenoviral vector,optimize conditions, and test production. (Months 12-18)
c) Determine cell cycle protein expression and cell kinetics in cells infected with either sod2 or sox9 adenoviral constructs. (Months 18-24)

Results of Studies in Task 2:

Induction of senescence in prostate epithelial cells by expression of mac25 results in suppression of tumor formation and secretion of proteins that may potentiate tumor growth in adjacent, non-senescent cells. Additionally, expression of mac25 modulates production of several additional proteins involved in senescence and differentiation, as well as elements of the extracellular matrix.

Mac25 increased senescence and decreased tumor formation of human prostate cancer cells.

Mac25 was first described as a gene that was down regulated in meningioma cell lines compared to benign leptomeningeal cells and then as a senescence-associated gene in mammary epithelial cells.[48,115] Bavik et al further demonstrated an increase in mac25 transcript in senescent prostate fibroblasts compared to proliferating fibroblasts **(ref)**.[41] We have shown that in normal prostate epithelial cells that transcript and protein levels of mac25 increased upon exposure to TGF- or retinoic acid, an inhibitor ofepithelial cell growth.[116] In addition, we found the levels of mac25 decreased in various prostate cancer cell lines (all epithelial based), in microdissections of prostate tumors, as well as in immunohistochemical staining of prostate cancer tissue.[47,116] Overexpression of mac25 in the M12 prostate cancer cell line led to increased levels of

senescence, an arrest in G1 of the cell cycle, and decreased growth and tumorigenicity *in vitro* and *in vivo* . cDNA arrays comparing M12mac25 cells with M12 cells demonstrated increases in the transcription factor

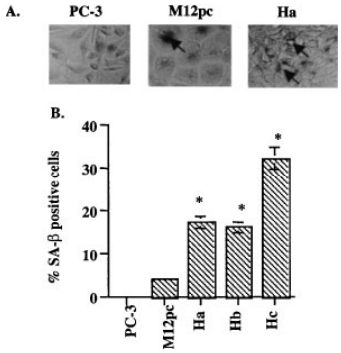

Figure 1. Senescence associated (SA)- β-galactosidase staining in (A) PC3, M12 control cells (M12pc), and a representative mac25 high expressing clone (Ha) and (B) the percentage of cells staining positive for SA- β -galactosidase in each cell type. The sta ining was performed four times. Arrows point to cells that stained positive for SA- β -galactosidase . No staining occurred in the PC3 cells, which do not undergo senescence and thus were used as a negative control.
*=P<0.01 compared to M12 control cells

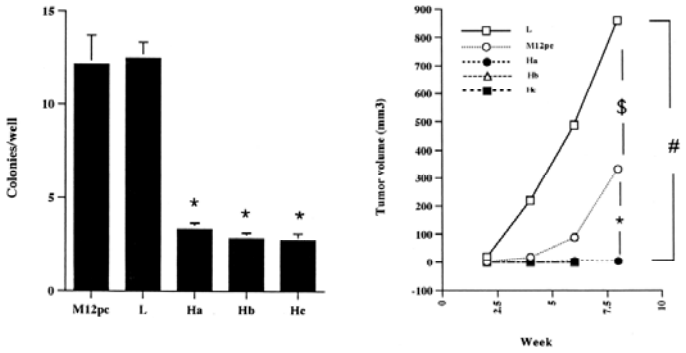

Figure 2. A. Colony growth in soft agar of M12 control, low (L), and high (Ha, Hb, Hc) mac25 expressing clones (±SE). *, P = 0.0001 versus M12 control and low (L). B. Change in tumor volume over an 8-week period in athymic , nude mice that were given s.c. injections of M12, low (L), and high (Ha, Hb, Hc) mac25 expressing clones. At week 8, Ha tumors were significantl y smaller than control tumors (*, P < 0.01) and L tumors (#, P < 0.001). Furthermore, control tumors were significantly smaller ($, P < 0.001) than L tumors. Because tumors did not form in the Hb and Hc mice, they could not be included in this statistical comparison.

Sox9 (SRY-related HMG box 9). The M12Sox9 cell lines decreased cell proliferation and tumor growth. Array data on the M12Sox9 line revealed alterations in extracellular matrix components, including an increase in the laminin α4 chain.

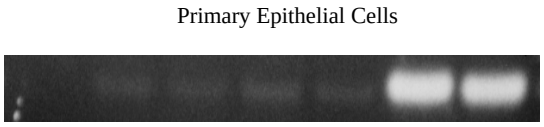

Figure 3. SOX9 induces laminin subunit 4 in primary prostate epithelial cells. SOX9 expression was accomplished with an adenoviral SOX9 construct. The increase in laminin 4 was confirmed in each cell line by RT-PCR. lacZ is an adenoviral control vector (84)

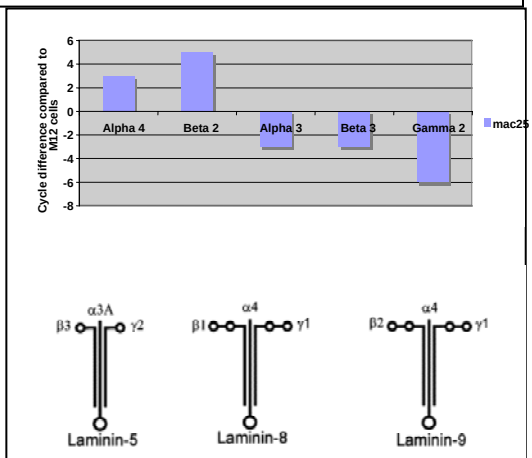

Figure 5, Real-time PCR comparing expression levels of mRNA for the various laminin chains (LN). C) General laminin structures (modified from Patarroyo, et al, 2002 [Sem Cancer Biol; 12:197-207]) of the primary laminins detected in the M12 (primarily LN 5) and M12mac25 cells (primarily LN 9 and LN 8).

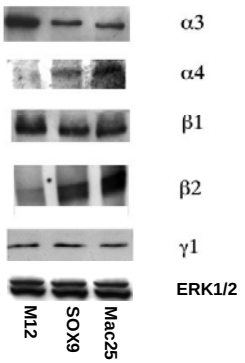

Figure 4. Laminin subunit expression in the M12 human prostate epithelial cell line infected with control adenoviral vector or SOX9 adenoviral construct, or mac25. These changes were also confirmed at the transcript level by Northern analysis (data not shown)

C.3. Regulation and Activity of Cancer

C.3.1. Mac25 alters laminin M12 cells and PrECs infected with LNα4 compared to M12 control cells. PCR confirmed these results. In

Laminins in Prostate Senescence and

subunit expression: cDNA arrays on adenoviral SOX9 showed an increase in Subsequent Western blotting and real-time addition, Western immunoblots and real-

time PCR on primary prostate epithelial cells also showed an increase in LN∝4 following SOX9 infection (**Figure3**). Westerns blots done on whole cell lysates from stably transfected M12/SOX9 or mac25 cells (which have elevated expression of SOX9) demonstrated an increase in LNα4 and β2 and a decrease in LNβ3 compared to the M12 cells (**Figure 4**). Results were confirmed with Qt-rtPCR. LNα4 protein has not been previously shown to be present in prostate epithelium (**Figure 5**). The changes detected so far indicate a shift from LN-5 (α3a∝3 γ2), 6 (α3b β1 γI), or 7 (α3β β2 γ1) to LN-8 in malignant cells and new expression of LN-8 or LN-9 (α4 β2 γ1) in senescent cells. The consequence of these initial findings in malignant prostate epithelium is not known, nor is it clear which factors determine the differential expression of LN-8 and LN-9. However, data from other systems which indicate that a shift to LN-9 is associated with quiescence, and new expression of LN-8 in proliferating vessels walls and cancerous epithelium is consistent with data showing that LN-8 facilitates tumor invasion and its in vivo expression correlates with a poor prognosis.

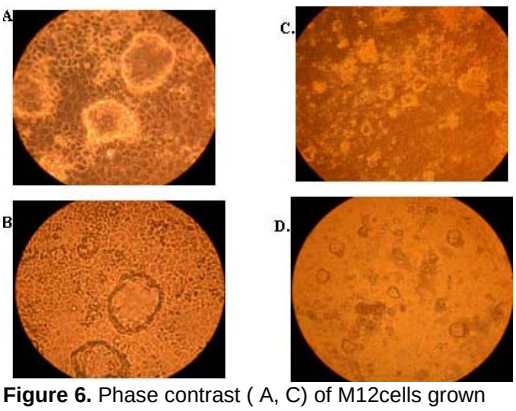

Figure 6. Phase contrast (A, C) of M12cells grown on ECM prepared from LN∝4 subunit transfected M12 cells. Compared to ECM from wtM12 cells in which the M12 cells grow aas a flat cuboidal layer 72 hrs after plating, there is marked "piling up " of cells on the LN∝4 ECM suggesting more aggressive growth.

When M12 cells were plated on ECM prepared from M12 cells transfected with an ∝4 expression vector (increased laminin 8),M12∝4 cells, there was a marked loss of contact inhibited and anchorage-independent growth consistent with a more aggressive phenotype induced by the senescent ECM, (**figure 6)**. When we compared the growth of the M12LNα4 expressing cells in soft agar to parent M12cells, and the senescent M12mac25 cells, the LN∝4 cells formed significantly more colonies in soft agar than M12 control cells, p> 0.001, whereas the mac25 senescent cells had very low colony formation in soft agar compared to either M12 or LN∝4M12, p <0.01, **Figure 7**. This is consistent with our published data that mac25 M12 senescent cell are poorly tumorigenic in a nude mouse tumor assay compared to M12 cells (7). Changes in integrin expression from cell lysates of M12 cells in which we have expressed different laminin isoforms are shown in **Figure 7**.

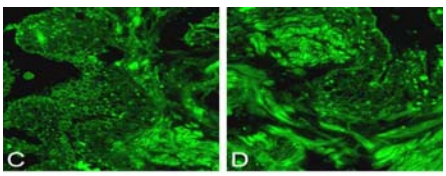

Figure. 8. Laminin α4 staining of human prostate cancer. C) An area of abnormal epithelium where the matrix surrounding the cells is positively stained. D) An area of the tumor where the normal architecture is disrupted showing that invasive epithelial cells are the most positively stained.

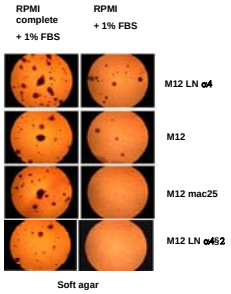

Figure 7. Soft agar growth demonstrating enhanced growth of M12LN∝4 cell growth in absence of epithelial growth media. Whereas, senescent mac25 cells and α4ß2 cells are fully dependent on epithelial media.

In contrast, when M12 cells expressing LN∝4 and ß2 laminin subunits (increased laminin 9) M12 ∝4ß2, colony growth in soft agar was suppressed similar to the M12 mac25 cells, figure 7 (put another blank circle below M12 mac 25, if you don't have a new picture let me know and I will do it.)

C.3.4. Laminin expression in normal and malignant prostate tissue: Human prostate tissue with normal regions and adjacent tumor was stained with antibodies to LN-1 (α1β1γ1) and the α4 subunit. In normal prostate LNα4 was detected around smooth muscle bundles and in the media of blood vessels, but not in epithelium. In areas of cancer, tongues of epithelial cells penetrating the epithelial acini were brightly stained for LNα4 (**Figure 8**). These observations indicate that there is new expression of LNα4 in areas of tumor.

In summary, these data demonstrate the the changes in laminin composition generated by senescenct prostate epithelial cells demonstrate the potential mechanism for induction of antagonistic pleiotropy exhibited by senesce in the prostate environment . Determination of how these changes in laminin expression function to either enhance or suppress tumor formation and growth will permit targeting laminin signaling through human antibodies to the integrin receptors for laminin to treat prostate cancer.

Task 3:Analyze the interaction between mac25 and androgen-responsive pathways. We will determine if reexpression of the AR regulates the expression of either SOD-2 or SOX9, and if SOD-2 or SOX9 can alter androgen receptor transcription activity. Production of specific proteins associated with differentiation, including cytokeratins and cadherins, will also be assayed in cells transfected with mac25, sod-2, sox9, or AR.

a) Determine timing and expression of sod2 and sox9, by Western and Northern blotting, in cells carrying the inducible temperature-sensitive AR vector (Months 21-24)
b) Measure PI3 and IGF-1R signaling in M12/AR, M12/sod2, and M12/sox9 cells. In cells which produce only sod2 or only sox9, meaure signaling in presence and absence of adenoviral infection with construct for the gene product not present. (Months 24-30)
c) Test cytokeratin, cadherin, and ERK expression in cells and conditions described above, by immunocytochemistry and Western/Northern blot analysis. (Months 31-36).

* Results of Task 3 are reported in the attached paper Plymate SR, Roberts CTJr, Tennant MK, Haugk k, Woodke L, Marcelli M, Ware JL, 2004 IGF-IR Regulation of Androgen Receptor Signaling in progression to Metastatic Prostate Cancer. Prostate. 61:276-284

Task 4: Assess the extent to which either sod-2 or sox9, via their activities in intracellular signalling and transcriptional regulation, can account for the gene expression pattern associated with tumor suppression by mac25. This will be accomplished by the use of microarrays of cell cycle or apoptotic genes, which will be screened using RNA from cells transfected with sod-2 or sox9.

- **Results of Task 4 are published in the attached papers.**

Bavik, C Coleman, I Dean, J Knudsen, B Plymate, S Nelson, PS The Gene Expression Program of Prostate Fibroblast Senescence Modulates Neoplastic Epithelial Cell Proliferation Through Paracrine Mechanisms. 2006 Cancer Research 66:794-802.

. Reed, MJ Karres,N Eyman,D Cruz' A Brekken' RA Plymate, SR 2006 Tumor cell dependent effects of aging on tumor growth and angiogenesis. Epub Nov 27 Int J Cancer

Wu, JD Haugk, K Woodke, L Nelson, P, Coleman, I Plymate, SR. 2006
Interaction of IGF signaling and the androgen receptor in prostate cancer progression. J Cell Biochem. 99:392-401

Key Research Accomplishments

- Defining the mechanisms for Mac25 suppression of tumor growth
- Demonstrating the contribution of senescent cells to tumor growth
- Demonstrating interaction of the IGF-IR and Androgen Receptor
- Demonstrate that tumor cells alter their interactions with the microenvironment depending on the laminin subunits they contribute to the ECM.

Reportable Outcomes

Drivdahl R, Tennant MK, Sprenger CT, Nelson PS, Plymate SR 2004 Transcription Factor SOX9 Regulation of Prostate Cancer Growth. Oncogene. 3;23(26):4584-93

Plymate SR, Roberts CTJr, Tennant MK, Haugk k, Woodke L, Marcelli M, Ware JL, 2004 IGF-IR Regulation of Androgen Receptor Signaling in progression to Metastatic Prostate Cancer. Prostate. 61:276-284

Bavik, C Coleman, I Dean, J Knudsen, B Plymate, S Nelson, PS The Gene Expression Program of Prostate Fibroblast Senescence Modulates Neoplastic Epithelial Cell Proliferation Through Paracrine Mechanisms. 2006 Cancer Research 66:794-802.

.Reed, MJ Karres,N Eyman,D Cruz, A Brekken, RA Plymate, SR 2006 Tumor cell dependent effects of aging on tumor growth and angiogenesis. Epub Nov 27 Int J Cancer

Wu, JD Haugk, K Woodke, L Nelson, P, Coleman, I Plymate, SR. 2006
Interaction of IGF signaling and the androgen receptor in prostate cancer progression. J Cell Biochem. 99:392-401

Conclusions: The most significant conclusion that is going to be derived from the work on this proposal is the relationship of tumor cell contribution to the extra cellular environment and tumor growth. This was unexpected when we started this proposal and this work has not been completed. However, based on the findings generated in this DOD proposal Dr. Plymate has received a 5yr NCI/NIH U54 Program Project to further develop these interactions.

Appendix

Oncogene (2004) 23, 4584–4593

www.nature.com/onc

Suppression of growth and tumorigenicity in the prostate tumor cell line M12 by overexpression of the transcription factor SOX9

Rolf Drivdahl[1,2], Kathy H Haugk[1], Cynthia C Sprenger[3], Peter S Nelson[2,4], Marie K Tennant[2] and Stephen R Plymate*[,1,2]

[1]*Veterans Affairs Puget Sound Health Care System, Seattle, WA 98105, USA;* [2]*Department of Medicine, University of Washington School of Medicine, Seattle, WA 98105, USA;* [3]*Molecular and Cell Biology Program, University of Washington School of Medicine, Seattle, WA 98105, USA;* [4]*Fred Hutchinson Cancer Research Center, Seattle, WA 98107, USA*

Overexpression of mac25 in the prostate cancer cell line M12 effects a dramatic reversal of the transformed phenotype. cDNA array analysis of RNA from cells overproducing the mac25 protein (M12/mac25) indicated upregulation of the sex determining transcription factor SOX9. In this study, we have confirmed increased expression of SOX9 in M12/mac25 cells and have further investigated the physiological effects of increased SOX9 production. Greatly increased levels of SOX9 RNA and mature protein were demonstrated in cells transfected with a SOX9 cDNA (M12/SOX9), and gel mobility shift assays confirmed binding of nuclear protein from these cells to an oligonucleotide containing the SOX9 consensus binding sequence. M12/SOX9 cells assumed the spindle-shaped morphology characteristic of M12/mac25 cells, suggesting that SOX9 mediates some effects of mac25. Elevated expression of SOX9 resulted in a decreased rate of cellular proliferation, cell cycle arrest in G0/G1, and increased sensitivity to apoptosis. Tumor development in athymic nude mice was inhibited by 80%. Finally, prostate-specific antigen and the androgen receptor, two genes whose expression is characteristic of differentiated cells, were both upregulated in M12/SOX9 cells. These data indicate that SOX9 contributes to growth regulation by mac25 via inhibition of cell growth and promotion of differentiation.
Oncogene (2004) **23,** 4584–4593. doi:10.1038/sj.onc.1207603
Published online 12 April 2004

Keywords: SOX9; prostate; androgens; IGF; cancer

Introduction

Insulin-like growth factor binding protein-related protein 1 (IGFBP-rP1), originally termed mac25 in meningial and mammary cell lines, has also been called tumor cell adhesion factor (TAF), prostacyclin stimulating factor (PSF), or angiomodulin, depending on cell context (Swisshelm *et al*., 1995; Kato *et al*., 1996; Oh *et al*., 1996; Kishibe *et al*., 2000). It was cloned as a gene that is decreased in meningioma cell lines compared to primary cultures of benign leptomeningeal cells (Murphy *et al*., 1993) and as a senescence-associated gene from human mammary epithelial cells (Swisshelm *et al*., 1995). We have previously demonstrated increased mac25 expression in senescent human prostate epithelial cell cultures (Lopez-Bermejo *et al*., 2000), and research on a variety of malignancies has demonstrated that mac25 is a potential tumor suppressor protein. Burger *et al*. (1997) identified loss of heterozygosity in 50% of breast cancer tissues, and expression of a transfected mac25 cDNA in MCF-7 breast cancer cells resulted in decreased cell proliferation, an increase in noncycling cells with arrest at G0/G1, and a significant increase in senescence-associated β-galactosidase (Wilson *et al*., 2002). In murine SV40-T-induced hepatocellular cancer, mac25 is silenced by methylation (Komatsu *et al*., 2001). Production of mac25 has been shown to decrease in metastatic prostate cancer (Hwa *et al*., 1998); re-expression of the protein in a human prostate epithelial cell line inhibited tumor formation *in vivo* when the transfected cells were placed in nude mice, and *in vitro* it resulted in an increased sensitivity to apoptosis, increased cell doubling time, decreased invasion, and altered cell morphology (Sprenger *et al*., 1999). mac25 has also been demonstrated to have a nuclear localization sequence, and in the M12 human prostate tumor cell line, it localized to the nucleus in association with neuroendocrine differentiating protein 25.1 (Wilson *et al*., 2001). These data suggest that mac25 may act by directly activating transcription of one or more effector molecules that are responsible for tumor suppression activity.

As a first step in the identification of genes induced by mac25 expression in prostate epithelial cells, we have performed cDNA array analysis of M12 cells overexpressing IGFBP-rP1/mac25, and on M12 cells transfected with empty vector (Plymate *et al*., 2003). Among several gene products determined to be upregulated in M12/mac25 cells was the transcription factor SOX9, a critical protein in male gonadal development and in

*Correspondence: SR Plymate, Harborview Medical Center, Box 359755, 325 9th Ave, Seattle, WA 98104, USA;
E-mail: splymate@u.washington.edu
Received 24 November 2003; revised 28 January 2004; accepted 30 January 2004; Published online 12 April 2004

chondrogenesis. SOX9 belongs to a family of transcription factors named for their DNA-binding domain (SRY-related HMG box); it activates transcription and causes DNA bending (Marshall and Harley, 2000; Koopman *et al*., 2001). Mutations or deletions in humans result in campomelic dysplasia syndrome manifest as chondro-dysplastic dwarfism, chondrocyte sarcomas, and sex reversal or intersex if the subject is XY (Kanai and Koopman, 1999; Olney *et al*., 1999; Preiss *et al*., 2001). SOX9 is a downstream effector of SRY, which in turn is dependent on the activity of androgens and the androgen receptor (AR) (Kent *et al*., 1996; Bowles and Koopman, 2001). The central importance of this factor in development is illustrated by the observation that in XX transgenic mice, production of SOX9 results in completely normal testis development and spermatogenesis (Healy *et al*., 1999; Vidal *et al*., 2001; Clarkson and Harley, 2002). SOX9 has not been studied in prostate cells, but its role in cell differentiation and its potential for interaction with androgens and the AR suggest that it may have powerful tumor suppressive activity. In the current study, we have investigated the effects of SOX9 on growth, apoptosis, and tumorigenicity in prostate cancer cells by transfection of the SOX9 cDNA into the M12 human prostate cancer cell line. Our results demonstrate effects of SOX9 on cell growth and gene expression consistent with mediation of mac25 activity through promotion of differentiation and inhibition of malignant proliferation.

Results

SOX9 expression in M12 prostate cancer cells

cDNA array analysis performed in our laboratory had indicated potential regulation of SOX9 in M12 cells which overproduce mac25 following transfection with mac25 cDNA (Plymate *et al*., 2003). These results were confirmed by Northern blot analysis, as shown in Figure 1a. A low level of expression of a 4.5 kb mRNA species, the expected size of SOX9 mRNA, was apparent in M12 cells transfected with empty vector (M12pC). This expression was markedly increased in M12/mac25. Transfection of M12 with the 2 kb SOX9 cDNA resulted in expression of the transgene in two clones at an approximately 12-fold higher level than in M12pC cells. Although Panda *et al*., (2001) reported that overexpression of a SOX9 transgene in CFK2 cells enhanced production of the endogenous transcript, we did not observe any similar effect in the M12 cells. Western

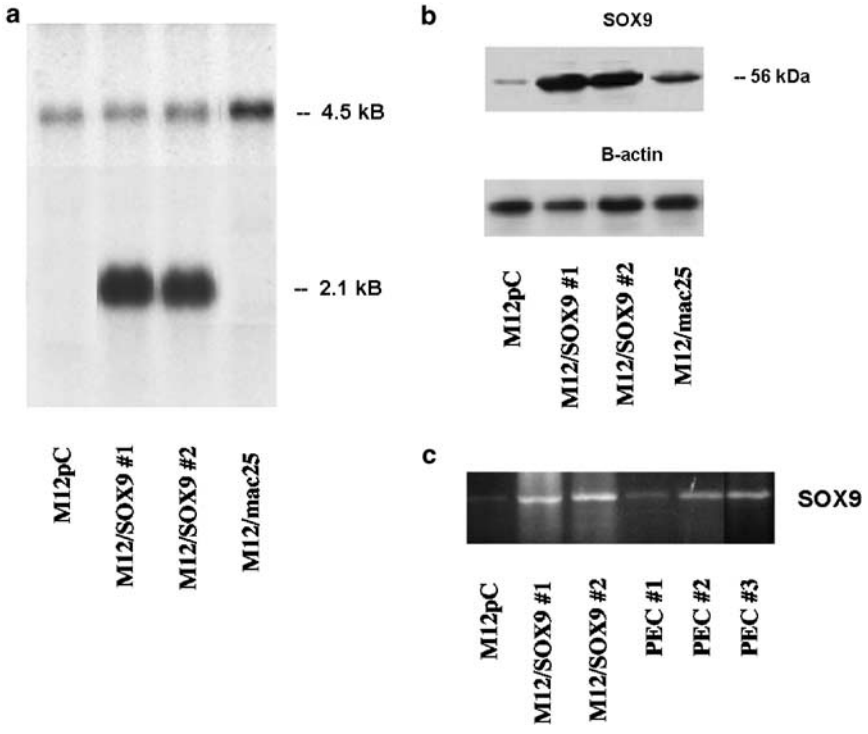

Figure 1 SOX9 mRNA and protein expression in M12 clones transfected with SOX9 plasmid expression construct. Individual colonies isolated from transfection plates in cloning rings were plated in defined medium (RPMI/ITS) containing 5% FCS; after allowing the cells to attach for 24 h, the medium was replaced with serum-free RPMI/ITS and cells were grown to approximately 80% confluence. RNA was extracted from cell monolayers and analysed for the production of SOX9 mRNA by Northern hybridization as described in the text (**a**). Protein was extracted from parallel cultures and analysed by Western blotting with specific antibody for SOX9; 100 μg of total protein was loaded in each well (**b**). Expression of SOX9 in normal prostate epithelial cells was evaluated by RT–PCR, using specific primers for SOX9 (**c**). Controls (M12pC) are M12 transfected with nonrecombinant pCDNA3. Results obtained with M12/mac25 cells are included for comparison

immunoblotting using a polyclonal SOX9 antibody demonstrated increases in SOX9 protein which parallel the changes in mRNA (Figure 1b).

In order to ascertain that SOX9 expression is not simply an aberrant feature of either transfected or tumor cell lines, we performed reverse transcription (RT)–PCR analysis of SOX9 expression in primary cultures of nonmalignant prostate epithelial cells. The data in Figure 1c indicate that SOX9 mRNA is expressed in three separate populations of these cells at readily detectable levels.

To determine that the transfected SOX9 was generating an active nuclear transcription factor, we performed gel mobility shift assays using a double-stranded oligomer corresponding to a portion of the N-cadherin promoter containing a SOX9 consensus binding site. Nuclear extracts were prepared from near-confluent cultures of M12pC and M12/SOX9, incubated with ^{32}P-labelled oligomer, and analysed by nondenaturing electrophoresis as described in Materials and Methods. Figure 2a demonstrates binding of the labelled oligomer to nuclear protein from SOX9-transfected cells; binding at lower levels was apparent in M12pC control cells. Inclusion of unlabelled N-cadherin promoter oligomer in the reaction effectively reduced formation of the shifted band, indicating the specificity of binding. The presence of a nonspecific competitor DNA (AP1 oligomer) had no effect. The Northern hybridization experiment shown in Figure 2b demonstrates that the ability to bind the N-cadherin promoter oligonucleotide correlates with increased production of cadherin mRNA.

Alteration of cell morphology

A particularly striking characteristic of SOX9-transfected M12 cells was the development of an elongated, spindle-shaped morphology, in contrast to the more cuboidal appearance of M12pC cells (Figure 3). As seen in the figure, this phenomenon is also evident in mac25-transfected cells, suggesting that SOX9 upregulation plays a key role in this and other physiological effects of mac25. Morphological changes may result in part from increased transcription of adhesion proteins such as cadherins, as well as the reported redistribution of actin filaments brought about by SOX9 (Panda *et al*., 2001). Such alterations of cellular architecture reflect a fundamental prodifferentiation activity of SOX9.

Regulation of cellular proliferation and cell cycle distribution

SOX9 stimulates cellular differentiation in a number of cell types, including Sertoli cells and chondrocytes (Graves, 1998; Healy *et al*., 1999; Olney *et al*., 1999; Marshall and Harley, 2000; Koopman *et al*., 2001), and it would be expected that this activity is coincident with inhibition of cell proliferation and cell cycle progression (Panda *et al*., 2001). Accordingly, we performed analyses of the increase in cell number in M12pC and M12/SOX9 clones using the MTS assay. M12/mac25 cells were included for comparison. As shown in Figure 4a, the total cell number was reduced by 30 and 37% in the two SOX9-expressing clones, compared with 35% in the M12/mac25 cells. Similar results were

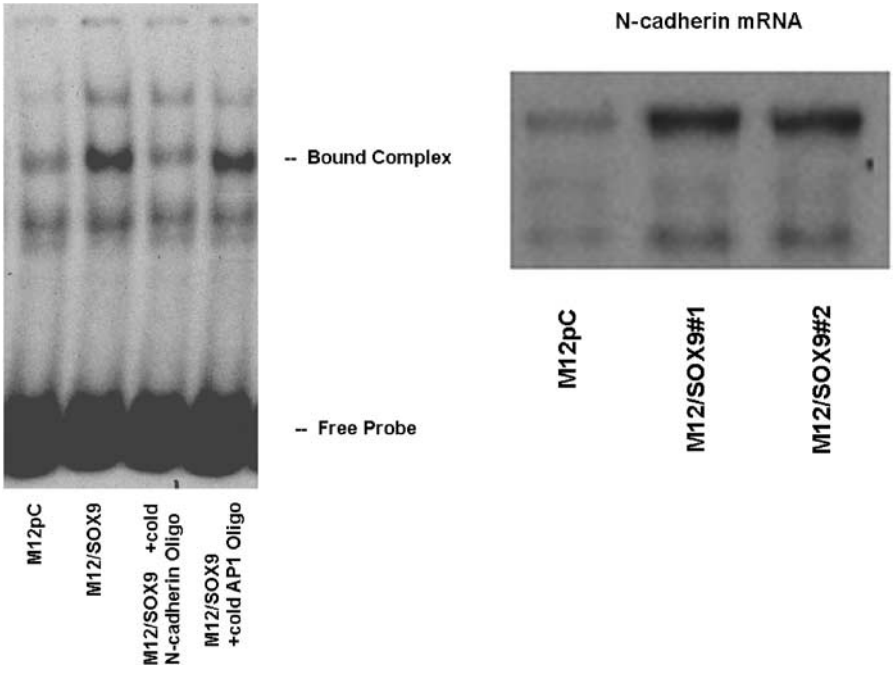

Figure 2 Binding of nuclear protein from M12 and M12/SOX9 clones to double-stranded N-cadherin promoter oligonucleotide. Nuclear extracts were prepared from near-confluent cell cultures in 60 mm dishes, as described in Materials and Methods. Binding assays were performed with the ^{32}P-labelled oligonucleotide in the presence or absence of nuclear extracts, and also in the presence of fivefold excess of unlabelled N-cadherin promoter oligonucleotide or unlabelled AP1 oligonucleotide from Promega Corp (**a**). (**b**) Results of Northern hybridization analysis using a ^{32}P-labelled oligonucleotide probe for N-cadherin

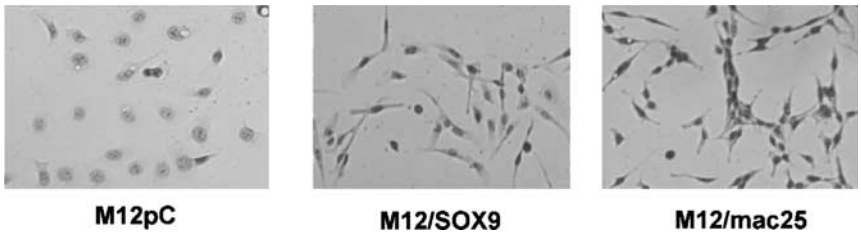

Figure 3 Comparative cellular morphology of M12pC and M12/SOX9 clones: (**a**) M12pC controls; (**b**) M12/SOX9#1; (**c**) M12/mac25

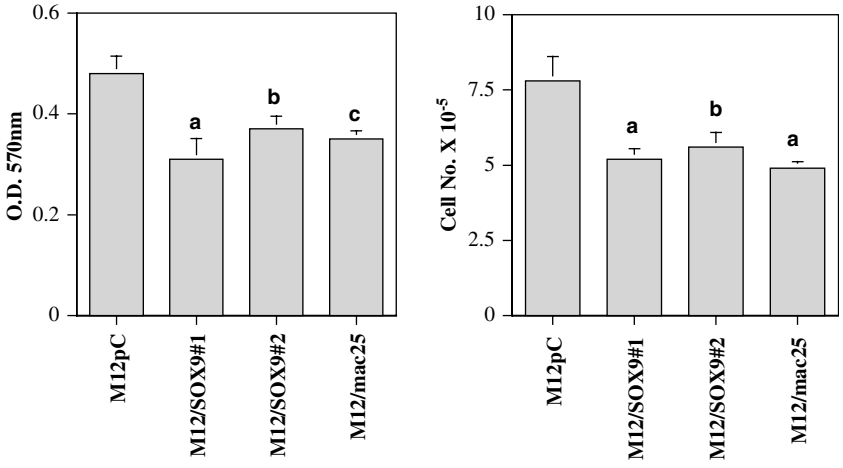

Figure 4 Growth of M12/SOX9 clones in monolayer culture. Cells were seeded in either 48-well plates (for MTT assay) or 60 mm culture dishes (for cell counting) in RPMI/ITS with 5% FCS; they were changed to serum-free conditions after 24 h. Fresh medium was added daily. Cell growth was assessed 96 h after plating. Data represent results of three separate experiments. Mean + s.e.m., $n = 4$. (**a**) $P < 0.01$ relative to corresponding controls; (**b**) $P < 0.05$; (**c**) $P < 0.005$

obtained with direct counting of cells (Figure 4b). Although M12pC cells are able to proliferate extensively in defined serum-free medium, the M12/SOX9 cells become inviable during extended serum-free culture in these conditions, apparently requiring mitogens in serum to counteract the effects of SOX9. These data suggest that cellular proliferation is inhibited by the actions of SOX9; however, as indicated below, SOX9 also sensitizes M12 cells to apoptotic cell death, which probably represents an additional contribution to the decrease in cell number.

Flow cytometry with propidium iodide of cells grown for 24 h in growth factor-free medium re-affirmed previous results with M12pC cells (Sprenger *et al*., 2002), in which the majority of cells were found in the G1 phase (mean = 71%), while M12/mac25 cells accumulated in the apoptotic sub-G0/G1 and to a lesser extent in G1; very few were identified in the G2/M phase. Expression of SOX9 produced a pattern that emulated that of M12/mac25, with 61% of cells found in G0/G1, 17% in G1, and no measurable G2/M fraction. In parallel experiments, cells were synchronized in G2/M with 5 μM nocodazole for 20 h and then analysed by flow cytometry as before. Nocodazole was selected as the synchronizing agent because it synchronizes cells in G2/M and thus clearly demonstrates delay of cells in G1. Figure 5 demonstrates that synchronized M12pC cells accumulate in the G2/M phase, but M12/SOX9 cells were found primarily in the G1 phase. Virtually identical results have been previously reported for M12/mac25 (Sprenger *et al*., 2002). Thus, both mac25 and SOX9 overexpression effect growth retardation and G1 arrest, probably creating an increased susceptibility to apoptotic cell death, as discussed below.

Effect of SOX9 expression on apoptosis in M12 cells

Previous work from this laboratory has demonstrated that in addition to its inhibition of cell proliferation and cell cycle progression, mac25 also promotes apoptotic cell death, an expected accompaniment to reduced growth and enhanced differentiation. As shown in Figure 6, this is also a feature of SOX9 expression. Increased susceptibility to apoptosis, with a consequent decrease in cell number and viability, was indicated by the demonstration of increased cleavage of poly(ADP-ribose) polymerase (PARP). PARP is a nuclear protein specifically cleaved by caspase-3 and -6, generating a signature 85 kDa product. Appearance of the 85 kDa band in addition to the unmodified 115 kDa band is therefore a marker for activation of caspases in apoptosis (Rosenthal *et al*., 1997; Simbulan-Rosenthal *et al*., 1999). Results depicted in Figure 6 demonstrate that the intensity of the 85 kDa band, relative to M12pC

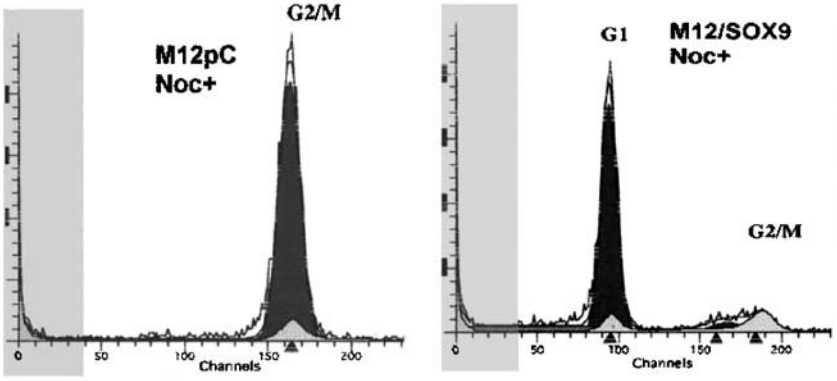

Figure 5 Flow cytometry with propidium iodide of M12pC cells and M12/SOX9 clone #1. Cells were synchronized by treatment with 5 μM nocodazole for 20 h and then analysed by flow cytometry as described in the text. Phases of the cell cycle are labelled

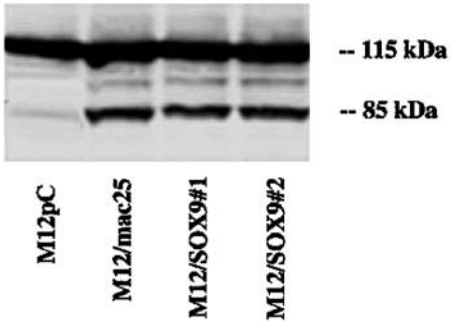

Figure 6 Apoptosis in M12 clones. Tumor cells were grown to near confluence and then incubated with 5 μM etoposide, a DNA topoisomerase inhibitor and an inducer of apoptosis, for 8 h. Attached cells were scraped into 1 ml of 1 × PBS, recovered by centrifugation and resuspended in 200 μl RIPA buffer (PBS containing 1% NP-40, 0.1% SDS, and 0.5% sodium deoxycholate). Remaining procedures of sample preparation and Western blot analysis were as described previously, except that the polyacrylamide gel percentage was 7%. PARP was detected using a specific monoclonal antibody from Oncogene Research. Appearance of the signature 85 kDa band, resulting from cleavage by caspase-3 and -6, in addition to the unmodified 115 kDa band, is used as a marker for induction of apoptosis

controls, is greatly increased in both the M12/mac25 and M12/SOX9 cells.

Tumorigenesis in athymic nude mice

The severely diminished growth of M12/SOX9 cells and increased occurrence of apoptosis indicate a potent inhibition of the transformed phenotype; this phenomenon was further examined by *in vivo* experiments in athymic, nude male mice. As shown in Figure 7, constitutive expression of SOX9 strongly inhibited the ability of M12 cells to form tumors *in vivo*. When cells from either the M12pC controls or the M12/SOX9 line were injected subcutaneously into sets of 10 mice, all 10 control mice developed tumors after 8 weeks, compared to only three of the mice receiving M12/SOX9. Additionally, the tumors in the M12/SOX9-treated mice were significantly smaller: tumor volume in mice injected with M12/SOX9 was only 9.6% of the value observed in control mice.

Markers of cellular differentiation

The known functions of SOX9 in cellular development led us to further examine expression of markers for prostate differentiation. Tran *et al.* (2002) have demonstrated a correlation between stages of prostate epithelial cell development and production of prostate stem cell antigen (PSCA), AR, and prostate-specific antigen (PSA). The data in Figure 8 demonstrate that the parental M12 (control) cells belong to a 'late intermediate' stage of differentiation, as evidenced by readily detectable levels of PSCA mRNA and the absence of both AR and PSA. Increased expression of SOX9 resulted in expression of both PSA and AR indicating that, as in other tissues, SOX9 is involved in progression to a more differentiated phenotype. As might be expected with continuous expression of genes potentially deleterious to cell growth, AR and particularly PSA were most readily detected in cells from early passage following transfection; their expression is prone to silencing with increasing number of cell passages. The mechanism of silencing (e.g. promoter methylation or mutation) has not been determined.

Discussion

SOX9 expression is an absolute requisite for both male sexual differentiation and cartilage formation (Graves, 1998; Healy *et al*., 1999; Olney *et al*., 1999; Marshall and Harley, 2000; Koopman *et al*., 2001), and it has recently been reported to be necessary for neural crest development in *Xenopus* (Spokony *et al*., 2002). It has also been detected in breast, skin, brain, and kidney (Kent *et al*., 1996; Lefebvre *et al*., 1997; Afonja *et al*., 2002), but despite the implicit significance of SOX9 in male reproductive physiology, there have been no studies on its expression or activity in prostate tissue. We have found by cDNA array analysis that its production is stimulated in M12 prostate cancer cells by transfection

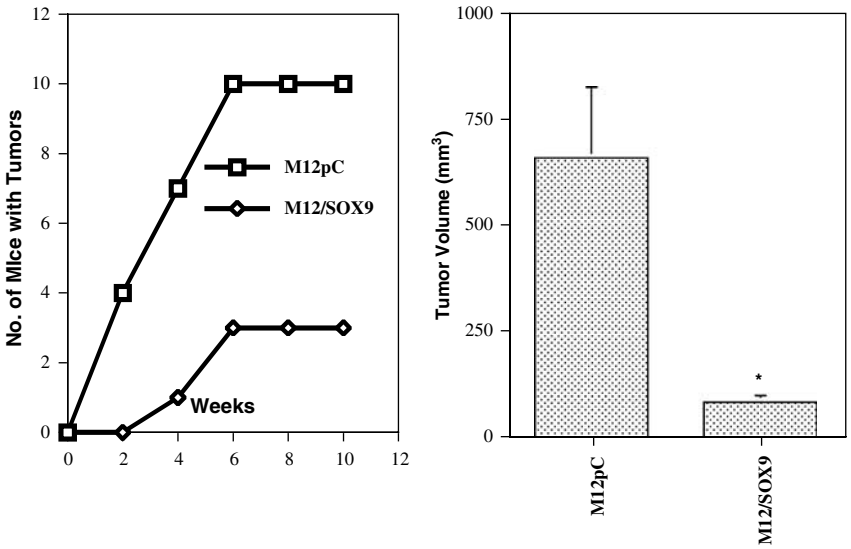

Figure 7 Rate of tumor volume increase in mice injected with M12pC or M12/SOX9 cells. Nude athymic male mice were injected subcutaneously with either M12/SOX9 or M12pcDNA control cells (1×10^6 cells/mouse) and maintained on a laboratory diet *ad libitum* for 8 weeks. Tumors were counted and measured weekly. * Significant difference from control ($P<0.005$)

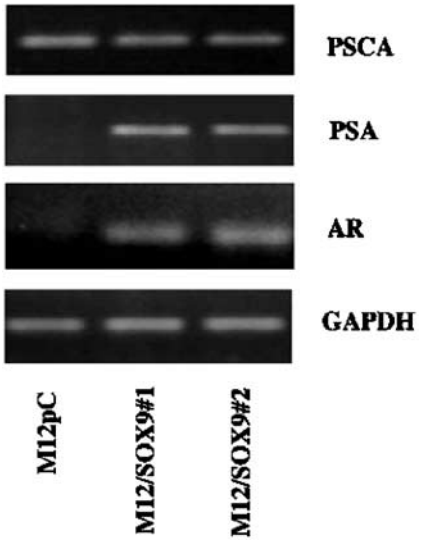

Figure 8 RT–PCR analysis of PSCA, AR, and PSA mRNAs in M12 and M12/SOX9 cell lines. RNA was extracted from cells in 60 mm dishes at approximately 80% confluence, and 1 μg was used in RT–PCR reactions with rTh polymerase and specific primers as described in Materials and methods

with a cDNA for mac25. mac25 has been shown to inhibit prostate tumor cell growth (Sprenger *et al*., 1999), and it was theorized that SOX9 may serve as a downstream mediator of mac25 tumor suppression activity. The data presented here establish that elevated production of SOX9 in itself is sufficient to initiate a sequence of events associated with tumor suppression, including reduced cellular proliferation, increased apoptosis, cell cycle arrest, and inhibition of tumor growth *in vivo*. The similar and distinctive morphological changes induced by both mac25 and SOX9 further suggest that many of these growth effects at least partially derive from stimulation of SOX9 expression.

Several factors have been shown to stimulate SOX9 synthesis, including androgens in Sertoli cells (Koopman *et al*., 2001), retinoids in TC6 cartilage and T-47D breast cancer cells (Afonja *et al*., 2002), and fibroblast growth factors in differentiating chondrocytes (Murakami *et al*., 2000). SOX9 was implicated as a critical intermediary in the differentiating activities of these factors and, at least in chondrocytes and male development, it may qualify as the master regulator. The effects of mac25, SOX9, and the AR in prostate are intriguing in their similarity, suggesting that mac25 and SOX9 may mimic prodifferentiation and antitumor activities of gonadal steroids in cells that have either lost or mutated the AR, most notably in metastatic, androgen-independent prostate cancer. mac25 itself can be upregulated by retinoids in breast and prostate cells (Swisshelm *et al*., 1995; Hwa *et al*., 1998), and may therefore function in a cascade mechanism that leads to SOX9 induction and subsequent differentiation and growth inhibition. However, the SOX9 promoter was also reported to have three potential RARE sites, which would enable retinoids to activate directly SOX9 transcription (Afonja *et al*., 2002).

The identification of genes regulated by SOX9 will be a critical focus of further research on its actions in prostate. The col2a1 and col11a2 genes are established targets in chondrocytes (Healy *et al*., 1999), as is anti-Mullerian hormone (AMH) in Sertoli cells (Kent *et al*., 1996; Marshall and Harley, 2000). Panda *et al*. (2001) reported increased N-cadherin gene expression in SOX9-transfected CFK2 cells, a phenomenon of particular interest in view of the pronounced morphology changes observed. N-cadherin belongs to a group of calcium-dependent adhesion molecules, which connect cells with each other and with extracellular matrix

(Vleminckx and Kemmler, 1999). They play important roles in development, and the increased production of cadherins and/or other adhesion molecules could explain the elongated spindle shape assumed by CFK2/SOX9 cells (Panda *et al*., 2001) and the M12/SOX9 cell line. The data presented in Figure 2 clearly demonstrate upregulation of N-cadherin by SOX9 in M12 cells; binding of SOX9 produced in M12 cells to the N-cadherin promoter fragment indicates a direct effect on RNA transcription.

Our data demonstrate that SOX9 causes cells to accumulate at the G0/G1 stage of the cell cycle, or in G1 when cells are synchronized. Similar results were presented in the studies discussed above with CFK2 and T-47D cells (Panda *et al*., 2001; Afonja *et al*., 2002), and they are also entirely analogous to those reported previously for M12/mac25 cells (Sprenger *et al*., 2002). SOX9 regulates expression of known mitotic inhibitors, which could account for stalling in G1. Most notable is p21, which contains a SOX9 consensus binding sequence in its promoter and was transcriptionally activated in the study of CFK2 cells (Panda *et al*., 2001). p21 has been invoked as a potential mediator in control of prostate tumor cell growth by vitamin D, and a vitamin D response element has also been identified in the p21 promoter (Miller, 1999). Lu *et al*. (2000) have also established that androgens can induce p21. However, in a previous study, p21 was downregulated by mac25, whereas p27 was increased (Sprenger *et al*., 2002). In LNCaP cells, p27 was considered to be the major mediator of G1 arrest, and p27 levels declined during progression to an androgen refractory state (Murillo *et al*., 2001). It has also been reported that Akt interferes with AR activity (Lin *et al*., 2001) and also downregulates p27 (Graff *et al*., 2000) in prostate tumor cells; recent experiments in our laboratory indicate that Akt also downregulates SOX9, providing a further indication of a causal link between SOX9 and p27 expression. It will therefore be of interest to examine cell cycle genes whose expression is influenced by SOX9, and also to determine the requirement for SOX9 in the induction of these genes through the use of antisense or siRNA to inhibit SOX9 function.

The cDNA array studies with M12/mac25 cells also demonstrated upregulation of manganese-dependent superoxide dismutase (MnSOD2), which has been extensively studied as an anticancer agent due to its antioxidant activity (Li *et al*., 1998; Oberley, 2001). MnSOD2 acts as a tumor suppressor in M12 cells (Plymate *et al*., 2003). The mechanism of action for mac25 is unknown, but it has been shown to translocate to the nucleus and may act as a transcription factor (Wilson *et al*., 2001). It is not known at present if mac25 directly stimulates expression of both SOX9 and MnSOD2, and it would be equally plausible for SOX9 as a transcription factor to activate MnSOD2 expression. The putative function of SOD2 in signal transduction (Rhee *et al*., 2000) also offers a potential mechanism for transcriptional control of additional genes in M12/mac25 cells. The enzymatic activity of SOD2 generates H_2O_2, which influences protein phosphorylation (e.g. by inhibition of phosphatase activity), and in M12 cells either overproduction of SOD2 or treatment with H_2O_2 causes MAPK activation. In primary chondrocytes, SOX9 transcription was induced by fibroblast growth factors via activation of the MAPK pathway (Murakami *et al*., 2000). In an analogous situation, the AR is required for SOX9 expression in developing testis, and several studies have associated AR transactivation and induction of androgen target genes with the MAPK system (Reinikaninen *et al*., 1996; Yeh *et al*., 1999).

In summary, SOX9 acts as a tumor suppressor in M12 prostate cancer cells, inhibiting proliferation by causing cell cycle arrest in G0/G1. As a transcription factor with a crucial role in normal development, it induces genes involved in cellular differentiation, resulting in the formation of mature cells susceptible to senescence and apoptosis. Growth arrest may partially derive from stimulated transcription of mitotic inhibitors such as p21 or p27, while increased production of structural and adhesion proteins such as collagens and cadherins results in altered morphology and development of cell to cell and cell to matrix contacts. Further research will undoubtedly reveal additional genes targeted by SOX9. SOX9 may also mediate tumor suppression by mac25 in concert with other factors such as MnSOD2. mac25 has the potential to upregulate SOX9 expression directly, but generation of H_2O_2 by the activity of MnSOD2 presents another pathway for activation, via interaction with MAPK. Our future studies will focus on identification of the role of SOX9 in mediation of tumor suppression and identification of other genes which it recruits for growth inhibition and differentiation.

Materials and methods

Reagents

Tissue culture media and additives, antibiotics, bacterial growth media, guanidine isothiocyanate, phenol, and agarose were purchased from GIBCO (Grand Island, NY, USA). Defined fetal calf serum (FCS) was purchased from HyClone Laboratories (Logan, UT, USA). Random primers labelling kits, horseradish peroxidase-linked anti-rabbit secondary antibody, and enhanced chemiluminescence reagents (ECL) were purchased from Amersham Pharmacia Biotech (Piscataway, NJ, USA). Gene Screen nylon blotting membranes and ^{32}P-dCTP were obtained from NEN-DuPont (Boston, MA, USA). Nitrocellulose and polyacrylamide gel electrophoresis reagents were purchased from BioRad Laboratories (Richmond, CA, USA). The SOX9 antibody was obtained from Santa Cruz Biologicals, and restriction enzymes were obtained from Promega Corp. (Madison, WI, USA). The human SOX9 cDNA, a 2.1 kb sequence encompassing the full protein coding sequence (Lefebvre *et al*., 1997) and cloned into pCDNA3 (InVitrogen), was a gift of Dr David Goltzman.

Cell lines and culture

The M12 line was derived from tumors developed in nude mice injected with p69SV40T cells; these are human prostate epithelial cells immortalized with SV40T antigen (Bae *et al*., 1998). M12 cells express stem cell antigen (PSCA) and are

cytokeratin positive (Bae *et al*., 1998); they also express PSA when expression of the AR is induced (see below). Cells were maintained at 37°C in RPMI 1640 supplemented with 10 ng/ml EGF, 0.1 μM dexamethasone, 5 μg/ml insulin, 5 μg/ml transferrin, 5 ng/ml selenium, and 50 μg/ml gentamicin (RPMI/ITS), in a 95% air/5% CO_2 atmosphere. FCS (5%) was included at plating, and the medium was replaced with the defined medium after 24 h. Cells used in these experiments were determined to be free of mycoplasma using the Gen-Probe Mycoplasma TC Rapid Detection System (Gen-Probe, San Diego, CA, USA). Primary cultures of benign prostate epithelial cells were obtained from Clonetics Corp. (Rahway, NJ, USA) and cultured in DMEM containing 5% FCS.

Cell transfection

Plasmid DNA from a positive colony was linearized with *Pvu*I and introduced into M12 cells by liposome-mediated transfection with pFx-5 (InVitrogen) according to the manufacturer's instructions. Control cells were prepared by transfection with pcDNA3 alone; these are designated as M12pC. After 48 h, cells were passaged into selective medium containing 400 μg/ml G418 and cultured for 10 days. Individual colonies were isolated from the plate by trypsinization in cloning rings and maintained in growth medium containing 200 μg/ml G418. SOX9 mRNA and protein expression were determined by Northern and Western blotting as described below.

Western blotting

Cell lysates were prepared by addition of cold lysis buffer (30 mM HEPES, 150 mM NaCl, 1.5 mM $MgCl_2$, 1 mM EGTA, 10% Triton X-100) containing protease inhibitors and phosphatase inhibitors (Phosphatase Inhibitor Cocktail II, Sigma) to monolayer cultures. Total protein concentration was determined with the BCA protein assay kit (Pierce Biological). A measure of 100 μg of each sample was boiled in 100 μl of SDS sample buffer (0.05 M Tris, pH 6.8, 2% SDS, 0.025% bromphenol blue). Samples were then subjected to electrophoresis in 12% SDS–polyacrylamide gels and transferred electrophoretically to nitrocellulose as described by Hossenlopp *et al*. (1986). The transfer buffer contained 15 mM Tris base, 120 mM glycine, and 5% methanol. Membranes were washed successively in Tris-buffered saline (TBS is 20 mM Tris-HCl, pH 7.5, containing 0.15 M NaCl), TBS/3% NP-40, TBS/1% BSA, and TBS/0.1% Tween 20. They were incubated overnight at 4°C with appropriate antibodies in TBS/0.1% Tween 20 and washed two times with TBS/0.1% Tween 20 and three times with TBS. Bands were detected using horseradish peroxidase-linked anti-rabbit secondary antibody and enhanced chemiluminescence reagents (ECL system, Amersham Corp., Arlington Heights, IL, USA), according to the manufacturer's protocol.

RNA extraction and analysis

RNA was extracted from cells by a minor modification of the procedure of Chomczysnki and Sacchi (1987), as previously described (Drivdahl *et al*., 2001). RNA was dissolved in 100% formamide and fractionated by electrophoresis in 1.25% agarose gels containing 0.66 M formaldehyde and 20 mM MOPS buffer, pH 7.2; 0.5 μg of ethidium bromide was added to each sample to stain the RNA (Lehrach *et al*., 1977; Fourney *et al*., 1989). Following electrophoresis, the RNA was visualized by UV illumination on a Fotodyne transilluminator. Visual analysis of ethidium bromide staining of the 28S and 18S RNA bands was used as a preliminary indication of the integrity and uniform loading of RNA. RNA was then transferred to Gene Screen by capillary blotting in 10 × SSC and crosslinked to the membrane with the Stratalinker apparatus from Stratagene Corp. (La Jolla, CA, USA).

Reverse transcription–PCR

Total RNA was obtained as described above and RT–PCR amplification was carried out using the Tth DNA polymerase (Promega) according to the manufacture's directions for RT–PCR reactions. The primer sets were designed using the MacVector DNA sequence analysis program and synthesized by InVitrogen Corp. (La Jolla, CA, USA). Total RNA (1 μg) was transcribed for 20 min at 70°C with 10 nM of the downstream primer. Amplification conditions consisted of an initial denaturing step at 95°C for 4 min, annealing at 60°C for 1 min, and extension/polymerization at 72°C for 1.5 min with a 3 s increment per cycle (35 cycles were performed). In all, 0.5 μM of each primer was used in the PCR reaction. PCR products were analysed by electrophoresis in 1.5% agarose gels, stained with ethidium bromide, and visualized with a FotoDyne UV transilluminator. The following primer pairs were used for these experiments:

SOX9:	Forward:	AGGTGCTCAAAGGCTACGACT
	Reverse:	AGATGTGCGTCTGCTCCGTG
AR:	Forward:	CCAGTCCCACTTGTGTCAAAAGC
	Reverse:	TACTTCTGTTTCCCTTCAGCGG
PSA:	Forward:	GGTGACCAAGTTCATGCTGTG
	Reverse:	GTGTCCTTGATCCACTTCCG
PSCA:	Forward:	TGACCATGAAGGCTGTGCTGCTT
	Reverse:	TCGGTGTCACAGCACGTGATGT

cDNA probes and hybridization

Northern blots were prehybridized at 43°C in a Hybaid roller bottle oven (Intermountain Scientific, Salt Lake City, UT, USA); the prehybridization solution was 50% formamide, 6 × SSC, 5 × Denhardt's solution, 0.1 M $NaPO_4$ (pH 7.2), 10 mM sodium pyrophosphate, and 50 μg/ml sonicated herring sperm DNA (Ulrich *et al*., 1984). ^{32}P-labelled probes were prepared from cDNA templates by the random primers technique (Feinberg and Vogelstein, 1983). The SOX9 probe template was a 980 bp *Eco*R1/*Pst*1 fragment of the human cDNA. Probes were denatured in 0.3 M NaOH, neutralized, and added directly to the prehybridization solution. Hybridization proceeded overnight at 43°C. The blots were washed at moderate stringency (1 × SSC, 0.1% SDS, 65°C) and exposed to a Kodak X-OMAT AR5 film with an intensifying screen at −70°C. Bands were quantitated with an image analyser equipped with the MCID version 4.2 software (Imaging Research, St Catherine, Ontario, Canada).

Cell proliferation assays

The rate of cellular proliferation in culture was measured by a colorimetric MTT assay, using the Cell Titer 96 AQ_{ueous} kit from Promega, as previously described (Damon *et al*., 1998). M12pC, M12/mac25, and M12/SOX9 cells were seeded in 48-well plates at 5000/well and assayed after 96 h of growth at 3°C. The tetrazolium salt and dye solution for MTT assay were added to cells 4 h prior to color determination and incubated at 37°C. Quantitation was accomplished by reading absorbance at 570 nm.

To validate MTT results by direct measurement of cell number, cells were plated in 60 mm dishes (500 000 cells/dish) and grown for 96 h as in the MTT assay. They were removed from plates by trypsinization, resuspended in 1 × phosphate-buffered saline (PBS), and counted in a hemocytometer.

Growth of tumors in nude mice

Nude athymic male mice (8-week-old) were injected subcutaneously with either M12/SOX9 or M12pC cells (1×10^6 cells/mouse, suspended in $1 \times$ PBS) and maintained on a laboratory diet *ad libitum* for 10 weeks. Tumors were counted and measured weekly, and tumor volume was calculated by the formula $(lw^2)/2$, where l and w are the length and width of the tumor, respectively. Statistical analysis included Kruskal–Wallis test for rates of tumor formation and Mann–Whitney U-test for tumor volumes. After 10 weeks, tumors were removed and digested with 0.1% type I collagenase and 50 μg/ml DNase I by the technique of Peehl and Stamey (1986). Dispersed cells were plated in RPMI growth medium with 5% FCS for 24 h, and the medium was then replaced with defined serum-free medium. Protein and RNA lysate were prepared and analysed by Northern and Western blotting to confirm retention of SOX9 expression.

Apoptosis assay

Apoptosis was assessed by demonstrating cleavage of PARP by Western blotting (Drivdahl *et al*., 2001). Cells were plated in complete medium in 60 mm dishes. At 24 h after plating, cells were changed to RPMI/ITS. Both floating and adhered cells were collected from separate plates at 48 and 96 h after the complete medium was removed. Cell lysates were prepared as described above and fractionated on a 7% SDS–polyacrylamide gel. Western immunoblots were performed with an anti-PARP (polyadenosylribose polymerase) antibody that recognizes the 85 kDa cleaved fragment (Promega Co., Madison, WI, USA).

Flow cytometry

Flow cytometry was performed as described by Sprenger *et al*. (2002). Briefly, cells were grown to 80% confluence, trypsinized, recovered by centrifugation, and washed with $1 \times$ PBS. Cells (2×10^6) were resuspended in cold 70% ethanol to a final density of 1×10^6 cells/ml, then pelleted and resuspended in 1 ml of DNA staining solution (PBS, pH 7.4, containing 0.1% Triton X-100, 0.1 mM EDTA (pH 7.4), 0.05 mg/ml RNase A (50 U/mg), and 50 μg/ml propidium iodide). Cells were detected with a Becton-Dickinson FACS Caliber at a wavelength of 488 nm. Data were collected and analysed using CellQuest and ModFit software, respectively.

Gel mobility shift assay

Nuclear extracts were prepared using the NE-PER kit from Pierce (Rockford, IL, USA). A measure of 10 μg of nuclear protein was then incubated at room temperature for 10 min in binding buffer (4% glycerol, 1 mM $MgCl_2$, 0.5 mM EDTA, 0.5 mM DTT, 50 mM NaCl, 50 mM Tris-HCl (pH 7.5), and 50 μg/ml poly(dI-dC). Total volume was 9 μl. A measure of 1 μl of ^{32}P-labelled oligonucleotide ($1–2 \times 10^5$ cpm) was then added and incubation continued for 20 min. Parallel reactions were performed with either no extract or with unlabelled competitor oligomers as described in the figure legend. Complexes were separated by electrophoresis on a nondenaturing 4% polyacrylamide gel. The gel was then dried and bands located by autoradiography.

The oligonucleotide sequence used for SOX9 binding represents a fragment of the human N-cadherin promoter, as described by Panda *et al*. (2001). The double-stranded target was generated by annealing oligomers 5′ggCCTCATTTA-**CATTGTT**GTAACCAAAAGT and 5′-ggACTTTTGGTTA-C**AACAATG**TAAATGAGG; the boldface letters designate the SOX9 consensus binding sequence. DNA was end-labelled using T4 polynucleotide kinase and gamma ^{32}P-ATP (Sambrook *et al*., 1989), and unincorporated label was removed on a Sephadex G-25 spin column. Total incorporation into DNA was measured in a BIOSCAN/QC-1000 single-well counter.

Acknowledgements
This research was supported by PO1-CA85859 (to SRP and PSN), and RO1-56283 and Veterans Affairs Merit Review Program to SRP.

References

Afonja O, Raaka BM, Huang A, Das S, Zhao X, Helmer E, Juste D and Samuels HH. (2002). *Oncogene*, **21,** 7850–7860.
Bae VL, Jackson-Cook CK, Maygarden SJ, Plymate SR, Chen J and Ware JL. (1998). *Prostate*, **34,** 275–282.
Bowles J and Koopman P. (2001). *Genome Biol.*, **2,** 10251–10254.
Burger A, Zhang X, Li H, Ostrowski J, Beatty B, Venanzoni M, Papas T and Seth A. (1997). *Oncogene*, **16,** 2459–2467.
Chomczysnki P and Sacchi N. (1987). *Anal. Biochem.*, **162,** 156–159.
Clarkson MJ and Harley VR. (2002). *Trends Endocrinol. Metab.*, **13,** 106–111.
Damon SE, Maddison L, Ware JL and Plymate SR. (1998). *Endocrinology*, **139,** 3456–3464.
Drivdahl RH, Sprenger CC, Trimm K and Plymate SR. (2001). *Endocrinology*, **142,** 1990–1998.
Feinberg AP and Vogelstein B. (1983). *Anal. Biochem.*, **132,** 6–13.
Fourney RM, Day RS and Paterson MC. (1989). *Focus*, **10,** 5–7.
Graff JR, Konicek BW, McNulty MN, Wang Z, Houck K, Allen S, Paul JD, Hbaiu A, Goode RG, Sandusky GF, Vessella RL and Neubauer BL. (2000). *J. Biol. Chem.*, **275,** 24500–24505.
Graves JA. (1998). *BioEssays*, **20,** 264–269.
Healy C, Uwanogho D and Sharpe PT. (1999). *Dev. Dyn.*, **215,** 69–78.
Hossenlopp P, Seurin D, Segovia-Quinson B, Hardouin S and Binoux M. (1986). *Anal. Biochem.*, **154,** 138–143.
Hwa V, Tomasini-Sprenger C, Bermejo AB, Rosenfeld RG and Plymate SR. (1998). *J. Clin. Endocinol.*, **83,** 4355–4362.
Kanai Y and Koopman P. (1999). *Hum. Mol. Genet.*, **8,** 691–696.
Kato M, Sato H, Tsukada T, Ikawa Y, Aizawa S and Nagayoshi MA. (1996). *Oncogene*, **12,** 1361–1364.
Kent J, Wheatley SC, Andrews JE, Sinclair AH and Koopman P. (1996). *Development*, **122,** 2813–2822.
Kishibe J, Yamada S, Okada Y, Sato J, Ito A, Miyazaki K and Sugahara K. (2000). *J. Biol. Chem.*, **275,** 15321–15329.
Komatsu K, Okazaki Y, Tateno M, Kawai J, Konno H, Kusakabe K, Yoshiki A, Muramatsu M, Held WA and Hayashizaki Y. (2001). *Biochem. Biophys. Res. Commun.*, **276,** 109–117.
Koopman P, Bullejos M and Bowles J. (2001). *J. Exp. Zool.*, **290,** 463–474.
Lefebvre V, Huang W, Harley VR, Goodfellow PN and deCrombrugghe B. (1997). *Mol. Cell. Biol.*, **17,** 2336–2346.
Lehrach H, Diamond D, Wozney JM and Boedtker H. (1977). *Biochemistry*, **16,** 4743–4749.

Li N, Oberley TD, Oberley LW and Zhong W. (1998). *J. Cell. Physiol.*, **175,** 359–369.
Lin HK, Yeh, Kang HY and Chang C. (2001). *Proc. Natl. Acad. Sci. USA*, **98,** 7200–7205.
Lopez-Bermejo A, Buckway CK, Devi GR, Hwa V, Plymate SR, Oh Y and Rosenfeld RG. (2000). *Endocrinology*, **141,** 4072–4080.
Lu S, Jenster G and Epner DE. (2000). *Mol. Endocrinol.*, **14,** 753–760.
Marshall OJ and Harley VR. (2000). *Mol. Genet. Metab.*, **71,** 455–462.
Miller GJ. (1999). *Cancer Metastasis Rev.*, **17,** 353–360.
Murakami S, Kan M, McKeehan WL and deCrombrugghe B. (2000). *Proc. Natl. Acad. Sci. USA*, **97,** 1113–1118.
Murillo H, Huang H, Schmidt L, Smith DI and Tindall DJ. (2001). *Endocrinology*, **142,** 4795–4805.
Murphy M, Pykett M, Harnish P, Zang K and George D. (1993). *Cell Growth Differ.*, **4,** 715–722.
Oberley LW. (2001). *Antioxidants Redox Signal.*, **3,** 461–472.
Oh Y, Nagalla S, Yamanaka Y, Kim H, Wilson E and Rosenfeld R. (1996). *J. Biol. Chem.*, **271,** 30322–30325.
Olney PN, Kean LS, Graham D, Elsas LJ and May KM. (1999). *Am. J. Med. Genet.*, **84,** 20–24.
Panda D, Miao D, Lefebvre V, Hendy G and Goltzman D. (2001). *J. Biol. Chem.*, **276,** 41229–41236.
Peehl DM and Stamey TA. (1986). *In vitro Cell Dev.*, **22,** 82–90.
Plymate SR, Haugk KH, Sprenger CC, Nelson PS, Tennant MK, Zhang Y, Oberley LW, Zhong W, Drivdahl RH and Oberley TD. (2003). *Oncogene*, **22,** 1024–1034.
Preiss S, Argentaro A, Clayton A, John A, Jans D, Ogata T, Nagai T, Barroso I, Schafer A and Harley VR. (2001). *J. Biol. Chem.*, **276,** 27864–27872.
Reinikaninen P, Palvimo JJ and Janne OA. (1996). *Endocrinology*, **137,** 4351–4357.
Rhee SG, Bae Y, Lee SR and Kwon J. (2000). *Science Sign. Trans. Knowl. Environ.*, **53,** 1–6.
Rosenthal DS, Ding R, Simbulan-Rosenthal CM, Vaillancourt JP, Nicholson DW and Smulson M. (1997). *Exp. Cell Res.*, **232,** 313–321.
Sambrook J, Fritsch EF and Maniatis T. (1989). *Molecular Cloning: A Laboratory Manual*. Cold Spring Harbor Laboratory: Cold Spring Harbor, NY.
Simbulan-Rosenthal CM, Rosenthal D, Luo R and Smulson M. (1999). *Mol. Cell. Biochem.*, **193,** 137–148.
Spokony RF, Aoki Y, Saint-Germain N, Magner-Fink E and Saint-Jeannet JP. (2002). *Development*, **129,** 421–432.
Sprenger CC, Damon SE, Hwa V, Rosenfeld RG and Plymate SR. (1999). *Cancer Res.*, **59,** 2370–2375.
Sprenger CC, Vail ME, Evans K, Smurdak J and Plymate SR. (2002). *Oncogene*, **21,** 140–147.
Swisshelm K, Ryan K, Tsuchiya K and Sager R. (1995). *Proc. Natl. Acad. Sci. USA*, **92,** 4472–4476.
Tran CP, Lin C, Yamashiro J and Reiter RE. (2002). *Mol. Cancer Res.*, **1,** 113–121.
Ulrich A, Berman CH, Dull TJ, Gray A and Lee JM. (1984). *EMBO J.*, **3,** 361–364.
Vidal VP, Chaboissier MC, Rooij DG and Schedl A. (2001). *Nat. Genet.*, **28,** 216–217.
Vleminckx K and Kemmler R. (1999). *BioEssays*, **21,** 211–220.
Wilson EM, Oh Y, Hwa V and Rosenfeld RG. (2001). *J. Clin. Endocrinol. Metab.*, **86,** 4504–4511.
Wilson HMP, Birnbaum R, Poot M, Quinn LS and Swisshelm K. (2002). *Cell Growth Differ.*, **13,** 205–213.
Yeh S, Lin HK, Kang HY, Thin TH, Lin MF and Chang C. (1999). *Proc. Natl. Acad. Sci. USA*, **96,** 5458–5463.

Androgen Receptor (AR) Expression in AR-Negative Prostate Cancer Cells Results in Differential Effects of DHTand IGF-I on Proliferation and AR Activity Between Localized and MetastaticTumors

Stephen R. Plymate,[1]* Marie K. Tennant,[1] Stephen H. Culp,[2] Lillie Woodke,[1] Marco Marcelli,[3] Ilsa Colman,[4] Peter S. Nelson,[1,4] Julie M. Carroll,[5] Charles T. Roberts Jr.,[5] and Joy L. Ware[2]

[1]*Department of Medicine, University of Washington, Seattle, Washington*
[2]*Department of Pathology, Medical College of Virginia, Virginia Commonwealth University, Richmond, Virginia*
[3]*Department of Medicine, Baylor College of Medicine, Houston, Texas*
[4]*Fred Hutchinson Cancer Research Center, Seattle, Washington*
[5]*Department of Pediatrics, Oregon Health and Science University, Portland, Oregon*

BACKGROUND. Two features of the progression from organ-confined to metastatic prostate cancer are dysregulation of the androgen receptor (AR) and a decrease in insulin-like growth factor-type-I receptor (IGF-IR) expression. The purpose of this study was to determine the effect of changes in IGF-IR expression on AR activity.

METHODS. M12 human prostate cells were stably transfected with an AR expression construct to produce the M12-AR parental (PAR) cell line. PAR cells were implanted orthotopically into nude mice and M12-AR primary (PRI) cell lines were derived from intraprostatic tumors and metastatic cell lines (MET) were derived from PRI tumors that had metastasized to diaphragm or lung.

RESULTS. Tumor formation in the prostate by PAR cells was decreased significantly compared to M12 controls. PAR, PRI, and MET cells expressed equivalent amounts of AR protein; however, IGF-IR expression was increased significantly in PAR and PRI cells. IGF-IR expression decreased in MET lines to the levels seen in M12 control cells. IGF-I significantly enhanced dihydrotestosterone (DHT)-stimulated, but not basal, AR transcriptional activity in PRI cells. In MET cells, IGF-I significantly suppressed DHT-stimulated transcriptional activity. In MET cells in which the IGF-IR was re-expressed from a retroviral vector, the effects of DHT and IGF-I on AR activity were similar to those seen in PRI cells.

CONCLUSIONS. This study demonstrates that the changes in IGF-IR expression exhibited by this model of metastatic progression cause significant alterations in AR signaling and suggest that this interaction may be an important aspect of the changes seen in AR function in disease progression in vivo. *Prostate 61: 276–290, 2004.*

KEY WORDS: **prostate cancer; androgen receptor; IGF-IR**

Marie K. Tennant and Stephen H. Culp contributed equally to this article.

Grant sponsor: Lematta Foundation of Southwest Washington (to C.T.R.); Grant sponsor: NIH (to J.L.W. and S.R.P.); Grant number: RO1DK52683; Grant sponsor: DAMD (to C.T.R.); Grant number: DOD PC10273; Grant sponsor: NIH (to S.R.P. and P.S.N.); Grant number: PO1-CA85859; Grant sponsor: Veterans Affairs Research Program (to S.R.P.).

*Correspondence to: Stephen R. Plymate, Harborview Medical Center, Box 359755, 325 9th Ave, Seattle WA 98104.
E-mail: splymate@washington.edu
Received 5 December 2003; Accepted 27 February 2004
DOI 10.1002/pros.20099
Published online 22 April 2004 in Wiley InterScience (www.interscience.wiley.com).

INTRODUCTION

More than 220,000 cases of prostate cancer are diagnosed each year, and this incidence is projected to increase to 380,000 per year by 2025 due to the aging population. Prostate cancer is the second leading cause of cancer deaths in men and the seventh cause of all cancer deaths (~30,000 per year) [1]. From a treatment perspective, these data highlight a significant problem, because one focus of treatment should be on those men with prostate cancer who will eventually die from their disease. Although prostate-specific antigen (PSA) levels and disease stage and grade are useful parameters for designing initial treatment strategies, more information on the pathobiological factors and cellular markers that define the group of men with disease that will progress is urgently needed to tailor effective follow-up therapy.

Two important features in the progression of prostate cancer from organ-confined, androgen-sensitive disease to metastatic disease are the dysregulation of androgen receptor (AR)-regulated target genes and a marked change in levels of the type 1 insulin-like growth factor receptor (IGF-IR), a transmembrane tyrosine kinase coupled to the ERK and PI3′ kinase (PI3K) cascades [2–5]. Although these changes could be considered independent epigenetic phenomena, increasing evidence indicates there is a close relationship between IGF-IR signaling and AR action. Lin et al. [6] have shown that the apoptotic activity of the AR seen after its transfection into an AR-negative prostate cancer cell line is suppressed by increased expression of the IGF-IR and subsequent stimulation of the PI3K pathway. The suggested mechanism for this IGF-IR-mediated activity was phosphorylation of the AR at serine residues 210 and 790, although not all studies detected serine phosphorylation [7]. In contrast, Li et al. [8] have shown that suppression of the PI3K pathway by re-expression of PTEN in LNCaP cells that lack a functional PTEN results in decreased AR signaling. In addition to the PI3K pathway, Bakin et al. [9] has shown that increased signaling through the ERK pathway enhances sensitivity to androgen in LNCaP cells, while inhibition of the ERK pathway restores androgen responsiveness in the androgen-independent LNCaP C4-2 subline. Additionally, some investigators had originally suggested that there was direct activation of the AR by IGF-I [10]. More recent studies, however, suggest that IGF signaling does not directly activate the AR, but that the IGF-activated IGF-IR influences AR transcriptional activity [11]. The mechanisms underlying these effects are not well defined, but may involve IGF-induced expression of AR co-regulators or alteration of AR function itself [12].

Since both IGF-IR expression levels and the activity of the ERK and PI3K pathways are altered during progression to metastatic prostate cancer, it is likely that some of the apparently contradictory interactions seen between IGF-IR signaling components and AR transcriptional activity in different studies are a result of differences in cellular context [13–15]. If, for example, the nature and extent of dysregulation of AR function varies with the source of the cell type, i.e., whether the cell is derived from an intraprostatic or metastatic environment, then the differences in the genes expressed in response to IGF-IR–AR interactions may be significant factors in metastatic progression. Identification of these alterations in gene expression may provide potential new markers to identify those tumors that have the potential to progress. In addition, these genes would identify mechanisms leading to progression of disease and, thus, provide potential targets for intervention.

The purpose of this study was to determine the effect of changes in IGF-IR expression during tumor progression on AR signaling. We demonstrate that, in the M12 human prostate cancer cell line in which the AR has been re-expressed, there are significant differences in IGF-IR expression depending on whether the cell was derived from an intraprostatic tumor or a metastasis. In addition, activation of the IGF-IR in these different tumor cell types resulted in marked qualitative and quantitative changes in dihydrotestosterone (DHT)-stimulated AR transactivation. Furthermore, re-expression of the IGF-IR in metastatic derivatives of the AR-expressing M12 cell line resulted in a reversion of the androgen response pattern back to that seen in AR-expressing M12 cells prior to metastasis.

MATERIALS AND METHODS

Generation of AR-Expressing Stable Transfectants

The establishment, characterization, and maintenance of the SV40 large T antigen-immortalized human prostate epithelial cell line P69 and its M12 sublines have been previously described [16,17]. In brief, non-neoplastic prostate epithelial cells were immortalized by transfection with an SV40-T antigen expression vector to generate the P69 cell line. Serial passage of sublines of P69 cells in athymic nude mice generated the M12 subline, which is consistently tumorigenic and metastatic after orthotopic injection. Neither P69 nor M12 cells express AR mRNA.

M12 cells were transfected with a pcDNA 3.1 expression vector (Invitrogen, Carlsbad, CA) containing a cDNA encoding the full-length, wild-type AR [18]. M12 cells transfected with the insertless pcDNA 3.1 expression vector served as negative controls (M12 controls). Cells were transfected using lipofectamine

plus (Life Technologies, Rockville, MD) according to the manufacturer's instructions. G418-resistant colonies were selected in 800 μg/ml G418 (Gibco BRL, Grand Island, NY), and the clone expressing the most intense AR band by Western immunoblot was designated as the M12-AR parental clone (PAR). Cells were then cultured with a 200 μg/ml maintenance dose of G418.

Establishment of PAR Sublines

Sixteen athymic nude mice were injected orthotopically with PAR cells using the technique originally described by Stephenson et al. [19]. Cells (2×10^6) were injected into the dorsal prostate (Harlan Sprague–Dawley, Madison, WI). Of the 10 mice that developed a macroscopic primary tumor, 4 mice also developed metastases to the diaphragm. The primary tumors and the metastases were recovered, the cells isolated by collagenase digestion, and G418-resistant cell lines were re-established. The primary tumor sublines were designated M12-AR primary (PRI), and the metastatic sublines were designated M12-AR metastatic (MET). Three mice were injected orthotopically with 2×10^6 cells each from one of the MET lines and each of these animals developed metastases to the diaphragm. One metastasis from each of the three animals was digested, cell lines established, and used in this study as MET lines. All protocols involving athymic nude mice were approved by the VCU Institutional Animal Care and Use Committee (IACUC).

Construction of AR/IGF-IR-Expressing Cell Lines

These lines were constructed by infecting either the PRI or MET sublines with the LXSN retroviral vector containing an IGF-IR cDNA (LISN) as previously described [20]. Clones were then picked from each infected cell line that over-expressed the IGF-IR. Control cells were infected with the LXSN vector alone. Clones were selected for dual expression of AR and IGF-IR by Western immunoblotting for IGF-IR and AR expression. Because of the high level of infection with the retroviral vector, the majority of clones over-expressed IGF-IR. Three IGF-IR-expressing clones from both the PRI and MET cell lines were selected for this study.

Isolation of Nuclear Protein

Cells were collected using a 1% trypsin/EDTA solution and washed once with ice-cold PBS. The cells were resuspended in a solution of 10 mM HEPES–KOH, 1.5 mM $MgCl_2$ 10 mM KCl, 0.5 mM dithiothreitol at pH 7.9. The suspended cells were allowed to swell on ice for 10 min. Cells were then vortexed and pulse spun. The supernatant was discarded and the pellet resuspended in ice cold buffer of 20 mM HEPES–KOH, 25% (v/v) glycerol, 420 mM NaCl, 1.5 mM $MgCl_2$, 0.2 mM EDTA, 0.5 mM dithiothreitol at pH 7.9. The mixture was incubated on ice for 20 min then centrifuged for 2 min at 2,000*g* at 4°C. The supernatant was removed and kept at −70°C until used for Western blots. All extracts contained protease inhibitors (Complete Protease Inhibitor Tablet, Roche, Indianapolis, IN).

Western Immunoblotting

Cell lysates were collected by addition of cold lysis buffer (30 mM HEPES, 150 mM NaCl, 1.5 mM $MgCl_2$, 1 mM EGTA, 10% Triton X-100) containing protease and phosphatase inhibitors (Phosphatase Inhibitor Cocktail II, Sigma, St. Louis, MO) to monolayer cultures. Total protein concentration was determined with the BCA protein assay kit (Pierce Biological). Fifty micrograms of cell lysates were separated on polyacrylamide gels and then transferred to nitrocellulose membranes (BioRad, Hercules, CA). Antibodies recognizing the AR, IGF-IR, phosphorylated Akt, and total ERK were purchased from Santa Cruz Biotechnology, Inc. (Santa Cruz, CA), antibody recognizing phosphorylated ERK from Cell Signaling Technologies (Beverly, MA), and Akt from Biosource, Inc. (Camarillo, CA). To control for loading of protein in the AR and IGF-IR Westerns, immunoblots were stripped and re-probed with a β-actin monoclonal antibody (Sigma). Protein was detected using the ECL Plus kit from Amersham (Buckinghamshire, England). An LKB 2222-020 Ultrascan XL laser densitometer (Pharmacia LKB, Uppsala, Sweden) was used to quantify the signal.

ReverseTranscription-PCR and DNA Sequencing

Total RNA from PRI and MET cells was extracted using RNAeasy Mini Kits (Qiagen, Inc., Chatsworth, CA) according to the manufacturer's suggestions. RT-PCR amplification of exons 1–8 of the transgene-derived AR mRNA was done with primers designed to cross intron/exon junctions to rule out amplification of genomic DNA. Primer sets also produced PCR products with overlapping sequences in order to provide reliable sequence in all regions. Primers were obtained from Invitrogen. Tth DNA polymerase (Promega) was used according to the manufacturer's directions for RT-PCR reactions. Total RNA (1 μg) was transcribed for 20 min at 70°C with 10 nM of the reverse primer. Amplification conditions consisted of an initial denaturing step at 95°C for 4 min, annealing at 60°C for 1 min, and extension/polymerization at 72°C for 1.5 min with a 3-sec increment per cycle for a total of 35 cycles. Each primer of 0.5 μM was used in the PCR reactions. DNA sequencing of the PCR product was

performed by Elim Biopharmaceuticals, Inc. (Hayward, CA), using the Big Dye Terminator Ready Reaction Kit (Applied Biosystems, Perkin-Elmer Corp., Torrance, CA).

Proliferation of PRI and MET Cells in Response to DHT

The growth rate of PRI and MET cells in the presence or absence of 10^{-10} M DHT was determined by counting the number of cells as a function of time. Three parallel wells for each time point and treatment were plated. Cells were trypsinized and counted with a hemocytometer 48, 72, and 96 hr after plating. Serum-free media with or without DHT was changed daily.

MTT Assays

Proliferation of the various M12-AR cell lines in the presence of DHT was also measured using the CellTiter 96 AQ_{ueous} One Solution Reagent (Promega). Cells were seeded in 12-well plates at 5×10^4 cells/well in medium with 5% charcoal-stripped serum (CSS) (HyClone). The day after plating, cells were treated in serum-free medium in triplicate under the following conditions: (A) serum-free medium; (B) 10^{-10} M DHT (Sigma); (C) 0.5 nM rh-IGF-I (IGF) (R & D Systems); (D) 15 particles/cell AKT adenovirus (a generous gift provided by Ken Walsh, Boston, MA); (E) 25 μM LY294002 (Sigma); and (F) 20 μM PD98059 (New England Biolabs). Efficiency of adenovirus infection was determined and adjusted for by infection of parallel plates with adenovirus expressing β-galactosidase. Following 48 hr of treatment, 150 μl of CellTiter 96 Reagent was added to each well, and 30 min later, the plates were read on a Wallac Victor^2 1420 fluorescent plate reader at an excitation wave length of 490 nm.

Promoter Activity Assays

Reporter assays were performed as previously described [22]. Transient transfections of PRI and MET cells with the triple AR probasin-luciferase promoter (AAR_3) (a generous gift from Dr. Robert Matusik) were performed using lipofectamine plus (Life Technologies) according to the manufacturer's protocol. The AAR_3 construct is an artificial reporter containing three repeats of the rat probasin ARE1 and ARE2 regions upstream of the thymidine kinase promoter [21]. Briefly, 7.5×10^4 cells were seeded in 12-well plates in RPMI medium containing 5% FBS. The following day, each well received 1.2 μg of vector DNA, 6 μl plus reagent, and 3 μl of lipofectin reagent in serum-free medium. After a 3-hr exposure to the lipofectamine/DNA/plus mixture, the medium was supplemented with 5% FCS and incubation was continued for 18 hr.

For DHT dose-response studies, transfection medium was removed and the cells were treated in triplicate for 24 hr with DHT (10^{-8}, 10^{-10}, 10^{-12} M) in serum-free medium. The effect of IGF-I on DHT-stimulated luciferase activity was determined by treating cells with 0.5 nM IGF for 1 hr prior to addition of 10^{-10} M DHT for 24 hr. To determine DHT-induced luciferase activity in response to PI3K activators or inhibitors and MEK inhibitors, transfection medium was removed and the cells were treated in triplicate with serum-free medium as follows: (A) serum-free medium; (B) 10^{-10} M DHT; (C) 25 μM LY294002; (D) 25 μM LY294002 + DHT (10^{-10} M); (E) 15 particles/cell AKT; (F) 15 particles/cell AKT + DHT (10^{-10} M); (G) 20 μM PD98059; and (H) 20 μM PD98059 + DHT (10^{-10} M); (I) 15 particles/cell (dn)AKT; (J) 15 particles/cell (dn)AKT + DHT (10^{-10} M). Efficiency of adenoviral infections, as well as negative adenoviral control effects, was determined by using an adenoviral-lacZ vector, which exhibit >90% infection efficiency. Replication-deficient adenoviral AKT (AKT) and (dn) adenoviral AKT ((dn)AKT) vectors were a generous gift from Dr. K. Walsh. The replication-deficient adenoviral LacZ control was constructed using the Invitrogen adenoviral kit (Invitrogen). Cells were initially treated with LY294002 or PD98059 for 2 hr prior to addition of DHT for an additional 24 hr. Cells were infected with adenoviral AKT or dominant-negative (dn)AKT constructs 24 hr prior to the addition of DHT. In preliminary studies, we have shown that the 24-hr time period allows for significant expression of either AKT or (dn)AKT protein (data not shown). The percent increase in DHT-induced luciferase activity was compared to its respective control; e.g., AKT + DHT versus AKT alone. To determine whether IGF-I was able to affect AR-induced luciferase activity, LY294002 or PD98059 was added 2 hr prior to the addition of DHT, and IGF-I (0.5 nm) was added 1 hr prior to addition of DHT treatment for 24 hr. Again, the percent increase in luciferase activity was compared to its re spective control; e.g., AKT + IGF-I + DHT/AKT + IGF-I alone.

Luciferase activity was determined using the Luciferase Assay System (Promega) according to the manufacturer's protocol. Each sample lysate (200 μl/well) was combined with the luciferase substrate by injection and analyzed on a System Luminometer 400 (Nichols Institute Diagnostics, San Clemente, CA). Transfection efficiency was determined by transfection of triplicate wells with a pGL-3 control vector, in which luciferase expression is driven by the SV40 promoter (SV40-Luc). The AAR_3 or SV40-Luc constructs were transfected 24 hr prior to the start of any treatment to assure similar transfection efficiency, regardless of treatment. In addition, as previously described, transfection efficiency

determined by the SV40-Luc constructs were confirmed by β-galactosidase as previously described [22]. PRI cells exhibited a 2.2-fold greater transfection efficiency than the MET cells, and this was corrected for in the analysis of the luciferase results. Separate triplicate wells were transfected with a pGL-3 basic luciferase reporter vector, which served as a non-specific control. All samples were done in triplicate and repeated at least three times.

Microarray Fabrication

Arrays containing a non-redundant set of 6,000 prostate-derived cDNA clones from the Prostate Expression DataBase (PEDB), a public sequence repository of expressed sequence tag (EST) data derived from human prostate cDNA libraries [23], were prepared as previously described by Lin et al. [24].

Probe Construction and Hybridization

Total RNA was isolated from each of the cell treatments using TRIzol (Life Technologies, Gaithersburg, MD) according to the manufacturer's directions. Fluorescently-labeled probes were made from 30 μg total RNA in a reaction volume of 20 μl containing 1 μl anchored oligo-dT primer (Amersham), 0.05 mM Cy3-dCTP (Amersham), 0.05 mM dCTP, 0.1 mM each of dGTP, dATP, dTTP, and 200 U Superscript II reverse transcriptase (Life Technologies). Hybridization of array slides was performed as previously described [24].

Image Acquisition and Data Analyses

Fluorescence intensities of the immobilized targets were measured using a laser confocal microscope (Molecular Dynamics). Quantitative data were obtained with the SpotFinder V 2.4 program written at the University of Washington. Local background hybridization signals were subtracted prior to comparing spot intensities and determining expression ratios. Each cDNA was represented twice on each slide, and the experiments were performed in duplicate, producing 4 data points per cDNA clone per hybridization probe. Intensity ratios for each cDNA clone hybridized with probes derived from the respective treatments were calculated. Gene-expression levels were considered significantly different between the two conditions if all four replicate spots for a given cDNA demonstrated a ratio >2 or <0.5, and the signal intensity was greater than 2 standard deviations above the image background. In order for a gene to be considered as regulated by AKT, the changes in expression were required to occur in both LY294002 and (dn)AKT-treated cells. Confirmation of differences in expression of selected genes was accomplished by either real-time RT-PCR using a Roche Light-Cycler™ or Northern blot.

Statistics

All the above experiments were repeated at least three times, and figures are representative of the results. All studies were performed on two PRI and three MET cell lines. Results are means of each group. Each experiment was performed on similar passages of PRI or MET cells. Results were considered significant if the probability value was less than 0.05. For the in vivo tumorigenicity assays, Fisher's exact test was used to assess any significance in tumor formation. Repeated-measures ANOVAs were performed to determine significance between cell proliferation counts, MTT, and promoter assays, followed by Fisher's PLSD post-hoc test. Unpaired *t*-tests were used to examine differences measured by Western immunoblots.

RESULTS

Tumorigenicity of AR-Expressing Cells and Establishment of Sublines

Confirmation of stable expression of the AR in M12 cells and the primary (PRI) and metastatic (MET) sublines is presented in Figure 1A. Note that there is an increase in AR in the nuclear extracts in each of the constructs following addition of DHT. As shown in Figure 1B, the MET subline also has a functional AR similar to its parental MET line shown in Figure 1A. In Figure 1C, we demonstrate that there is no detectable AR mRNA in the M12 line, but clear expression of AR mRNA in the M12-AR PRI and MET sublines. Quantitative RT-PCR demonstrated that there was equivalent AR mRNA expression in the PRI and MET lines (data not shown).

To assess the effect of AR expression on the tumorigenicity of M12 cells, 2×10^6 cells of the PAR clone were injected into the dorsal prostate of male athymic nude mice. As shown in Table I, 16 of the 26 mice injected with the PAR cells developed macroscopic primary tumors within 3 months. In contrast, 25 out of 25 mice injected with M12 control cells developed macroscopic primary tumors within 6–8 weeks of injection. PAR-injected mice also developed significantly fewer tumors than mice injected with M12 and M12 empty vector control cells ($P < 0.05$). In addition to primary tumors, four PRI mice also demonstrated visible metastases to the diaphragm and microscopic metastases to the lungs. The diaphragm metastases were removed, and the cells were re-injected orthotopically into athymic nude mice. Of the four metastatic tumors injected orthotopically into mice, all four developed large tumors (>1-cm diameter) in the same time

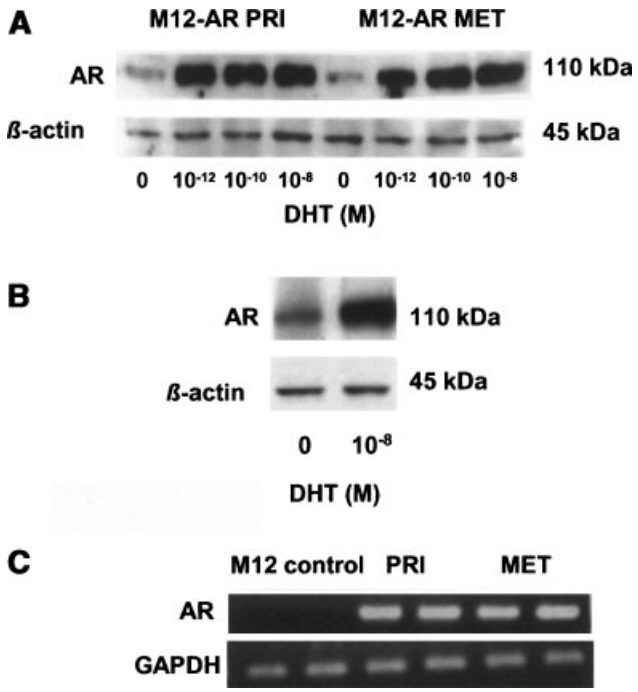

Fig. 1. **A**: Western immunoblot of androgen receptor (AR) in nuclear extracts from MI2-AR primary (PRI) and metastatic (MET) cells treated for 24 hr with increasing concentrations of dihydrotestosterone (DHT). Note the similar expression levels and increased nuclear accumulation of AR in response to DHT treatment in both cell lines. **B**: Western immunoblot of AR in MET subline BI cells treated with 10^{-8} M DHT. β-Actin was used as a loading control. **C**: RT-PCR of AR mRNA from MI2 control (AR-negative), PRL, and MET cells. Note the lack of AR mRNA in the MI2 control cells.

frame as the M12 control cells, and these cells were again collagenase-digested and cell lines re-established. The animals were followed for another 2 months and metastatic tumors again appeared in the lungs and diaphragm, confirming the transition from a primary prostatic to metastatic phenotype. All subsequent assays were performed on cells from the initial metastatic cell line (MET cells) and two additional metastatic sublines.

Sequencing of the AR mRNA and Expression of Signaling Molecules

Sequence analysis of the AR mRNA in the MET cells revealed no AR mutations (data not shown). PRI and MET cells expressed immunodetectable levels of AR (Fig. 1) and IGF-IR protein (Fig. 2A). AR expression was readily detected at similar levels in PRI and MET cells by quantitative RT-PCR and Western immunoblotting, Figure 1, as previously described [25]. No changes in PTEN expression by Western immunoblot were noted between the cell types (data not shown). As shown in Figure 2, IGF-IR levels assessed by Western immunoblotting were increased by stable expression of the AR. IGF-IR levels were increased even further in the PRI cell line, while in the MET line, IGF-IR expression was decreased to 64% of the M12 control level.

Proliferation and Viability of AR-Expressing MI2 Cells

As shown in Figure 3A, MET cells exhibited a faster population doubling time than the PRI cells. This increase in growth rate was apparent by 96 hr, as the MET cells had tripled their cell number in 24 hr as opposed to the approximate doubling of cell number observed continuously in the PRI cells and earlier in the MET cells. Addition of 10^{-10} M DHT caused slower cell growth in the PRI cells. This decrease was significant at 72 and 96 hr ($P < 0.03$). There was no significant difference in growth rate in the MET cells in the presence of 10^{-10} M DHT. MTT assays were also performed to verify the cell proliferation counts, as well as to examine cell viability under various conditions.

TABLE I. Cell Lines, Androgen Receptor (AR) Status, and Number of MiceThat Developed Tumors Within I2 Weeks After Orthotopic (Intraprostatic-Dorsal Lobe) Injection of 2×10^6 Cells Into Athymic Nude Mice

Cell line	AR status	Mice with tumor/ total mice injected	Time to detectable tumor (weeks)
M12 control-intact	Negative	25/25	6–8
M12 parental-intact	Positive	16/26	12
M12 control-castrate	Negative	10/10	6–8
M12 parental-castrate	Positive	3/10	12
M12-MET	Positive	4/4	6–8[a]
M12 MET sublines	Positive	12/12	6–8[a]

Time to detectable tumor indicates time at which palpation of the abdomen suggested tumor growth that was confirmed with pathology.
[a]Indicates that the animal could not be allowed to proceed to the 12-week time point because of tumor volume.

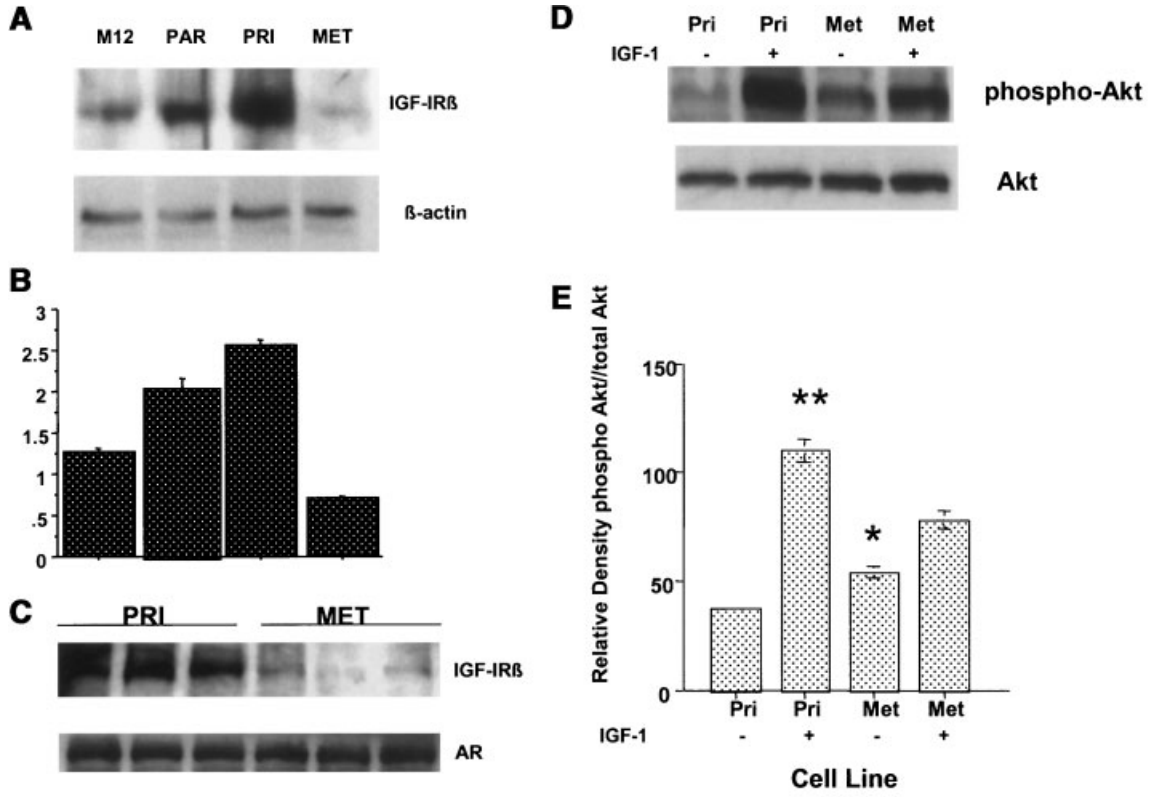

Fig. 2. **A**: Western immunoblot of IGF-IR β subunit in MI2 control, MI2-AR parental (PAR), primary (PRI), and metastatic (MET) cell extracts. Note the marked increase in IGF-IR in the PAR and PRI cell lines and the marked decrease in the MET cell line. β-Actin was used as a loading control. **B**: Relative differences in IGF-IR expression between cell lines based upon the combined results of three Western blots corrected for loading with actin controls. $^{*}P < 0.01$ compared to MI2 control cells. **C**: Western immunoblot of IGF-IR β subunit and AR from clones from three PRI and MET tumors. Note the consistent decrease in IGF-IR in the three MET clones compared to the three PRI clones. **D**: Western immunoblot of phosphorylated Akt (phospho-Akt) and total Akt from PRI and MET clones with and without addition of IGF-I, 50 ng/ml, 20 min prior to collection of lysates. **E**: Densitometric quantitation of Figure 4D. Note the increase in phospho-Akt in response to IGF-I; this increase was significantly greater in the PRI cells compared to MET cells, $^{**}P < 0.01$ and basal phospho-Akt increase in MET compared to PRI cells $^{*}P \leq 0.05$. Akt quantitation is the mean of three separate experiments.

PRI cells had a significant decrease ($P < 0.0002$) in cell viability with 10^{-10} M DHT, while DHT had no affect on MET cell viability, in accordance with the proliferation experiment (Fig. 3B). Also in agreement with cell counts, MET cells had increased cell viability compared to the PRI cells ($P < 0.001$), suggesting that they had a higher growth rate. MTT assays were also done in the presence of 0.5 nM IGF-I, 15 particles/cell AKT adenovirus, 25 μM LY294002, and 20 μM PD98059. In the PRI cells, IGF-I significantly increased cell viability ($P < 0.0001$) compared to no treatment, while LY294002 and PD98059 significantly decreased cell viability ($P < 0.0002$). In the MET cells, only LY294002 had an effect on cell viability as measured by MTT assay.

We also assessed whether the effects of PD98059 and LY294002 in the MTT assay were due to changes in proliferation or apoptosis. In the PRI cells, PD98059 caused a decrease in proliferation and an increase in apoptosis as determined by propidium iodide staining and flow cytometry and PARP and caspase 3 cleavage; in contrast, in the MET cells, there was no effect of PD98059 on apoptosis and minimal effects on proliferation at the concentration used. Flow cytometry, PARP, and caspase 3 assays were performed as previously described [26–28]. The effect of LY294002 on the MTT in both PRI and MET cells was due to apoptosis. In the MET cells, LY294002 significantly decreased cell viability compared to no treatment ($P < 0.0002$).

Effect of DHT and IGF-I on AR Activity in AR-Expressing PRI and MET Cells

To assess the transcriptional regulatory activity of the expressed AR protein, PRI and MET cells were transiently transfected with an AAR_3-probasin luciferase reporter and treated for 24 hr with varying doses of DHT. In both PAR and MET cells, there was a

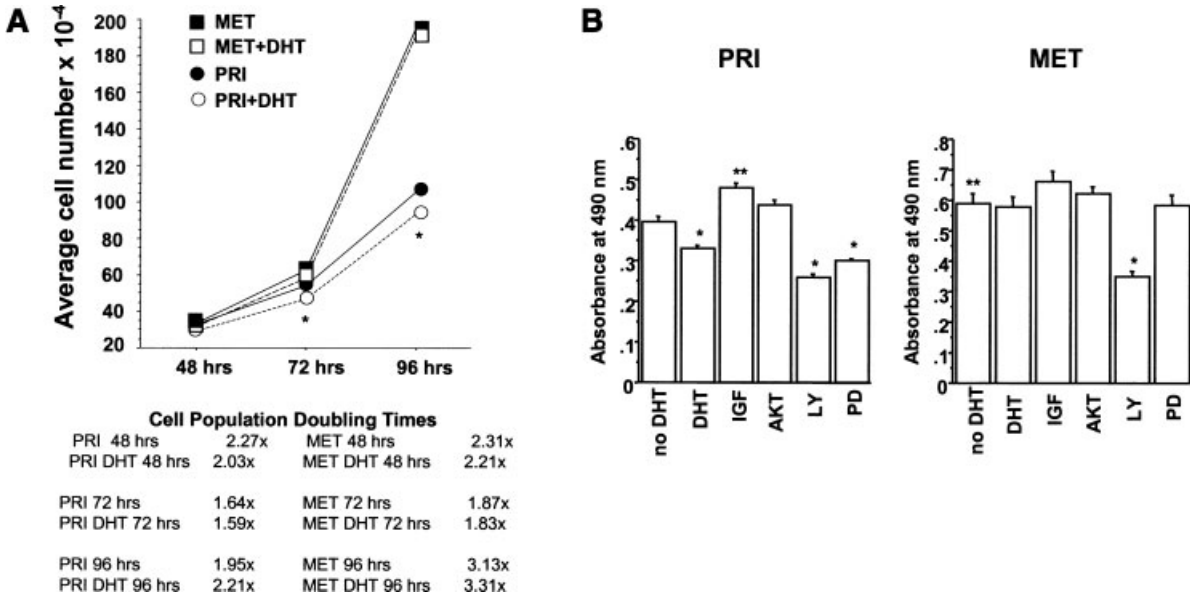

Cell Population Doubling Times

PRI 48 hrs	2.27x	MET 48 hrs	2.31x
PRI DHT 48 hrs	2.03x	MET DHT 48 hrs	2.21x
PRI 72 hrs	1.64x	MET 72 hrs	1.87x
PRI DHT 72 hrs	1.59x	MET DHT 72 hrs	1.83x
PRI 96 hrs	1.95x	MET 96 hrs	3.13x
PRI DHT 96 hrs	2.21x	MET DHT 96 hrs	3.31x

Fig. 3. **A**: PRI and MET cell population counts at 48, 72, and 96 hr in the presence or absence of 10^{-10} M DHT. In the PRI cells, DHT reduced cell number at 72 and 96 hr compared to PRI cells without DHT (*$P < 0.05$; SEM bars are within the point markers). DHT had no effect on MET cells, which exhibited an increased growth rate compared to PRI cells. This was noted at 96 hr, when the MET cells began tripling their growth rate as opposed to the approximate doubling observed continuously in the PRI cells and previously in the MET cells. **B**: MTT assay indicating cell viability after 72 hr after treatment of PRI or MET cells with DHT (10^{-8} M), IGF-I (20 ng/ml), 15 particles/cell AKT adenovirus, 25 μM LY294002, or 20 μM PD98059. *$P \leq 0.01$ compared to no DHT, **$P < 0.001$ compared to no DHT. The relative contributions of apoptosis and proliferation to cell viability are discussed in the text.

significant increase in promoter activity at 10^{-8} and 10^{-10} M DHT compared to no DHT ($P < 0.002$), while 10^{-12} M DHT did not significantly increase reporter activity (Fig. 4A). PRI and MET cells both exhibited maximal DHT-induced AR activity at 10^{-8} M DHT. PRI and MET cells were then treated with 0.5 nM IGF-I in the presence or absence of 10^{-10} M DHT (Fig. 4B). In PRI cells, IGF-I caused a significant increase in DHT-induced luciferase activity compared to cells treated with DHT alone ($P < 0.0001$). The opposite effect was observed in MET cells, with IGF-I causing a significant decrease in DHT-induced luciferase activity ($P < 0.0002$).

Effect of PI3K and ERK Pathway Inhibition on DHT-Stimulated AR Activity

Since the primary signaling pathways activated by the IGF-IR are the PI3K and ERK cascades, and prostate cancer cells exhibit autocrine production of IGF ligands, we next examined the effects of alterations in these two pathways on AR transcriptional activity in order to determine if one or both of these pathways modulates the effects of the IGF-IR seen in the PRI and MET cell lines [25].

PRI and MET cells were treated with 25 μM LY294002, 15 particles/cell AKT adenovirus, 15 particles/cell (dn)AKT adenovirus, or 20 μM PD98059 for 2 hr prior to addition of 10^{-10} M DHT for 24 hr. Twenty five micromolar LY294002 or (dn) adenoviral AKT, in the presence of 10^{-10} M DHT, caused a significant reduction in DHT-induced luciferase activity in the PRI cells ($P < 0.002$; Fig. 4C). The results with the (dn)Akt construct are not shown, since they were similar to LY294002. Both the AKT adenovirus and PD98059 caused a significant increase in DHT-induced luciferase activity ($P < 0.01$), while, in MET cells, the opposite effect was observed. Namely, LY294002 and 15 particles/cell (dn)AKT adenovirus caused a significant increase in DHT-induced luciferase activity ($P < 0.01$), while AKT and PD98059 caused a significant decrease in AR promoter activity ($P < 0.0002$). To determine whether IGF-I was able to modulate the observed effects of (dn)AKT, LY294002, or PD98059 treatment, PRI and MET cells were treated with the above reagents for 2 hr, followed by 0.5 nM IGF-I treatment for 1 hr prior to addition of 10^{-10} M DHT for 24 hr. As seen in Figure 4D, in the PRI cells, IGF-I treatment abolished the decrease in DHT-induced luciferase activity with LY294002 and (dn)Akt treatment. PRI cells treated with IGF-I had significantly higher DHT-induced luciferase activity than cells treated with DHT alone ($P < 0.0002$). In the MET cells, the opposite effect was again observed. IGF-I treatment significantly decreased

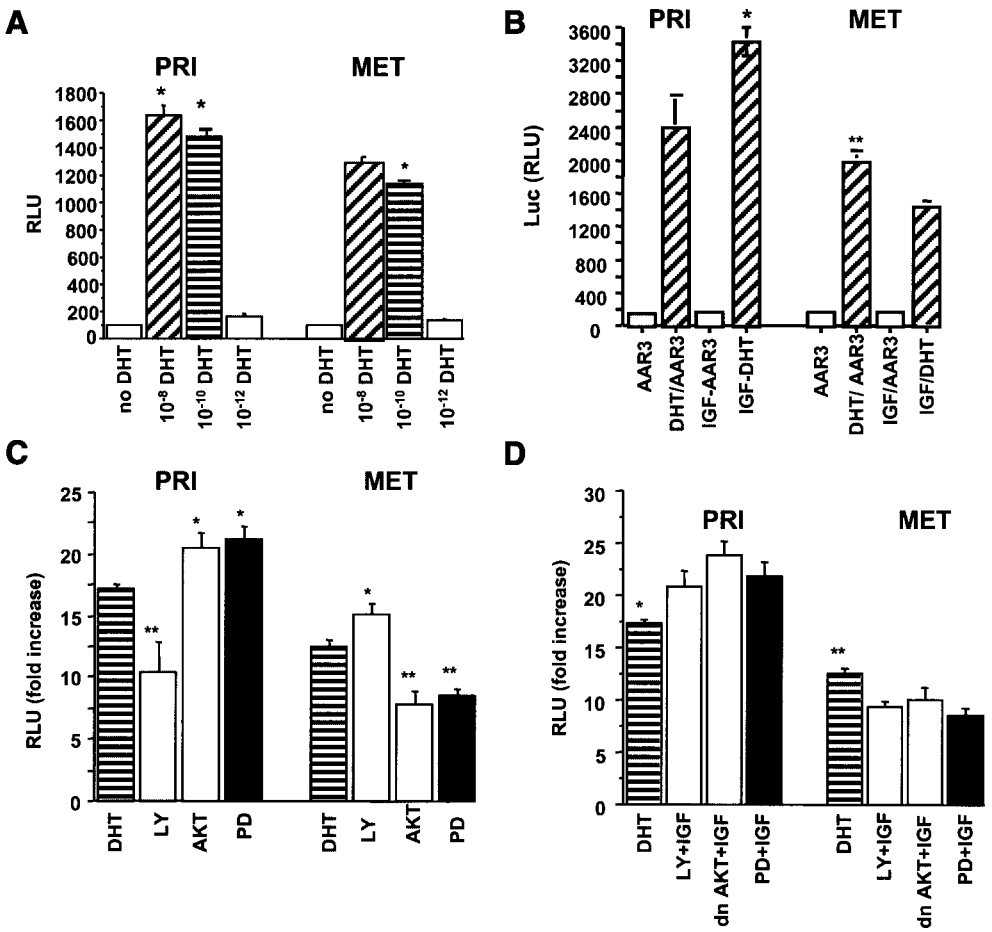

Fig. 4. Luciferase reporter activity in PRI and MET cells. **A**: DHT-induced luciferase activity in PRI and MET cells transfected with the AAR_3 promoter construct following DHT (10^{-8}, 10^{-10}, and 10^{-12} M) treatment for 24 hr. In PRI and MET cells, 10^{-8} and 10^{-10} M DHT significantly increased promoter activity (*$P < 0.01$). In the MET cells, 10^{-8} M DHT significantly decreased promoter activity compared to 10^{-10} M DHT (**$P < 0.05$). Furthermore, the increase in promoter activity at 10^{-8} and 10^{-10} M DHT in the MET cells was significantly less than the respective increase observed in the PRI cells (**$P < 0.01$). **B**: Luciferase activity in PRI and MET cells treated with 0.5 nM IGF-I for 1 hr prior to addition of 10^{-10} M DHT for 24 hr. PRI cells showed a significant increase in DHT-induced luciferase activity in the presence of IGF-I (*$P < 0.0001$), while MET cells showed a significant decrease in DHT-induced luciferase activity in the presence of IGF (**$P < 0.0002$). **C**: Luciferase reporter activity in PRI and MET cells treated with 25 μM LY294002, 15 particles/cell AKT adenovirus, or 20 μM PD98059 for 2 hr prior to addition of 10^{-10} M DHT for 24 hr. Results are expressed as a fold increase in DHT + treatment/treatment alone, for example, IGF-I + DHT treatment/IGF-I treatment alone. In the PRI cells, the presence of 25 μM LY294002 significantly reduced levels of DHT-induced luciferase activity (**$P < 0.002$), while AKT and PD98059 caused a significant increase in DHT-induced luciferase activity (**$P < 0.01$). In the MET cells, the opposite effect was observed; namely, LY294002 caused a significant increase in DHT-induced luciferase activity (*$P < 0.01$), while AKT and PD98059 caused a significant decrease in DHT-induced luciferase activity (**$P < 0.0002$). **D**: The effect of IGF-I treatment on luciferase activity in PRI and MET cells treated with 25 μM LY294002, 15 particles/cell AKT adenovirus, or 20 μM PD98059 for 2 hr prior to addition of 0.5 nM IGF-I for 1 hr followed by addition of 10^{-10} M DHT for 24 hr. In PRI cells, IGF-I reversed the decrease in DHT-induced luciferase activity caused by LY294002, and in the MET cells, IGF-I reversed the increase in DHT-induced luciferase activity seen with LY294002 (compare C and D). In the PRI cells, all cells treated with IGF-I had significantly higher DHT-induced luciferase activity (*$P < 0.0002$). In the MET cells, the opposite effect was observed, with all IGF-I-treated cells having significantly reduced DHT-induced luciferase activity (**$P < 0.0005$).

DHT-induced luciferase activity in IGF-I-treated cells ($P < 0.0005$), and IGF-I treatment overcame the increase in DHT-induced luciferase activity observed in the presence of LY294002 or (dn)AKT in the MET cells.

In order to confirm that the adenoviral AKT and (dn)AKT constructs performed appropriately, we infected M12 cells with 15 particles/cell of either AKT or (dn)AKT adenovirus. Cell lysates were collected 24 hr after infection and Western immunoblots performed. In Figure 5A, we confirm that the AKT construct increases the expression of AKT protein and phosphorylated AKT, and that the phosphorylation of the transfected AKT is stimulated by IGF-I treatment (Fig. 5B). In Figure 5B, we also confirm that LY294002

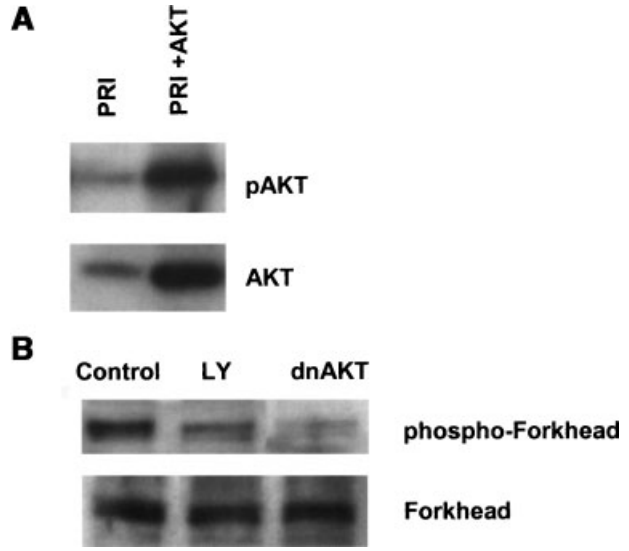

Fig. 5. **A**: Western immunoblot of cell lysates with either AKT or phospho-AKT (pAKT) antibody 24 hr following the addition of AKT adenovirus to the PRI cell line. Note the increase in total AKT protein as well as phosphorylated AKT in the AKT adenovirus-infected cells. **B**: Western immunoblot of forkhead and phospho-forkhead in whole-cell lysates from PRI cells. Note the decrease in forkhead phosphorylation with the addition of LY294002 and (dn)AKT adenovirus compared to untreated PRI cells.

and (dn)AKT markedly inhibit phosphorylation of the downstream AKT target, forkhead protein. Thus, these data confirm that the adenoviral AKT and (dn)AKT constructs function as expected in the time frame described.

Effect of IGF-IR Expression Level on AR Transcriptional Activity

The expression levels of the IGF-IR and AR proteins in representative clones of each construct are shown in Figure 6A,B, and the relative changes in AAR_3 reporter activity for these constructs are seen in Figure 6C. Increased expression of the IGF-IR (with the LISN vector) in the PRI cell line did not result in any qualitative change in AR-induced promoter activity, nor were there any qualitative differences noted between these two constructs when either the PI3K or ERK pathways were inhibited. In contrast, when the IGF-IR was re-expressed in the MET sublines, Figure 6C, AR-induced promoter activity reverted to that seen in the PRI lines. It should be noted that, in the progression from PRI to MET cells, there is a significant decrease in endogenous IGF-IR expression. This suggests that re-expression of the IGF-IR in MET cells results in the conversion of the IGF-regulated portion of AR transcriptional activity to the less-aggressive phenotype exhibited by PRI cells. On the other hand, the level of basal expression of the IGF-IR in the PRI cells is similar to that of poorly tumorigenic cell lines, and a further increase in IGF-IR expression does not result in a qualitative change in AR transcriptional activity.

Effects of IGF-IR re-Expression on AR Activity in PRI and MET Cell Lines Following Inhibition of the PI3K and ERK Pathways

As shown in Figure 6C, when the ERK pathway was inhibited with PD98059, there was an increase in DHT-stimulated reporter activity in the PRI line when the IGF-IR was re-expressed (Fig. 6C2) as compared to the PRI cells without the IGF-IR re-expressed (Fig. 6C1). There were no differences when AKT was inhibited between the PRI and PRI line with the IGF-IR re-expressed (data not shown). In contrast, in the MET line, when the IGF-IR was re-expressed, the response to inhibition of the ERK pathway (Fig. 6C5) resulted in a pattern similar to that seen in the PRI cells without IGF-IR re-expression (Fig. 6C1). More striking changes were noted with inhibition of the PI3K pathway, where there was a reversion to the PRI AKT response in the MET cell line when the IGF-IR was re-expressed (Fig. 6C3). These data suggest that re-expression of the IGF-IR in the metastatic cell lines returns the interaction between the AR and IGF-IR to that characteristic of the less-aggressive PRI cells. These findings are in agreement with earlier reports that a decrease in IGF-IR in prostate cancer is associated with a more aggressive phenotype [20,29–31].

AKT Inhibition Results in Differences in Expression of Androgen-Regulated Genes Between PRI and MET Cells

Since the AR functions as a transcription factor, we used cDNA microarrays to determine if alteration of IGF signaling results in differential regulation of genes expressed in response to androgens. RNA isolated from PRI and MET cells treated with DHT and treated with LY29004, (dn)AKT adenovirus, or vehicle was used to interrogate microarrays as described in ''Materials and Methods.'' The genes that were differentially regulated by both LY294002 and the (dn)AKT construct compared to vehicle control cells are shown in Table II. Of particular note are the changes in the expression levels of PSA, ets, and *TMPRSS2*, genes that contain well-defined androgen response elements in their promoters. Differences in PSA and TMPRSS2 mRNA levels were confirmed by quantitative, real-time RT-PCR, and LIM kinase mRNA levels by Northern blot (data not shown). These array data demonstrate that the changes we have described in the interaction between the between the IGF-IR and AR between primary and metastatic prostate cancer.

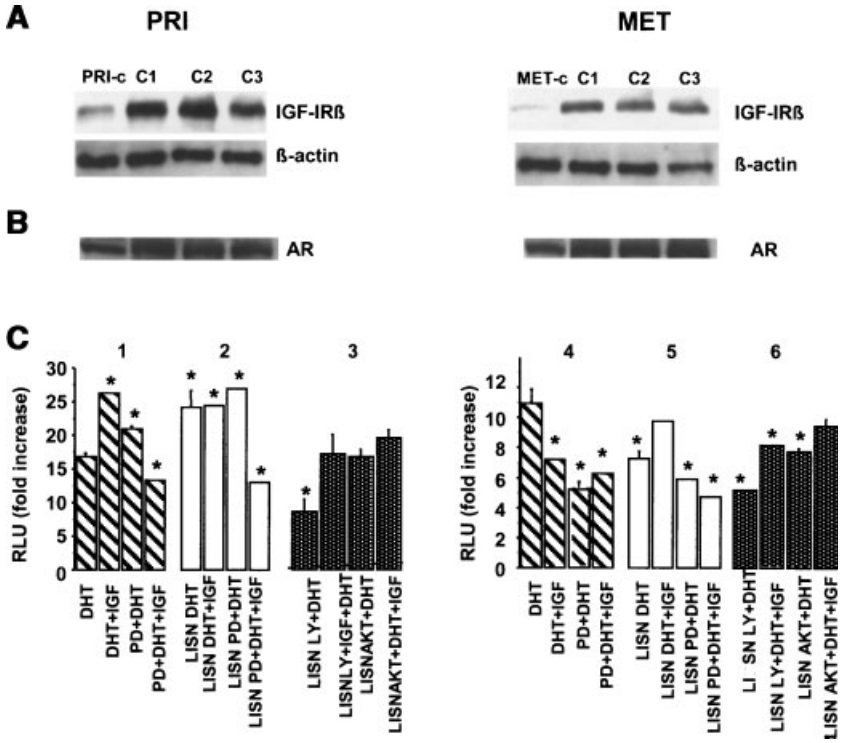

Fig. 6. Luciferase activity in PRI and MET cells with and without re-expression of the IGF-IR using the retroviral LISN IGF-IR expression vector. Control PRI (6CI) and MET (6C4) cells were infected using the LXSN empty retroviral cassette. The increase in IGF-IR expression is shown in (**A**) and persistence of AR expression in (**B**). PRI-c and MET-c indicate PRI or MET cells infected with the empty LXSN vector, and CI-3 indicate clones of either PRI or MET cells infected with the LISN IGF-IR vector. **C**: Re-expression of the IGF-IR in the PRI cells (6C2 and 3) results in a quantitative increase in reporter response, but no qualitative differences compared to the control cells. In contrast, in the MET cells, re-expression of the IGF-IR (6C5 and 6) results in a qualitative difference in AR activity, with conversion to the pattern seen in the PRI control cells. In this figure, we have included the effect of inhibition of ERK by the addition of PD98059 (PD, 6C2 and 5) and PI3K by the addition of LY294002 (LY, 6C3 and 6) or increased AKT by addition of the previously described AKT adenoviral construct (AKT, 6C3 and 6). $^*P \leq 0.01$ compared to the respective DHT-stimulated response for the PRI or MET cell line. Note that, in addition to the quantitative changes seen in the cells when the IGF-IR is expressed, in the MET line, there is also a qualitative difference in the MET-LISN cells, with a response similar to that seen in the PRI control cells. PRI and MET LY and AKT control responses are noted in Figure 4C,D.

TABLE II. Genes Differentially Regulated Between PRI and MET Cells Following Inhibition of AKT by LY294002 and (dn)AKT as Described in "Materials and Methods"

Gene name	Gene identification	Fold increase
Kallikrein-3 (prostate specific antigen (PSA))	gi[22345713	4.1
ets homologous factor	gi[7955288	3.2
Jumping translocation breakpoint	gi[4629922	2.4
Vascular cell adhesion molecule 1	gi[18201908	2.5
Epitheliasin (TMPRSS2)	gb[AF329454	2.0
B-cell CLL/lymphoma 2 (Bcl-2)	gi[20072667	2.0
Claudin 4	gi[2570124	2.7
LIM domain kinase 1	gi[565279	3.3
Anterior gradient 2 hormone	gi[21811148	5.1
Monoamine oxidase	gi[187354	6.2
Claudin 7	NM001307	6.2

In order to be considered differentially regulated, they had to be affected by both LY294002 and the (dn)AKT construct.

DISCUSSION

In this study, we have demonstrated there is a functional interaction between the AR and the IGF-IR, and that this interaction depends on the cell context in which the interaction takes place. More specifically, the determinants of cell context were whether the cell line had been derived from a primary prostate tumor or whether this line had developed metastatic capability. The relationship between the AR and growth factors in the prostate changes markedly in the progression from benign to metastatic prostate cancer. In the more benign cell, androgens stimulate prostate epithelial growth via a paracrine mechanism in which androgen stimulates the release of peptide growth factors from stromal cells. These growth factors, in turn, act through their cognate receptors on epithelial cells to stimulate growth. The role of the AR in the epithelial cell is related to differentiation and inhibition of cell growth [5]. This effect on cell growth and induction of more differentiated functions was seen in our PRI cells, where cell growth was inhibited by androgen, PSA was expressed, and tumor formation, as well as the latent period to tumor formation, was increased. These results are similar to those reported for other mouse and human immortalized epithelial cells [32,33]. However, the function of the AR in malignant metastatic cells changes, and activation of the AR no longer inhibits proliferation. Furthermore, since the cells acquire an autocrine production of growth factors, the relationship between the AR and stroma needed to maintain epithelial growth in the benign prostate is no longer necessary. Thus, in the malignant prostate epithelium, the AR is converted from a regulator of growth and differentiation to a potential ''oncogene'' that enhances cell proliferation and survival [5]. In the case of most human prostate cancer cell lines, as well as 25% or more of prostate cancers, mutation or decreased expression of the AR is associated with progression to malignancy. The concept of altered AR signaling in the progression to metastatic disease is documented in the present study, in which we demonstrate qualitative differences in androgen-stimulated AR transcriptional activity that are dependent on whether the target cell is derived from an intraprostatic or metastatic context. These differences in AR activity result in differences in the levels of expression of a set of androgen-regulated genes. Microarray analyses of P69 and M12 cell lines that compared differences in gene expression to differences in genes expressed in primary human benign and malignant prostate epithelial cells have recently been published [34]. The similarity of changes in gene expression patterns seen in the progression of P69 to M12 cells, in which there is a marked increase in malignant characteristics, and the changes seen between human benign and malignant microdissected primary prostate epithelial cells has recently been published [34]. This similarity supports the relevance of this model to the study of prostate cancer.

In addition to changes in AR signaling that have been described in progression to metastatic disease, there are also marked changes in the IGF-IR. In the initial transformation process, increased expression of the IGF-IR occurs. This initial increase in IGF-IR expression appears to be due, at least in part, to signaling from the AR [6]. However, the IGF-IR can transform cells in the absence of steroid receptors [35]. Some studies have indicated that the increase in IGF-IR expression allows IGF-IR-mediated growth and proliferation signals to predominate over the pro-apoptotic and differentiation pathways that also emanate from the IGF-IR [35]. Once the initial transformation step occurs and the intraprostatic cancer has been established, the level of IGF-IR expression decreases in models of prostate cancer progression [3]. This decrease in IGF-IR expression is accompanied by an increase in autocrine IGF-II production [25]. It is important to note that the decrease in IGF-IR expression does not mean that the IGF-IR is not functional. A number of studies have shown that interruption of the IGF axis in malignant prostate epithelial cell lines results in inhibition of growth. As we and others have shown, the decrease in IGF-IR appears to be an important step in the progression towards metastatic prostate cancer and is associated with an androgen-independent phenotype [3]. Re-expression of the IGF-IR in metastatic prostate cancer cells returns the cells to a less-aggressive phenotype [29,36]. Since recent studies have suggested that expression of the AR in metastatic, AR-negative human prostate epithelial cell lines results in an increase in IGF-IR expression that, in turn, activates AKT and suppresses the apoptotic activity of the AR, in this study we have followed the effects of the IGF system on the AR in a model of prostate cancer progression. The results of this study are consistent with those of previous investigators showing that expression of a wild-type AR in an AR-negative prostate cell line, including normal human and mouse epithelial cells that have been immortalized with either SV40-T or E6/E7 papilloma virus [32,33], resulted in a marked decreased in tumorgenicity whether cells were delivered by s.c. or orthotopic injection. The decrease in tumorgenicity was associated by a delay in passage through the G_1 stage of the cell cycle, with increased p21 and $p27^{kip}$ expression (data not shown). No tumors resulted from s.c. injection of M12-AR PRI cells; however, tumors did develop from the orthotopic injections, albeit with an increased latency period and decreased frequency of tumor

formation. Furthermore, one several of the orthotopic tumors developed diaphragmatic metastases. These metastases were removed, recultured as cell lines, and again injected in the orthotopic position. The latency period and incidence of tumor formation of the metastastic cells and the metastatic sublines returned to that of the original M12 AR-negative cells, suggesting that the cells had reverted to the AR-negative phenotype.

To determine, if there was an interaction between the IGF-IR and AR during progression to metastasis, we assayed AR activity with an AAR_3 reporter construct. Our results were surprising, in that there were both quantitative and qualitative differences in AR activity in primary and metastatic cells. Although there was a quantitative decrease in reporter activity between the contexts, this could not account for the quantitative differences seen between the cells. Further, when the IGF-IR was re-expressed in the metastatic cells to levels seen in the primary intraprostatic tumors, AR activity reverted to that seen in the primary cells. Specifically, in MET cells, IGF-I suppressed AR activity in response to DHT, while, in PRI cells, IGF-I enhanced this response. These findings are consistent with the concept that suppression of the potential differentiating effects of the AR occurs as prostate cancer becomes more aggressive. Further, these data demonstrate that, even though IGF-IR expression is decreased in metastatic prostate cancer, signaling through this receptor still has a functional effect on AR transactivation of androgen response elements.

Since the two major signaling pathways from the IGF-IR have each been shown to affect AR signaling, we examined the effects of these pathways in relation to IGF-IR activation in PRI and MET cells. Cell proliferation experiments revealed that, compared to the PRI cells, MET cells showed significantly increased proliferation whether or not DHT was present. In PRI cells, 10^{-8} and 10^{-10} M DHT were inhibitory to in vitro proliferation, while in MET cells, only 10^{-8} M DHT decreased cell viability. Interestingly, expression of AKT in PRI cells reversed the inhibitory effect of DHT on growth rate, while, in the MET cells, (dn)AKT had no effect. The decrease in proliferation in response to androgen is similar to the reported effects of androgen in AR-transfected PC-3 cells, as well as the effects of androgen administered to androgen-starved LnCaP cells [37–39].

DHT-activated AR activity was significantly greater in PRI cells than MET cells. DHT causes reduced cell growth and high induction of AR activity in the PRI cells, suggesting that DHT is causing genes in the proliferative shutoff pathway to be activated. Because DHT is less effective in activating the AR and inhibiting cell growth in the MET cells, it is possible that the AR is not as active in the MET cells. We are presently profiling which genes are turned on by DHT and AKT in PRI and MET cells.

We also examined the effect of PI3K inhibitors on AR activity. AKT alone has been demonstrated to increase the activity of the AR [40,41]. Although, we did observe an increase in AR activity after 24 hr of AKT expression in both the PRI and MET cells, the effect of AKT was not significant. In the PRI cells, AKT significantly increased DHT induced AR activity, while (dn)AKT and LY29004 significantly decreased DHT-induced AR activity. Because AKT increases AR activity and abolishes the reduction in cell growth observed with DHT, it is plausible that AKT, in the presence of DHT, increases AR activity, resulting in expression of proliferative genes rather than the induction of apoptotic genes associated with DHT alone. We are currently investigating this possibility. AKT also phosphorylates the AR at various sites [6,42] and it would be interesting to determine whether phosphorylation differs under different conditions. The results observed in PRI cells contrast with those observed in MET cells, where, in the presence of DHT, AKT caused a significant decrease in AR promoter activity, while (dn)AKT and LY294002 caused a significant increase in AR activity. Thus, it appears that, in the MET cells, AKT decreases cell proliferation and also decreases DHT-induced AR activity.

It appears that, in the PRI cells, AKT causes an increase in cell viability and also enhances AR activity, resulting in increased proliferation. However, the MET cells do not appear to respond to AKT or DHT with any significant change in cell viability; if anything, AKT appears to inhibit cell growth. Thus, it is interesting that AKT, which normally causes cell proliferation, is significantly increased in the MET cells, but does not appear to cause increased cell growth. One would assume that other pathways are active in the MET cells causing the significant increase in cell proliferation.

In contrast to the effects of AKT in the PRI cells, inhibition of the ERK pathway enhances signaling through the AR. This result is similar to that reported by Bakin et al. [9], in which attenuation of Ras signaling restored androgen sensitivity to AR-positive, but not hormone-refractory, LnCaP C4-2 cells. However, in the MET cells, inhibition of the ERK pathway resulted in a decrease in AR activity. This finding suggests that enhanced AR signaling through ERK is involved in the progression of prostate cancer. This is consistent with data from other studies. It also suggests that, in contrast to recent data on C4-2 cells and in contrast to the effects on the PRI cells, inhibition of ERK in MET cells can no longer return the cells to an androgen-sensitive state. Re-expression of the IGF-IR in the PRI line appears to further enhance AR signaling following inhibition of

the ERK pathway, but had no significant effects on the MET cells.

Since the AR is a transcription factor, we would expect to see differences between primary and metastatic tumors in gene expression following manipulation of the IGF signaling pathway. We elected to inhibit the PI3K pathway, since this pathway has been reported to alter IGF-IR signaling when activated through the IGF-IR. As we demonstrated, inhibition of AKT signaling resulted in differential expression of a subset of AR-regulated genes. We specifically selected from the array genes that are known to have an androgen response element in their promoter, e.g., kallikrein 3 (PSA), ets homologous factor, TMPRSS2, or genes that have been demonstrated to vary their expression either directly or indirectly in response to androgen. The array data substantiate that the context in which the AR is expressed results in alterations of AR signaling.

These studies have shown that there are interactions between changes in IGF-IR expression and AR activity. Since we have demonstrated that the changes occurred in the context of primary intraprostatic tumor compared to metastatic lesions, and that they were associated with the changes that have been described clinically for the IGF-IR in progression to metastasis, we suggest that signaling through the IGF-IR changes during progression to metastasis and may be involved in the dysregulation of the AR that results in its change from a differentiation and growth regulator in normal prostate to an oncogene and metastasis inducer in aggressive prostate cancer.

REFERENCES

1. Weir H, Thun M, Hankey B, Ries L, Howe H, Wingo P. Annual report to the nation on the status of cancer, 1975–2000, featuring the uses of surveillance data for cancer prevention and control. J Natl Cancer Inst 2003;95:1276–1299.
2. Tennant M, Thrasher J, Twomey P, Drivdahl R, Birnbaum R, Plymate S. Protein and messenger ribonucleic acid (mRNA) for the type 1 insulin-like growth factor (IGF) receptor is decreased and IGF-II mRNA is increased in human prostate carcinoma compared to benign prostate epithelium. J Clin Endocrinol Metab 1996;81:3774–3782.
3. Kaplan P, Mohan S, Cohen P, Foster B, Greenberg N. The insulin-like growth factor axis and prostate cancer: Lessons from the transgenic adenocarcinoma of mouse prostate (TRAMP) model. Cancer Res 1999;59:2203–2209.
4. Denmeade S, Lou W, Logren J, Malm J, Lilja H, Isaacs J. Specific and efficient peptide substrates for assaying the proteolytic activity of prostate-specific antigen. Cancer Res 1997;57:4924–4930.
5. Litvinov I, De Marzo A. Is the Achilles' heel for prostate cancer therapy a gain of function in androgen receptor signaling? J Clin Endocrinol Metab 2003;88:2972–2982.
6. Lin H, Yeh S, Kang H, Chang C. Akt suppresses androgen-induced apoptosis by phosphorylating and inhibiting androgen receptor. PNAS 2001;98:7200–7205.
7. Gioeli D, Ficarro S, Kwiek J, Aaronson D, Hancock M, Catling A, et al. Androgen receptor phosphorlyation: Regulation and identification of the phosphorylation sites. J Biol Chem 2002; 277:29304–29314.
8. Li P, Nicosia SV, Bai W. Antagonism between PTEN/MMAC1/TEP-1 and androgen receptor in growth and apoptosis of prostatic cancer cells. J Biol Chem 2001;M010226200.
9. Bakin R, Gioeli D, Bissonette E, Weber M. Attenuation of Ras signaling restores androgen sensitivity to hormone-refractory C4-2 prostate cancer cells. Cancer Res 2003;63:1975–1980.
10. Culig Z, Hobisch A, Cronauer M, Radmayr J, Hittmair A, Bartsch G, et al. Androgen receptor activation in prostatic tumor cell lines by insulin-like growth factor-I, keratinocyte growth factor, and epidermal growth factor. Cancer Res 1994;54:5474–5478.
11. Kollara A, Diamandis E, Brown T. Secretion of endogenous kallikreins 2 and 3 by androgen receptor-transfected PC-3 prostate cancer cells. J Steroid Biochem Mol Biol 2003;84: 493–502.
12. Reid K, Hendy S, Saito J, Sorenson P, Nelson C. Two classes of androgen receptor elements mediate cooperativity through allosteric interactions. J Biol Chem 2001;276:2943–2952.
13. Graff JR, Konicek BW, McNulty AM, Wang Z, Houck K, Allen S, et al. Increased AKT activity contributes to prostate cancer progression by dramatically accelerating prostate tumor growth and diminishing p27Kip1 expression. J Biol Chem 2000;275(32): 24500–24505.
14. Aguirre-Ghiso J, Estrada Y, Liu D, Ossowski L. ERK(MAPK) activity as a determinant of tumor growth and dormancy; regulation by p38(SAPK). Cancer Res 2003;63:1684–1695.
15. Drew L, Fine R, Raffo A, Petrylak D. Sustained activation of extracellular signal-regulated kinase (ERK) signaling in human prostate cancer LNCaP cells depleted of androgen. Prostate 2001;3:105–117.
16. Bae V, Jackson-Cook C, Maygarden S, Edelman W, Brothman A, Chen J, et al. A new model for cytogenetic analysis of human prostate cancer progression and metastasis. Proc Am Assoc Cancer Res 1995; Cancer Res 36:642 (abstract).
17. Bae V, Jackson-Cook C, Maygarden S, Chen J, Plymate S, Ware J. Metastatic sublines of an SV40 large T antigen immortalized human prostate epithelial cell line. Prostate 1998;34:275–282.
18. Tilley W, Marcelli M, Wilson J, McPhaul M. Characterization and expression of a cDNA encoding the human androgen receptor. Proc Natl Acad Sci USA 1989;86:327–331.
19. Stephenson R, Dinney C, Gohji K, Ordonez N, Killion J, Fidler I. Metastatic model for human prostate cancer using orthotopic implantation in nude mice. J Natl Cancer Inst 1992;17:951–957.
20. Plymate S, Bae V, Maddison L, Quinn L, Ware J. Type-1 insulin-like growth factor receptor re-expression in the malignant phenotype of SV40-T-immortalized human prostate epithelial cells enhances apoptosis. Endocrine 1997;7:1–6.
21. Snoek R, Rennie P, Kaspar S, Matusik R, Bruchovsky N. Induction of cell-free, in vitro transcription by recombinant androgen receptor peptides. J Steroid Biochem Mol Biol 1996; 59:243–250.
22. Damon S, Plymate S, Carroll J, Sprenger C, Dechsukhum C, Ware J, et al. Transcriptional regulation of insulin-like growth factor-I receptor gene expression in prostate cancer cells. Endocrinology 2001;142:21–27.
23. Hawkins V, Doll D, Bumgarner R, Smith T, Abajian C, Hood L, et al. PEDB: The prostate expression database. Nucleic Acids Res 1999;27(1):204–208.

24. Lin B, White J, Ferguson C, Bumgarner R, Friedman C, Trask B, et al. Part-1: A novel human prostate-specific androgen regulated gene that maps to chromosome 5q12 1. Cancer Res 2000; 60:858–863.
25. Guo N, Ye J, Liang S, Mineo R, Li S, Giannini S, et al. The role of insulin-like growth factor-II in cancer growth and progression evidenced by the use of ribozymes and prostate cancer progression models. Growth Horm IGF Res 2003;13: 44–53.
26. Plymate S, Haugk K, Sprenger C, Nelson P, Tennant M, Zhang Y, et al. Increased manganese superoxide dismutase (SOD-2) is part of the mechanism for prostate tumor suppression by Mac25/ insulin-like growth factor binding-protein-related protein-1. Oncogene 2003;22:1024–1034.
27. Sprenger C, Tennant M, Arnold H, Nelson P, Vail M, Plymate S. Insulin-like growth factor binding protein-related protein-1 (IGFBP-rP1/mac25) induction of cell-cycle arrest depends on expression of a senescence-associated cell phenotype. 83rd Annual Meeting of the Endocrine Society, Denver, CO, abstract, 2001.
28. Sprenger C, Damon S, Hwa V, Rosenfeld R, Plymate S. Insulin-like growth factor binding protein-related protein 1 (IGFBPrP1) is a potential tumor suppressor protein for prostate cancer. Cancer Res 1999;59:2370–2375.
29. Plymate S, Bae V, Madison L, Quinn L, Ware J. Re-expression of the type 1 insulin-like growth factor receptor inhibits the malignant phenotype of simian virus 40 T antigen immortalized human prostate epithelial cells. Endocrinology 1997;138:1728–1735.
30. Kaplan P, Mohan S, Cohen P, Foster B, Greenberg N. The insulin-like growth factor axis and prostate cancer: Lessons from the transgenic adenocarcinoma of mouse prostate (TRAMP) model. Cancer Res 1999;59:2203–2209.
31. Pennisi P, Barr V, Nunez N, Stannard B, LeRoith D. Reduced levels of IGF-IR in MCF-7 breast cancer cells leads to a more metastatic phenotype. 84th Annual Meeting of the Endocrine Society 2002:P1–P294.
32. Choo C, Ling M, Chan K, Tsao S, Zheng Z, Zhang D, et al. Immortalization of huan prostate epithelial cells by HPV 16 E6/ E7 open reading frames. Prostate 1999;40:150–158.
33. Whitacre D, Chauhan S, Davis T, Gordon D, Cress A, Miesfeld R. Androgen induction of in vitro prostate cell differentiation. Cell Growth Differ 2002;13:1–11.
34. Glinsky G, Krones-Herzig A, Glinskii A, Gebauer G. Microarray analysis of xenograft-derived cancer cell lines representing multiple experimental models of human prostate cancer. Mol Carcinog 2003;37:209–221.
35. Liu C, Adamson E, Mercola D. Transcription factor EGR-1 suppresses the growth and transformation of human HT-1080 fibrosarcoma cells by induction of transforming growth factor β1. Proc Natl Acad Sci 1996;93:11831–11836.
36. Baserga R. The contradictions of the insulin-like growth factor I receptor. Oncogene 2000;19:5574–5581.
37. Geck P, Szelei J, Jimenez J, Tien-Min L, Sonnenschein C, Soto A. Expression of novel genes linked to the androgen-induced, proliferative shutoff in prostate cancer cells. J Steroid Biochem Mol Biol 1997;63:211–218.
38. Geck P, Stagon L, Sonnenschein C, Soto A. AS3, a negative regulator of androgen-induced proliferative arrest in prostate cells. Am Assoc Cancer Res 2000;44(57):9.
39. Yuan S, Trachtenberg J, Mills G, Brown T, Xu F, Keating A. Androgen-induced inhibition of cell proliferation in an androgen-insensitive prostate cancer cell line (PC-3) transfected with a human androgen receptor complementary DNA. Cancer Res 1993;53:1304–1311.
40. Wen Y, Hu MC-T, Makino K, Spohn B, Bartholomeusz G, Yan D-H, et al. HER-2/neu promotes androgen-independent survival and growth of prostate cancer cells through the Akt pathway. Cancer Res 2000;60(24):6841–6845.
41. Datta S, Brunet A. Cellular survival: A play in three Akts. Genes Dev 1999;13:2905–2927.
42. Lin H, Wang L, Hu Y, Altuwaijri S, Chang C. Phosohorylation-dependent ubiquitylation and degradation of androgen receptor by Akt require Mdm2 E3 ligase. Embo J 2002;21:4037–4048.

The Gene Expression Program of Prostate Fibroblast Senescence Modulates Neoplastic Epithelial Cell Proliferation through Paracrine Mechanisms

Claes Bavik,[1] Ilsa Coleman,[1] James P. Dean,[1,2] Beatrice Knudsen,[3] Steven Plymate,[4] and Peter S. Nelson[1,2]

Divisions of [1]Human Biology, [2]Clinical Research, and [3]Public Health Sciences, Fred Hutchinson Cancer Research Center; [4]Department of Medicine, University of Washington, Seattle, Washington

Abstract

The greatest risk factor for developing carcinoma of the prostate is advanced age. Potential molecular and physiologic contributors to the frequency of cancer occurrence in older individuals include the accumulation of somatic mutations through defects in genome maintenance, epigenetic gene silencing, oxidative stress, loss of immune surveillance, telomere dysfunction, chronic inflammation, and alterations in tissue microenvironment. In this context, the process of prostate carcinogenesis can be influenced through interactions between intrinsic cellular alterations and the extrinsic microenvironment and macroenvironment, both of which change substantially as a consequence of aging. In this study, we sought to characterize the molecular alterations that occur during the process of prostate fibroblast senescence to identify factors in the aged tissue microenvironment capable of promoting the proliferation and potentially the neoplastic progression of prostate epithelium. We evaluated three mechanisms leading to cell senescence: oxidative stress, DNA damage, and replicative exhaustion. We identified a consistent program of gene expression that includes a subset of paracrine factors capable of influencing adjacent prostate epithelial growth. Both direct coculture and conditioned medium from senescent prostate fibroblasts stimulated epithelial cell proliferation, 3-fold and 2-fold, respectively. The paracrine-acting proteins fibroblast growth factor 7, hepatocyte growth factor, and amphiregulin (AREG) were elevated in the extracellular environment of senescent prostate fibroblasts. Exogenous AREG alone stimulated prostate epithelial cell growth, and neutralizing antibodies and small interfering RNA targeting AREG attenuated, but did not completely abrogate the growth-promoting effects of senescent fibroblast conditioned medium. These results support the concept that aging-related changes in the prostate microenvironment may contribute to the progression of prostate neoplasia. (Cancer Res 2006; 66(2): 794-802)

Introduction

Clinical prostate cancer is extremely rare in men ages <40, occurring with a frequency of 1 in 10,000 individuals (1). Unfortunately, the incidence increases dramatically over the ensuing decades to represent the most common noncutaneous malignancy in men >60 years of age, with a one-in-seven chance of cancer detection between ages 60 and 79 years. This relationship between prostate cancer incidence and aging is consistent across ethnic and racial groups. The prevalence of latent or indolent prostate carcinoma also increases in a dramatic fashion with aging. Sakr et al. (2) systematically examined prostate glands from young males and identified prostatic intraepithelial neoplasia in 0%, 9%, 20%, and 44%, and foci of histologic cancer in 0%, 0%, 27%, and 34% in the second, third, fourth, and fifth decades of age, respectively. Understanding the factors influencing the progression of these cancers to invasive and lethal forms represents an active area of research. Although secondary and tertiary events in the initiated epithelium contribute cellular characteristics driving neoplastic progression, it is also apparent that reactive or aging-related alterations in the tumor microenvironment provide necessary or sufficient influences that promote tumor cell invasion and metastasis.

The host microenvironment is increasingly viewed as an important active contributor to tumor growth and tumor suppression. Sternlicht et al. (3) reported that manipulation of the microenvironment through overexpression of stromelysin 1 could produce carcinomas derived from the adjacent parenchymal cells. Malignant breast epithelial cells can be epigenetically reprogrammed to a near-normal morphology with the appropriate microenvironment *in vitro* (4, 5). Conversely, morphologically normal breast tissue can exhibit invasive growth *in vivo* through alterations in the stromal environment (6). Exposure of mammary gland stroma to irradiation or carcinogens has been shown to promote tumor formation by nontumorigenic breast epithelial cells (7, 8), whereas normal breast stroma does not support tumorigenesis. Thus, the microenvironment provided by the stroma can be a powerful suppressor—or promoter—of malignant epithelial phenotypes caused by oncogenic mutations. In the context of prostate cancer, elegant studies by Olumi et al. (9) have shown that nontumorigenic prostate epithelial cells can become tumorigenic when cocultured with fibroblasts obtained from regions near tumors. Inactivation of the transforming growth factor-β (TGF-β) type II receptor gene in mouse fibroblasts resulted in intraepithelial neoplasia in the prostate and invasive cancers of the forestomach (10), a finding that further supports the important role of stroma in the process of carcinogenesis.

There is substantial evidence that aging-related changes can influence stromal-epithelial interactions leading to an environment permissive for neoplastic growth. Cellular senescence represents an aging-associated process and senescent cells accumulate in tissues with age (11, 12). Although senescent and tumor-associated

Note: C. Bavik is a Pacific Northwest Prostate Cancer Specialized Programs of Research Excellence fellow.

Requests for reprints: Peter S. Nelson, Division of Human Biology, Fred Hutchinson Cancer Research Center, Mailstop D4-100, 1100 Fairview Avenue North, Seattle, WA 98109-1024. Phone: 206-667-3377; Fax: 206-685-7344; E-mail: pnelson@fhcrc.org.

doi:10.1158/0008-5472.CAN-05-1716

reactive fibroblasts differ in growth potential and morphology, they share the ability to stimulate the proliferation and invasive behavior of initiated epithelial cells through direct contact or secreted factors. Work by Krtolica et al. (13) has shown the ability of senescent human fibroblasts to promote the growth and tumorigenesis of premalignant and malignant breast epithelial cells, a finding that provides a mechanistic link between stromal aging and carcinogenesis.

In this study, we sought to characterize the molecular alterations that occur during the process of prostate fibroblast senescence to identify factors in the aged tissue microenvironment capable of promoting the proliferation and potentially the neoplastic progression of prostate epithelium. We evaluated three mechanisms leading to cell senescence (i.e., oxidative stress, DNA damage, and replicative exhaustion) and identified a common and consistent program of gene expression that includes a subset of paracrine factors capable of influencing adjacent prostate epithelial growth. These results support the concept that aging-related changes in the prostate microenvironment may contribute to the genesis and progression of prostate neoplasia.

Materials and Methods

Cell culture. The methods for isolating and propagating the primary human prostate stromal cells used in this study were described previously (isolates PSC27, PSC31, and PSC36; ref. 14). Briefly, tissues from benign areas of radical prostatectomy specimens were collected under approval by the institutional review board. Stromal cells were cultured in PSC medium [80% MCDB131 (Invitrogen, Carlsbad, CA) supplemented with 10% FCS, nonessential amino acids, insulin, dexamethasone, transferrin, selenium, and 20% AmnioMax (Life Technologies, Carlsbad, CA)], and routinely subcultured 1:8. The human prostatic epithelial cell line BPH1 was derived from nonmalignant prostatic tissue with benign hyperplasia and immortalized by transfection with SV40-large T antigen and has been described previously (15). BPH1 cells were cultured in DMEM + 10% fetal bovine serum (FBS) at 37°C and 5% CO_2 until 80% to 100% confluent and routinely subcultured 1:8. The neoplastic metastatic M12 human prostate epithelial cell line and culture conditions have been described previously (16). BPH1 and M12 cells were transfected with pIRES2-EGFP (BD Bioscience, Palo Alto, CA) using LipofectAMINE 2000 (Invitrogen) according to the recommendations of the manufacturer. The cells were passaged 1:10 the next day into fresh medium and subsequently flow sorted in a FACSVantage (Becton Dickinson, Palo Alto, CA) with selection for green fluorescent protein (GFP) expression. Positive cells were seeded into DMEM + 10% FCS, expanded, and stored frozen in liquid nitrogen. These sublines were designated BPH1-GFP2 and M12-GFP2 and routinely subcultured under the same culture conditions as the parental cells. Human prostate epithelial cell lines DU145 and PC3 were routinely subcultured under the same culture conditions as BPH1 and used without modifications.

Senescence induction. Normal human prostate stromal cells (PSC27, PSC31, and PSC36) were grown in PSC medium until 80% confluent. The cells were then treated for 2 hours at 37°C with 1 mmol/L hydrogen peroxide (H_2O_2) as described by Chen et al. (17) or overnight with 100 μg/mL bleomycin in PSC medium. After treatment, the cells were rinsed thrice with PBS and left to recover 3 days in PSC medium. Following recovery, cells were designated PSC27ASB (PSC27 accelerated senescence by bleomycin), PSC27ASH (PSC27 accelerated senescence by H_2O_2), or PSC27N (presenescent PSC27). Hydrogen peroxide and bleomycin sulfate were purchased from Sigma-Aldrich Biotechnology LP (St. Louis, MO).

To generate cells at replicative senescence, PSC27 cells were cultured until cell doubling time >2 weeks (~45 cell doublings). At this time, the cells were considered to have reached replicative exhaustion and designated PSC27RS. Induction of senescence was verified by measuring the increase in senescence-associated β-galactosidase (β-Gal) activity essentially as described previously (11). Briefly, cells were washed in PBS and fixed 3 minutes in 10% neutral buffered formalin (Sigma, St. Louis, MO). The fixed cells were then washed in PBS and stained overnight in 1 mg/mL 5-bromo-4-chloro-3-indolyl β-D-galactoside, 40 mmol/L citric acid/sodium phosphate (pH 6.0), 5 mmol/L potassium ferricyanide, 5 mmol/L potassium ferrocyanide, 150 mmol/L NaCl, and 2 mmol/L $MgCl_2$. Expression of the β-Gal transcript was also quantified by PCR (see below).

***In vitro* cocultures of epithelium and fibroblasts.** BPH1-GFP2 cells were mixed with various proportions of PSC27N, PSC27ASB, PSC27ASH, or PSC27RS using cell numbers previously determined to form confluent lawns of fibroblasts in six-well plates. The fibroblast ratios were as follows: 100% PSC27N, 10% PSC27ASB/90% PSC27N, 30% PSC27ASB/70% PSC27N, 100% PSC27ASB, 10% PSC27ASH/90% PSC27N, 30% PSC27ASH/70% PSC27N, 100% PSC27ASH, 10% PSC27RS/90% PSC27N, 30% PSC27RS/70% PSC27N, and 100% PSC27RS. Each cell mixture was seeded in a six-well plate (20,000 BPH1-GFP2 cells per well) in DMEM with 0.5% FBS. The cultures were incubated for 3 days after which cells were detached with trypsin and the total cell number was determined by direct counting in a hemacytometer. The PSC/BPH1-GFP2 proportion was determined on a FACScan (Becton Dickinson) using GFP fluorescence as a marker for BPH1-GFP2 cells. M12-GFP cells were mixed with PSC27N or PSC27ASH to form confluent lawns of fibroblasts in six-well plates and analyzed as above. The means of the cell quantitation results from each experimental condition were compared using a two-sample Student's t test assuming unequal variances.

Culture of neoplastic prostate epithelial cells with senescent fibroblast conditioned medium and amphiregulin. Confluent cultures of PSC27N, PCS27ASB, PSC27ASH, and PSC27RS were rinsed thrice in PBS and incubated for 3 days in DMEM + 0.5% FCS. The supernatant was harvested and stored frozen at −80°C. Conditioned medium was thawed and diluted 1:1 with fresh DMEM + 0.5% FCS before use. BPH1-GFP2, DU145, or PC3 cells were seeded at 20,000 per well in six-well plates in conditioned medium or fresh DMEM + 0.5% FCS. The cultures were incubated for 3 days and the total number of cells was determined by direct counting in a hemacytometer.

To evaluate the effect of amphiregulin (AREG) on prostate epithelial cell growth, 20,000 BPH1-GFP2 cells were seeded per well in six-well plates in DMEM + 0.5% FCS containing increasing concentrations of AREG (0, 10^{-9}, and 10^{-8} mol/L). The cultures were incubated for 3 days and the cell numbers were quantitated. Separately, 20,000 BPH1-GFP2 cells were seeded per well in six-well plates in PSC27ASH and PSC27N-conditioned medium containing 100 ng/mL neutralizing anti-AREG antibodies (mouse monoclonal antihuman AREG IgG, MAB262; R&D Systems, Inc., Minneapolis, MN) or control mouse IgG. The cultures were incubated for 3 days, and the cell numbers were quantified by 3-(4,5-dimethylthiazol-2-yl)-2,5-diphenyltetrazolium bromide assay.

Quantitative reverse transcription-PCR. Total cellular RNA was isolated from cultured cells using the TRIzol reagent (Invitrogen) and 2 μg of total RNA was reverse transcribed using SuperScriptII Reverse Transcriptase (Invitrogen) according to the recommendations of the manufacturer. The RNA was then hydrolyzed 15 minutes at 65°C in 0.20 mol/L NaOH and 0.10 mol/L EDTA before neutralization with 0.33 mol/L Tris (pH 7.4). The cDNA was purified with a Qiagen (Valencia, CA) PCR clean-up column according to the recommendations of the manufacturer.

Primers specific for the genes of interest were designed using the web-based primer design service Primer3 provided by the Whitehead Institute for Biomedical Research (http://fokker.wi.mit.edu/cgi-bin/primer3/primer3_www.cgi). Before quantitative PCR analysis, the suitability of the PCR primers were examined using normal human prostate cDNA, Biolase Taq polymerase (Bioline, Foster City, CA), and the GeneAmp PCR system 9700 (Applied Biosystems, Randolph, MA). Briefly, 1 ng template cDNA was amplified with 0.3 μmol/L primers in 30 cycles of 94°C (15 seconds), 60°C (30 seconds), and 72°C (30 seconds). The PCR products were analyzed on a 4% agarose gel in 1× TAE with 5 μL 10 mg/mL ethidium bromide per 100 mL gel. The following primer pairs generated strong unique PCR products of the appropriate lengths and were selected for use in quantitative PCR reactions. Human glyceraldehyde-3-phosphate dehydrogenase (GAPDH; control):

ACTTCAACAGCGACACCCACTC (forward primer) and CACCCTGTTGCTGTAGCCAAA (reverse primer). Human β-actin (control): AAGGAGAATGGCCCAGTCCT (forward primer) and TGCTATCACCTCCCCTGTGTG (reverse primer). Human α-tubulin (control): GGTGACGTGGTTCCCAAAGA (forward primer) and GGTTTTGATGGTGGCAATGG (reverse primer). Human β-Gal: TTAGGATGTGCATTTTCACCTGA (forward primer) and CTTTGGCACTGCAGGGATG (reverse primer). Human manganese superoxide dismutase 2 (MnSOD2): ACTGCAAGGAACAACAGGCC (forward primer) and TCCCACACATCAATCCCCA (reverse primer). Human AREG: TGGATTGGACCTCAATGACA (forward primer) and AGCCAGGTATTTGTGGTTCG (reverse primer). Human fibroblast growth factor 7 (FGF7): CTGAGGATCGATAAAAGAGGCAA (forward primer) and ATTCTTCATCTCTTGGGTCCCTT (reverse primer). Human hepatocyte growth factor (HGF): GTTCCTGGTCGTGGATGTGC (forward primer) and TCGGACAAAAATACCAGGACG (reverse primer). Relative quantification of gene expression by quantitative PCR (40 cycles of 60°C annealing, 72°C extension and 95°C melting) was done on a 7700 Sequence Detector (ABI, Foster City, CA) using SYBR Green Master mix (ABI) and gene-specific primers according to the recommendations of the manufacturer.

cDNA microarray analysis. Custom Prostate Expression Database cDNA microarrays were constructed as previously described (18) using clones derived from the Prostate Expression Database, a sequence repository of human prostate expressed sequence tag data available to the public (www.pedb.org; ref. 19). A second microarray was constructed using ~17K cDNAs chosen from the Research Genetics sequence-verified set of IMAGE clones. The inserts of individual cDNA clones were amplified by PCR, purified, and spotted in duplicate onto glass microscope slides (Gold Seal, Becton Dickinson) with a robotic spotting tool (GeneMachine OmniGrid 100). Probes were generated from the PSC27, PSC31, and PSC36 prostate fibroblast cultures at steady state and following induction of senescence. Labeling with Cy3 and Cy5 fluorescent dyes and hybridization to the microarray slides were essentially as described (20).

Fluorescent array images were collected for both Cy3 and Cy5 using a GenePix 4000 B fluorescent scanner (Axon Instruments, Foster City, CA). The image intensity data were gridded and extracted using GENEPIX PRO 4.1 software (Axon Instruments), and spots of poor quality determined by visual inspection were removed from further analysis. All three stromal cell lines (PSC27, PSC31, and PSC36) and three senescence-inducing treatments [H_2O_2 treatment (ASH), bleomycin treatment (ASB), and replicative exhaustion (RS)] were hybridized against untreated controls to the Prostate Expression Database array. Each of these experiments was repeated with a switch in fluorescent labels to account for dye effects. The three cell lines treated with ASH were also hybridized to the human 17K microarray. Normalization of the Cy3 and Cy5 fluorescent signal on each array was done using Silicon Genetics GeneSpring 6.2 software (Silicon Genetics, Redwood City, CA) A print tip–specific Lowess curve was fit to the log-intensity versus log-ratio plot and 20.0% of the data was used to calculate the Lowess fit at each point. This curve was used to adjust the control value for each measurement. If the control channel was lower than 10, then 10 was used instead. Data were filtered to remove values from poorly hybridized cDNAs with average foreground minus background intensity levels <300. Data from the two duplicate cDNAs spots on each Prostate Expression Database chip as well as the duplicate arrays were combined and the average ratios were used for comparative analyses. Ratios were filtered to include only clones whose expression was measurable in at least 75% of the samples. Differences in gene expression associated with senescence were determined using the significance analysis of microarray procedure (http://www-stat.stanford.edu/~tibs/SAM/; ref. 21). A one-sample t test was used to determine whether the mean gene expression of all cell lines and all treatments differed from zero. Gene expression differences with a false discovery rate of ≤1% were considered significant. A multiclass test (one-way ANOVA) in Significance Analysis of Microarray was used to assess the differences between cell isolates.

Western blot analysis. Confluent cultures of PSC27N, PSC27ASH, PSC31N, and PSC31ASH in T150 flasks were rinsed thrice with PBS and the cultures were incubated for 3 days in DMEM with 0.5% FBS. The supernatant was harvested and stored frozen at −80°C. The protein was concentrated before SDS-PAGE by trichloroacetic acid precipitation as follows: 1 mL conditioned medium was precipitated for 1 hour on ice with 10% final trichloroacetic acid concentration. The tube was spun in microcentrifuge at 14,000 rpm for 45 minutes at 4°C. The supernatant was removed and the pellet was washed with 1 mL cold acetone. The centrifugation and acetone wash was repeated. After drying, the sample was dissolved in loading buffer, reduced by boiling with 1% DTT for 5 minutes, and separated on a NuPAGE MES 4% to 12% gel (Invitrogen) according to the instructions of the manufacturer. Purified recombinant human AREG (R&D Systems) was included as a positive control at quantities of 0.1 and 0.02 μg. The separated proteins were transferred to nitrocellulose membranes (Invitrogen) in a trans-blot semidry transfer cell (Bio-Rad, Hercules, CA). Nonspecific protein binding to the nitrocellulose membranes was saturated over night with 3% dry milk, 2% bovine serum albumin, and 0.1% Tween 20 in PBS (Blotto). The filters were then blotted with antibodies to AREG, FGF7 (R&D Systems), or HGF (Sigma) in Blotto for 3 hours at room temperature. Adhered primary antibodies were visualized with horseradish peroxidase–conjugated ImmunoPure secondary antibodies (Pierce, Rockford, IL) and the SuperSignal West Pico Staining system (Pierce) according to the instructions of the manufacturer. Western blot analysis was repeated with a second antibody recognizing AREG (AF262, R&D Systems).

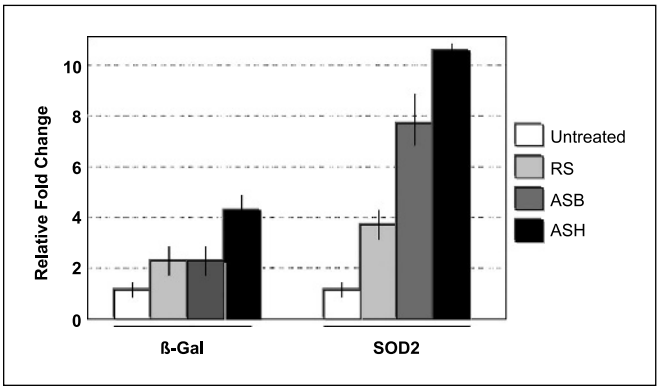

Figure 1. Induction and quantitation of prostate fibroblast senescence. RNA harvested from PSC27N, PSC27ASH, PSC27ASB, and PSC27RS cells was used as template for qRT-PCR measurements of transcripts encoding β-Gal and MnSOD2. GAPDH transcripts were quantified as an internal standard. Data are normalized so that relative expression of β-Gal and SOD2 in untreated cells equals 1.

RNA interference. An small interfering RNA (siRNA) duplex targeting the AREG mRNA and a GL2 control were designed according to previously published methods (22) and purchased from Integrated DNA Technologies (Coralville, IA; www.idtdna.com). Sequences of the siRNA used were CCACAAAUACCUGGCUATAdTdT (AREG) and CGUACGCGGAAUACUUCGAdTdT (GL2 control). The 21-nucleotide siRNA duplexes were transfected into prostate fibroblasts using OligofectAMINE (Invitrogen) according to the instructions of the manufacturer. Transfected cells were used 3 days after transfection.

Results

Induction of prostate fibroblast senescence. Several factors have been shown to induce a phenotype of cellular senescence (23, 24). In this study, we evaluated three senescence mechanisms that prostate fibroblasts could reasonably encounter in their natural environment: oxidative stress (17), DNA damage due to chemotherapy exposure (25), and replicative exhaustion (26). We studied three independent primary prostate stromal cell isolates (PSC27, PSC31, and PSC32) to determine both the consistency and variability of the phenotypic and gene expression features of the senescence program in this cell type. To verify a senescence phenotype associating with

each mechanism, we visually inspected cell cultures for morphologic features of senescence and measured expression of β-Gal by quantitative reverse transcription-PCR (qRT-PCR) and by staining at pH 6 (SA-β-Gal; ref. 11).

Primary prostate fibroblast isolates were treated with 1 mmol/L H_2O_2, 100 μg/mL bleomycin, or grown to replicative senescence. Morphologic changes previously associated with senescence, including cell enlargement and flattening, were clearly apparent (11, 13). SA-β-Gal staining was not observed in presenescent cell cultures but was readily visualized following each of the three treatments (data not shown). To provide a more quantitative measure, β-Gal and SOD2 transcripts were analyzed by qRT-PCR before and after treatments and compared relative to *GAPDH* gene expression. β-Gal expression increased 4.3-fold after ASH, 2.8-fold after ASB, and 2.3-fold in RS, relative to low-passage presenescent cells (Fig. 1). To ensure that these changes were due to senescence and not growth quiescence, PSC27 and PSC31 fibroblast isolates were cultured to confluence and further incubated 7 days under normal culture conditions. The quiescent PSC27 and PSC31 did not exhibit increases in β-Gal mRNA or SA-β-Gal staining compared with proliferating cells (data not shown).

The transcriptional program of prostate fibroblast senescence. To characterize common and unique features of the senescence program in prostate fibroblasts, we used cDNA microarray analysis to quantitate transcript abundance levels

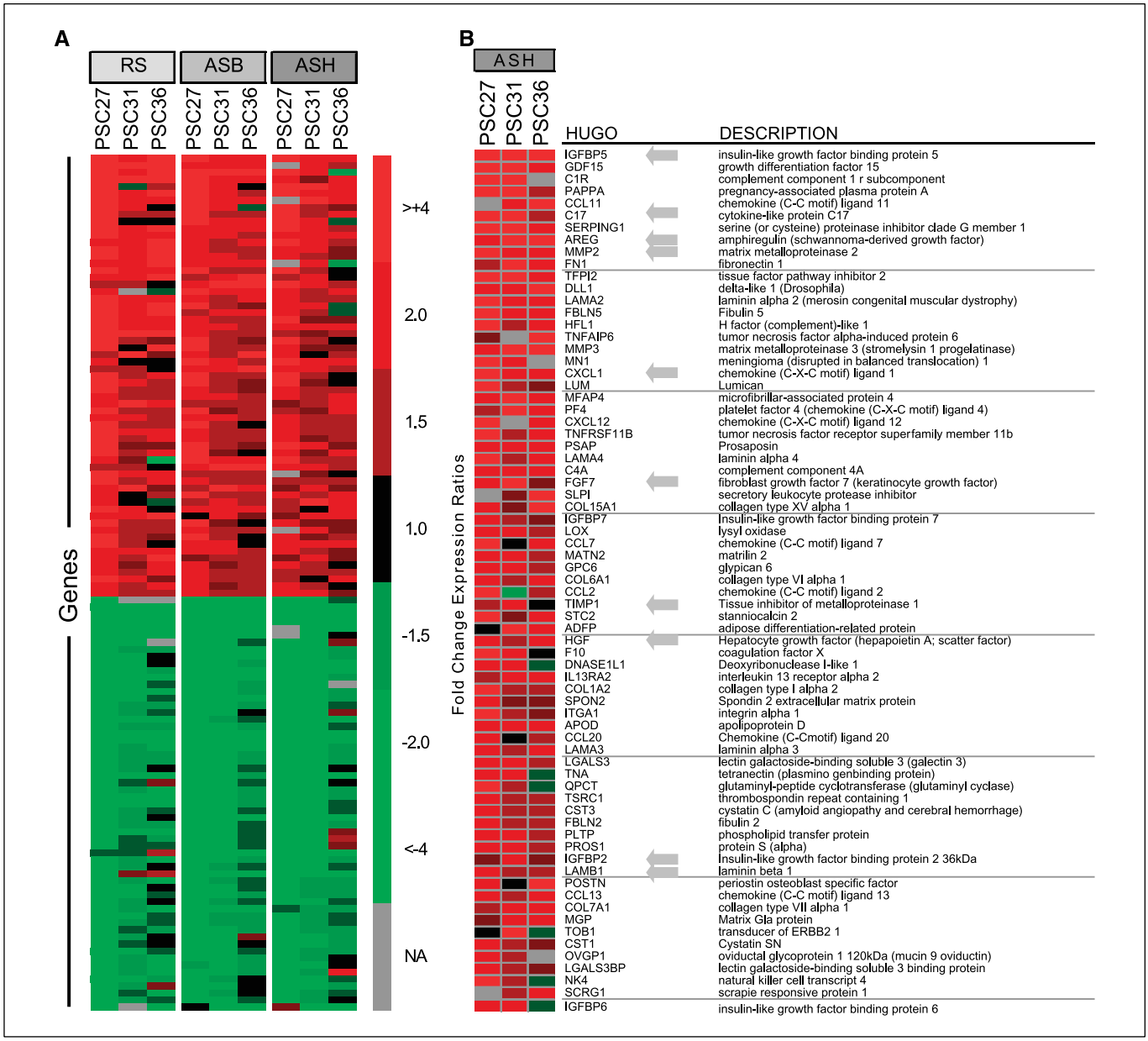

Figure 2. cDNA microarray analysis of gene expression changes associated with prostate fibroblast senescence. *A,* three primary prostate fibroblast isolates (PSC27, PSC31, and PSC36) were compared between presenescent and postsenescent states induced by three different mechanisms: ASH, ASB, and RS. Hierarchical clustering of consistent transcript alterations (false discovery rate <1%) across cell isolates and treatments. *B,* transcripts encoding extracellular proteins altered by different senescence mechanisms in PSC27 fibroblast cells. *Arrows,* transcript alterations verified by qRT-PCR.

Table 1. Verification of transcript alterations in senescent versus presenescent prostate fibroblasts

Gene symbol	Gene description	Fold-change: microarray	Fold-change: qRT-PCR
AREG	*Amphiregulin*	4.4	3.4
C17	*Cytokine-like protein C17*	5.3	2.2
CXCL1	*Chemokine (C-X-C motif) ligand 1*	3.4	8.2
FGF7	*Fibroblast growth factor 7*	2.8	2.5
HGF	*Hepatocyte growth factor*	2.5	5.1
IGFBP2	*Insulin-like growth factor binding protein 2*	3.4	26
IGFBP3	*Insulin-like growth factor binding protein 3*	4.6	34
IGFBP5	*Insulin-like growth factor binding protein 5*	14.1	53
IL-8	*Interleukin 8*	3.3	22
LAMB1	*Laminin β1*	2.1	9.6
MMP2	*Matrix metalloproteinase 2*	4.1	16
TIMP1	*Tissue inhibitor of metalloproteinase 1*	2.6	14

between presenescent PSC27, PSC31, and PSC36 fibroblasts and parallel cultures induced to senesce by H_2O_2, bleomycin, or replicative exhaustion. A one-sample *t* test comparing transcript abundance levels across a matrix of three fibroblast isolates and three senescence mechanisms—a total of nine experiments—identified 1,073 clones (representing 855 unique genes, 714 of which are characterized) with significant differential expression results across the nine senescent samples compared with presenescent controls (false discovery rate ≤ 1%). The consistency of these results is supported by direct comparisons of the three different senescence mechanisms to each other in which no clones were significantly differentially regulated (<1% false discovery rate). A comparison of the three different fibroblast isolates to each other at steady state determined that 436 clones were differentially expressed (<1% false discovery rate, one-way ANOVA). Although the expression of these genes differed significantly between cell isolates, upon further analysis, it was determined that although measurable, the differences were due to relatively small magnitudes of expression between the fibroblast isolates; on the other hand, the direction of expression changes for the vast majority of genes was concordant between all cell lines and treatments.

To prioritize genes for further study, we first sought to identify those with consistent alterations across cell lines and treatments, and exhibited magnitudes of increased transcriptional changes that might reasonably be measured at the protein level. Of the cDNAs represented on the Prostate Expression Database microarrays, 122 genes with significant expression changes also exhibited average fold changes of ≥2 in senescent versus presenescent cells (Fig. 2*A*). Additional profiling experiments using a larger clone set identified 588 additional genes with statistically significant gene expression alterations of ≥2-fold across the three fibroblast isolates following H_2O_2 treatment. We chose to focus on the 407 genes with elevated expression. Of these, we were particularly interested in the subset of 71 genes that encode extracellular proteins annotated in the Genome Ontology database with the potential to influence adjacent cells via paracrine mechanisms (Fig. 2*B*).

The identification of senescence-associated alterations in genes with documented roles as paracrine mediators of cell proliferation prompted further studies designed to confirm the microarray results for several genes in this functional category. We used quantitative RT-PCR to measure the senescence-associated increase of transcripts encoding AREG, cytokine-like protein C17 (C17), chemokine C-X-C motif-ligand 1 (CXCL1), FGF7, HGF, insulin-like growth factor binding protein (IGFBP) 2, IGFBP3, IGFBP5, interleukin 8 (IL-8), laminin β1 (LAMB1), matrix metalloproteinase 2 (MMP2), and tissue inhibitor of matrix metalloproteinase 1 (TIMP1). The mRNA abundance in senescent (PSC27ASH) and presenescent (PSC27N) cells from two unrelated experiments were normalized against GAPDH and were compared (Table 1). For each gene, the senescence-associated increase in expression originally measured by microarray hybridization was confirmed by qRT-PCR in a replicate biological experiment. The IGFBP mRNAs increased between 26- and 53-fold following senescence. IL-8, MMP2, and TIMP2 increased 22-, 16-, and 14-fold, respectively.

Evaluation of paracrine mediators of neoplastic epithelial cell growth. The identification of senescence-induced expression of transcripts encoding fibroblast proteins with the potential to influence epithelial proliferation prompted experiments designed to determine if senescent prostate fibroblasts could stimulate the growth of immortalized prostate epithelial cells when in close proximity. Primary prostate fibroblasts induced to senesce with H_2O_2, bleomycin, or replicative exhaustion were each cocultured with BPH1-GFP2 cells for 72 hours. To ensure that the coculture conditions of BPH1 with nonproliferating senescent fibroblasts were similar to that of untreated proliferation-competent fibroblasts, enough fibroblasts were used to form a confluent lawn immediately upon seeding without proliferation. PSC27ASH or PSC27ASB senescent fibroblasts stimulated the proliferation of the BPH1-GFP2 epithelial cells ~2.9-fold each relative to coculture with untreated PSC27N cells ($P < 0.001$ and $P < 0.001$, respectively; Fig. 3*A* and *C*). Senescent fibroblasts comprising 30% of the entire fibroblast population was sufficient to exert measurable effects on epithelial cell proliferation (Fig. 3*C*). PSC27RS senescent fibroblasts also stimulated epithelial cell proliferation although to a lesser extent (1.5-fold; $P < 0.001$; Fig. 3*B*). The stimulating effect of senescent fibroblasts was corroborated by the finding that PSC27ASH also stimulated the proliferation of the highly metastatic M12-GFP epithelial cells ~1.3-fold relative to coculture with untreated PSC27N cells ($P = 0.02$; Fig. 3*D*).

We next sought to determine if the influence of senescent prostate fibroblasts on epithelial growth resulted from soluble factors. We generated conditioned medium from presenescent PSC27N cells and senescent PSC27ASH, PSC27RS cells, and measured BPH1-GFP2 cell numbers after growth for 3 days in the different conditioned medium. The proliferation of BPH1-GFP2 cells was stimulated 1.8-fold ($P = 0.004$) and 1.6-fold ($P = 0.007$) with medium from PSC27ASB

and PSC27RS, respectively, when compared with medium conditioned with PSC27N cells (Fig. 4*A*). Consistent with these findings, conditioned medium from the senescent PSC27ASH stimulated the growth of tumorigenic DU145 and PC3 cells 1.2-fold ($P < 0.001$) relative to conditioned medium from presenescent PSC27N fibroblasts (Fig. 4*B*). These results suggest that a significant component of the senescent fibroblast proliferative influence toward epithelium is mediated through soluble factors.

Identification of AREG as a senescence-associated factor modulating the proliferation of neoplastic prostate epithelium. To confirm that senescence-associated transcript alterations produced corresponding changes in extracellular protein levels, we evaluated conditioned medium obtained from senescent PSC27 fibroblasts for the presence of FGF7, HGF, and AREG by Western blot analysis (Fig. 5*A*). The FGF7 antibody detected a strongly reactive protein with a molecular mass of ~25 kDa and a weakly reactive protein of molecular mass 75 kDa. Higher amounts of the 25 kDa protein were measurable in medium conditioned by senescent prostate fibroblasts compared with presenescent cells, whereas the 75 kDa protein was not appreciably altered. A 28 kDa form of FGF7 has previously been detected in medium conditioned by human embryonic lung fibroblasts (27). Western analysis of conditioned culture medium with an antibody recognizing HGF detected several proteins with apparent molecular masses of ~53, 35, and 30 kDa, and a faintly visualized protein with an apparent molecular mass of ~75 kDa. The weakly staining high molecular mass band is consistent with the intact precursor pro-HGF protein, whereas the lower molecular mass bands correspond to the heavy and light chains (28). Significantly higher amounts of all four proteins were detected in medium conditioned by senescent prostate fibroblasts cells compared with presenescent cells.

The AREG antibody detected a protein in fibroblast-conditioned medium with an apparent molecular mass of ~58 kDa. Considerably greater amounts of the protein were detected in medium conditioned by senescent fibroblasts compared with presenescent cells (Fig. 5*A*). Although the predicted molecular mass of AREG is ~20 kDa, size ranges of 60, 55, 28, 18, and 10 kDa have been found in medium conditioned by the human breast cancer cell line MCF-7 due to glycosylation (29). AREG sizes of 51 and 27 kDa have been measured in microsomal preparations from sheep mammary glands (30). To verify antibody specificity, we ran 0.1 μg of recombinant AREG and measured a predominant band at ~60 kDa and a faint band at ~20 kDa (Fig. 5*A*). A Western blot run with 0.02 μg AREG resulted in a shift of the predominant band to ~20 kDa. Repeating the Western analysis with a second AREG-specific antibody produced similar results (data not shown).

AREG has been shown to be expressed in prostate interstitial smooth muscle cells and to stimulate the proliferation of primary benign prostate epithelium (31). AREG expression has also been

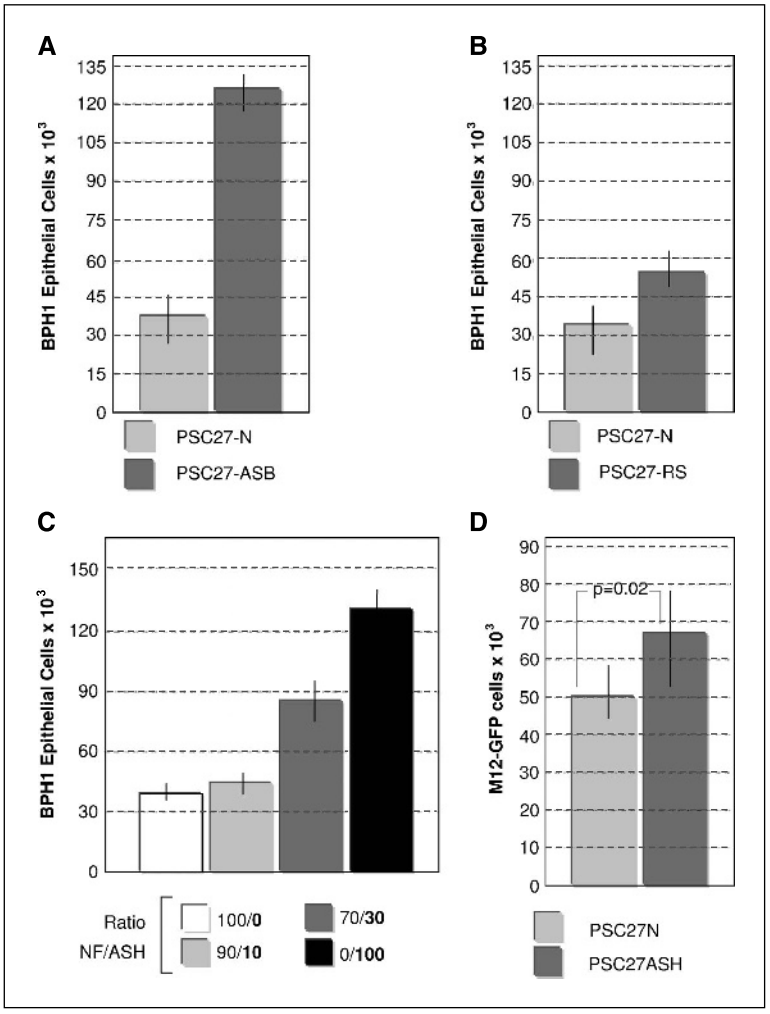

Figure 3. Stimulation of prostate epithelial cell proliferation by coculture with senescent prostate fibroblasts. *A,* BPH-1 immortalized prostate epithelial cell quantitation following coculture with presenescent (*PSC27-N*) or prostate fibroblasts induced to senescence with bleomycin treatment (*PSC27-ASB*) for 72 hours. *B,* BPH-1 immortalized prostate epithelial cell quantitation following coculture with presenescent or prostate fibroblasts at replicative exhaustion (*PSC27-RS*) for 72 hours. *C,* BPH-1 epithelial cell quantitation after 72 hours of coculture with various ratios of presenescent (*NF*) or H_2O_2-induced senescent fibroblasts (*ASH*). *D,* M12-GFP immortalized prostate epithelial cell quantitation following coculture with presenescent or prostate fibroblasts induced to senescence with H_2O_2 treatment (*PSC27ASH*) for 72 hours.

shown to be up-regulated in prostate cancers with altered subcellular localization patterns (32). To determine if AREG contributed to a component of the proliferative effect of senescent prostate fibroblasts toward prostate epithelium, we added recombinant AREG to BPH1-GFP2 cells for 72 hours and quantitated cell numbers. AREG concentrations of 1×10^{-8} mol/L stimulated the proliferation of BPH1-GFP2 cells 2.4-fold relative to cells grown in the absence of AREG ($P < 0.01$; Fig. 5*B*). Senescent fibroblast conditioned medium treated with anti-AREG-neutralizing antibodies lost a small but significant component of the growth-promoting effects relative to complete conditioned medium ($P = 0.002$; Fig. 5*C*). To corroborate these findings, we treated fibroblasts with AREG or control RNA interference (RNAi). The senescence-induced expression of AREG was not noticeably affected by control RNAi but was reduced 46-fold by AREG RNAi (Fig. 5*D*). Conditioned medium from senescent fibroblasts treated with AREG-specific siRNA lost a small but significant component of the growth-promoting effects ($P = 0.04$; Fig. 5*E*). These results suggest that multiple paracrine-acting factors secreted or liberated from senescent prostate fibroblasts contribute to epithelial growth stimulation.

Discussion

The "host" microenvironment is increasingly viewed as an important active contributor to tumor growth and tumor suppression. The somatic mutation theory of cancer postulates that carcinomas result from a single somatic cell that accumulates multiple DNA mutations or chromosomal alterations over time: genotypic changes result in phenotypes of uncontrolled growth (33). This concept explains many aspects of tumorigenesis but other important observations indicate that additional influences must be operative. For example, embryos transplanted into ectopic sites (e.g., peritoneal cavity) can behave like malignant neoplasms (e.g., teratocarcinomas). Conversely, embryonal carcinoma cells injected into murine blastocycts contribute to normal tissues and organs in cancer-free adult mice (34). Thus, the microenvironment provided by the stroma can be a powerful suppressor—or promoter—of malignant phenotypes caused by oncogenic mutations. This is true both during embryogenesis and in adult tissues (reviewed in ref. 35).

The importance of cellular context as a contributor to carcinogenesis has led to alternative explanations for the development and progression of epithelial malignancies. One hypothesis, designated the Tissue Organization and Field Theory (reviewed in ref. 36), builds on an extensive body of work in embryology involving morphogenetic fields of cellular interactions that collectively dictate cellular differentiation and tissue organization through cellular contacts and diffusible gradients of morphogens (37–39). In agreement with the Tissue Organization and Field Theory are observations that tumors exhibit striking similarities to "wounds that do not heal" (40). The "reactive" stroma surrounding carcinomas display morphologic and biochemical characteristics akin to changes associated with wound healing: fibroblast and epithelial proliferation, cell migration, recruitment of inflammatory cells, and angiogenesis. Recent studies using microarray-based expression profiling have shown striking similarities between signatures of fibroblast serum response and human tumors (41). Whereas the concept of a wound-associated or reactive stroma implies that the microenvironment is altered in response to an extrinsic (e.g., epithelial) event,

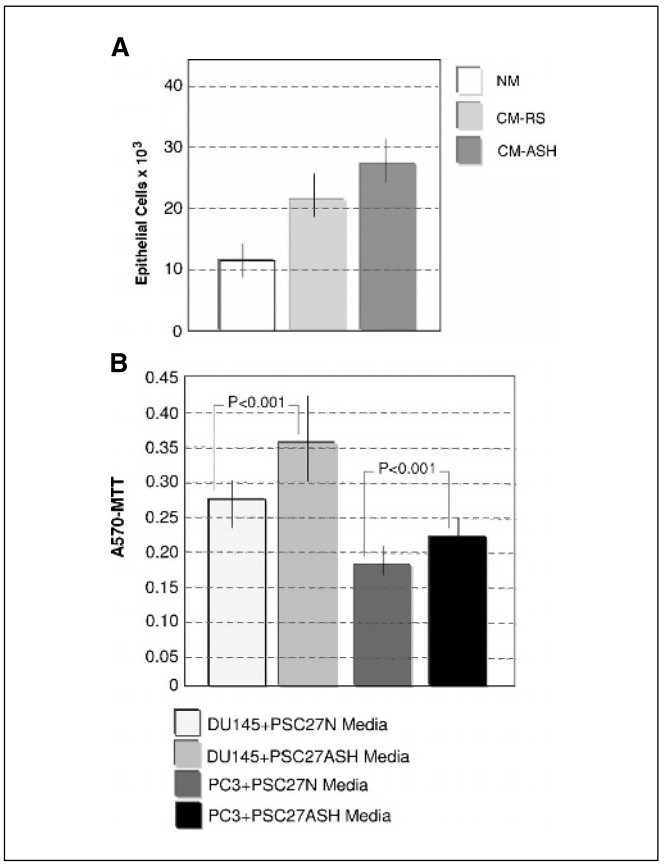

Figure 4. Stimulation of neoplastic prostate epithelial cell proliferation by conditioned medium from senescent prostate fibroblasts. *A,* quantitation of BPH-1 prostate epithelial cell proliferation after 72 hours of culture in normal medium (*NM*), medium conditioned by prostate fibroblasts at replicative exhaustion (*CM-RS*), or prostate fibroblasts induced to senescence with H_2O_2 (*CM-ASH*). *B,* quantitation of DU145 and PC3 prostate epithelial cell proliferation after 72 hours of culture in medium conditioned by normal prostate fibroblasts (*N*), or prostate fibroblasts induced to senescence with H_2O_2 (*ASH*).

it is also plausible that intrinsic stromal alterations are operative as primary or permissive events allowing for, or magnifying, a reactive phenotype. Studies of the tumor-promoting effects of senescent fibroblasts on breast carcinogenesis and the findings reported here suggest that age-dependent stromal processes operate as a tissue-modifying field effect.

The substantial number of reproducible molecular changes identified in this study that associate with prostate fibroblast senescence includes a host of extracellular proteins with well-described capabilities for influencing the growth or survival of cells in the locoregional environment. Paracrine-acting proteins identified in our study included HGF/scatter factor, a protein originally identified as a fibroblast-derived epithelial cell motility factor and a potent mitogen of hepatocytes (42). HGF has been shown to disrupt epithelial cell morphogenesis, regulate the breakdown of cell-to-cell junctions, and stimulate the migration and invasion of single cells (43, 44). HGF expression has been shown to increase in skin fibroblasts from old individuals and in response to IGFs that increase with aging (45, 46). HGF can coactivate androgen receptor signaling, leading to androgen-independent prostate cancer growth (47, 48). The important influence of stroma and HGF on the development of neoplastic growth was recently shown in experiments analyzing mice with

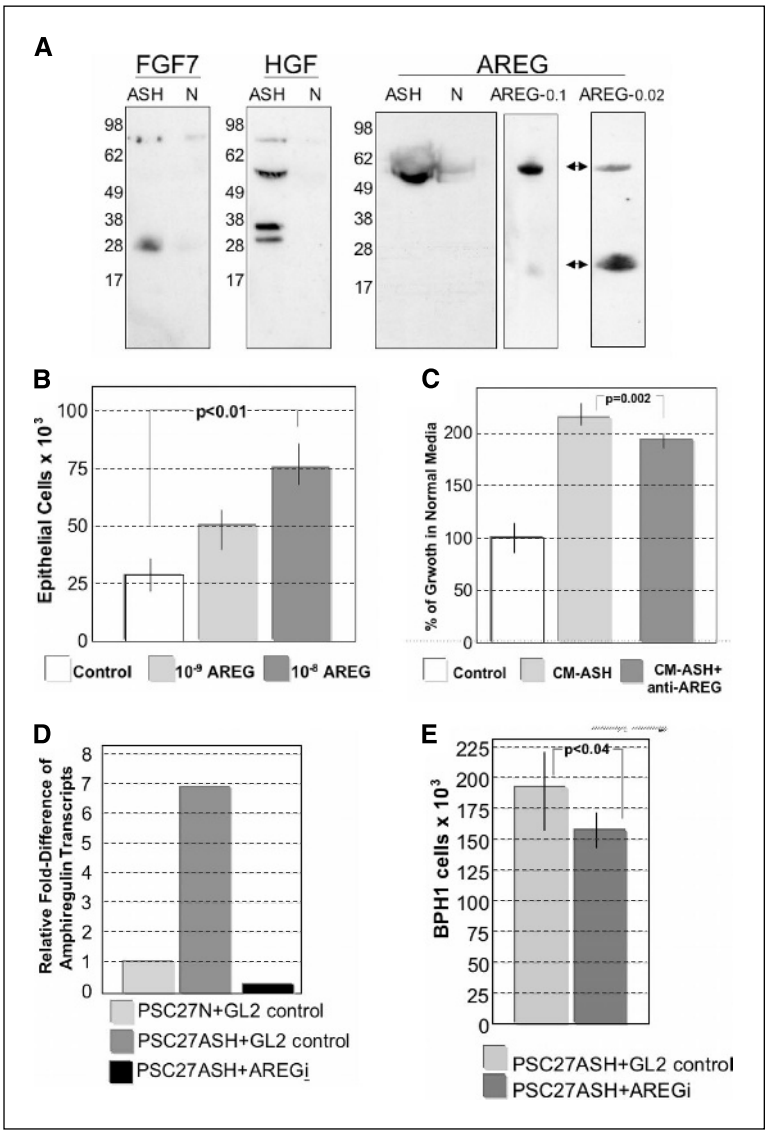

Figure 5. Senescence-associated AREG-mediated proliferation of immortalized prostate epithelium. *A,* Western analysis for quantitation of FGF7, HGF, and AREG in conditioned medium from presenescent fibroblasts or fibroblasts induced to senesce with H_2O_2. The FGF7 antibody detected a strongly reactive protein with a molecular mass of ~25 kDa and a weakly reactive protein of molecular mass 75 kDa. A 28 kDa form of FGF7 has previously been identified in medium conditioned by human embryonic lung fibroblasts. The HGF-reactive antibody detected several proteins with apparent molecular masses of ~53, 35, and 30 kDa, and a faintly visualized protein with an apparent molecular mass of ~75 kDa. The weakly staining high molecular mass band is consistent with the intact precursor pro-HGF protein, whereas the lower molecular mass bands correspond to the heavy and light chains. The AREG-reactive antibody detected a predominant protein of ~58 kDa. AREG forms of this size have been identified in conditioned medium from epithelial cells due to glycosylation. *AREG-0.1* and *AREG-0.02,* control recombinant AREG protein at 0.1 and 0.02 μg. Highly concentrated AREG has been reported to aggregate (information provided by manufacturer). *Arrows,* AREG reactivity at ~58 and ~20 kDa. *B,* quantitation of BPH-1 epithelial cells following treatment with varying concentrations of recombinant AREG. *C,* quantitation of BPH-1 prostate epithelial cell growth when treated with conditioned medium from presenescent fibroblasts (*Control*), conditioned medium from fibroblasts induced to senesce with H_2O_2 (*CM-ASH*), or CM-ASH with the addition of neutralizing antibody to AREG (*CM-ASH + anti-AREG*). *D,* quantitation of AREG transcripts in control RNAi (*GL2*) and AREG RNAi (*AREGi*)–treated normal (*PSC27N*) and senescent (*PSC27ASH*) fibroblasts determined by qRT-PCR. *E,* quantitation of BPH-1 prostate epithelial cell growth when treated with conditioned medium from fibroblasts induced to senesce with H_2O_2 and treated with AREG RNAi or GL2 RNAi.

targeted deletions of the TGF-β type II receptor specifically in fibroblasts. These mice developed invasive gastric cancers and prostate intraepithelial neoplasia through a mechanism involving stromally derived HGF (10).

Other senescence-induced mitogenic factors identified in this study include FGF7/KGF, IGFBPs, and AREG. AREG is a heparin-binding member of the epidermal growth factor family that influences the survival, growth, or progression of multiple human cancers, including myeloma (49), breast (50), lung (51), pancreas (52), and prostate (31, 32). AREG has been shown to function as a survival factor, protecting hepatocytes from Fas-mediated liver injury, and cooperating with IGF-I to inhibit apoptosis of lung carcinoma cells through phosphorylation of Bad (51). In the context of prostate carcinogenesis, AREG mediates androgen-stimulated cell proliferation in the LNCaP prostate cancer cell line, suggesting the presence of an androgen-regulated autocrine loop involving the epidermal growth factor receptor and AREG. The important role for AREG in mediating the survival of prostate cancer cells to castration was recently shown through studies reporting a 5-fold increase in tumor AREG protein expression following androgen depletion (53). Blockade of the HER1 tyrosine kinase receptor in conjunction with castration significantly increased tumor involution compared with castration alone.

In summary, the molecular signature of prostate fibroblast senescence includes a cohort of factors capable of influencing the survival and proliferation of adjacent prostate epithelium. The local production of these mitogens and prosurvival factors could exert important affects on preneoplastic lesions originally instigated by predisposing genetic variables, carcinogens, or chronic inflammation (54). Further, these findings suggest an explanation for the paradoxical age-associated increases in hormonally driven prostatic diseases, such as cancer and benign hyperplasia in the setting of age-associated declines in testosterone, whereby increases in mitogens from the aged stroma substitute for androgen loss.

Acknowledgments

Received 5/18/2005; revised 10/25/2005; accepted 10/31/2005.

Grant support: Seattle Cancer and Aging Program; Cancer Center Support Grant pilot funds CA015704; and NIH grants CA85859, CA97186, and DK65204 (P.S. Nelson).

The costs of publication of this article were defrayed in part by the payment of page charges. This article must therefore be hereby marked *advertisement* in accordance with 18 U.S.C. Section 1734 solely to indicate this fact.

We thank Michael Taylor for the construction of BPH1-GFP2 cells.

References

1. Hsing AW, Tsao L, Devesa SS. International trends and patterns of prostate cancer incidence and mortality. Int J Cancer 2000;85:60–7.
2. Sakr WA, Haas GP, Cassin BF, Pontes JE, Crissman JD. The frequency of carcinoma and intraepithelial neoplasia of the prostate in young male patients. J Urol 1993; 150:379–85.
3. Sternlicht MD, Lochter A, Sympson CJ, et al. The stromal proteinase MMP3/stromelysin-1 promotes mammary carcinogenesis. Cell 1999;98:137–46.
4. Kenny PA, Bissell MJ. Tumor reversion: correction of malignant behavior by microenvironmental cues. Int J Cancer 2003;107:688–95.
5. Bissell MJ, Radisky D. Putting tumours in context. Nat Rev Cancer 2001;1:46–54.
6. Kuperwasser C, Chavarria T, Wu M, et al. Reconstruction of functionally normal and malignant human breast tissues in mice. Proc Natl Acad Sci U S A 2004; 101:4966–71.
7. Barcellos-Hoff MH, Ravani SA. Irradiated mammary gland stroma promotes the expression of tumorigenic potential by unirradiated epithelial cells. Cancer Res 2000;60:1254–60.
8. Maffini MV, Soto AM, Calabro JM, Ucci AA, Sonnenschein C. The stroma as a crucial target in rat mammary gland carcinogenesis. J Cell Sci 2004;117:1495–502.
9. Olumi AF, Grossfeld GD, Hayward SW, Carroll PR, Tlsty TD, Cunha GR. Carcinoma-associated fibroblasts direct tumor progression of initiated human prostatic epithelium. Cancer Res 1999;59:5002–11.
10. Bhowmick NA, Chytil A, Plieth D, et al. TGF-β signaling in fibroblasts modulates the oncogenic potential of adjacent epithelia. Science 2004;303:848–51.
11. Dimri GP, Lee X, Basile G, et al. A biomarker that identifies senescent human cells in culture and in aging skin *in vivo*. Proc Natl Acad Sci U S A 1995;92:9363–7.
12. Castro P, Giri D, Lamb D, Ittmann M. Cellular senescence in the pathogenesis of benign prostatic hyperplasia. Prostate 2003;55:30–8.
13. Krtolica A, Parrinello S, Lockett S, Desprez PY, Campisi J. Senescent fibroblasts promote epithelial cell growth and tumorigenesis: a link between cancer and aging. Proc Natl Acad Sci U S A 2001;98:12072–7.
14. Gmyrek GA, Walburg M, Webb CP, et al. Normal and malignant prostate epithelial cells differ in their response to hepatocyte growth factor/scatter factor. Am J Pathol 2001;159:579–90.
15. Hayward SW, Dahiya R, Cunha GR, Bartek J, Deshpande N, Narayan P. Establishment and characterization of an immortalized but non-transformed human prostate epithelial cell line: BPH-1. In Vitro Cell Dev Biol Anim 1995;31:14–24.
16. Bae VL, Jackson-Cook CK, Maygarden SJ, Plymate SR, Chen J, Ware JL. Metastatic sublines of an SV40 large T antigen immortalized human prostate epithelial cell line. Prostate 1998;34:275–82.
17. Chen QM, Bartholomew JC, Campisi J, Acosta M, Reagan JD, Ames BN. Molecular analysis of H_2O_2-induced senescent-like growth arrest in normal human fibroblasts: p53 and Rb control G_1 arrest but not cell replication. Biochem J 1998;332:43–50.
18. Nelson PS, Clegg N, Arnold H, et al. The program of androgen-responsive genes in neoplastic prostate epithelium. Proc Natl Acad Sci U S A 2002;99:11890–5.
19. Hawkins V, Doll D, Bumgarner R, et al. PEDB: the Prostate Expression Database. Nucleic Acids Res 1999; 27:204–8.
20. Bonham M, Arnold H, Montgomery B, Nelson PS. Molecular effects of the herbal compound PC-SPES: identification of activity pathways in prostate carcinoma. Cancer Res 2002;62:3920–4.
21. Tusher VG, Tibshirani R, Chu G. Significance analysis of microarrays applied to the ionizing radiation response. Proc Natl Acad Sci U S A 2001;98:5116–21.
22. Gschwind A, Hart S, Fischer OM, Ullrich A. TACE cleavage of proamphiregulin regulates GPCR-induced proliferation and motility of cancer cells. EMBO J 2003; 22:2411–21.
23. Ben-Porath I, Weinberg RA. The signals and pathways activating cellular senescence. Int J Biochem Cell Biol 2005;37:961–76.
24. Itahana K, Campisi J, Dimri GP. Mechanisms of cellular senescence in human and mouse cells. Biogerontology 2004;5:1–10.
25. Chang BD, Broude EV, Dokmanovic M, et al. A senescence-like phenotype distinguishes tumor cells that undergo terminal proliferation arrest after exposure to anticancer agents. Cancer Res 1999;59:3761–7.
26. Linskens MH, Harley CB, West MD, Campisi J, Hayflick L. Replicative senescence and cell death. Science 1995;267:17.
27. Rubin JS, Osada H, Finch PW, Taylor WG, Rudikoff S, Aaronson SA. Purification and characterization of a newly identified growth factor specific for epithelial cells. Proc Natl Acad Sci U S A 1989;86:802–6.
28. Miyazawa K, Shimomura T, Naka D, Kitamura N. Proteolytic activation of hepatocyte growth factor in response to tissue injury. J Biol Chem 1994;269: 8966–70.
29. Martinez-Lacaci I, Johnson GR, Salomon DS, Dickson RB. Characterization of a novel amphiregulin-related molecule in 12-*O*-tetradecanoylphorbol-13-acetate-treated breast cancer cells. J Cell Physiol 1996; 169:497–508.
30. Forsyth IA, Taylor JA, Keable S, Turvey A, Lennard S. Expression of amphiregulin in the sheep mammary gland. Mol Cell Endocrinol 1997;126:41–8.
31. Adam RM, Borer JG, Williams J, Eastham JA, Loughlin KR, Freeman MR. Amphiregulin is coordinately expressed with heparin-binding epidermal growth factor-like growth factor in the interstitial smooth muscle of the human prostate. Endocrinology 1999; 140:5866–75.
32. Bostwick DG, Qian J, Maihle NJ. Amphiregulin expression in prostatic intraepithelial neoplasia and adenocarcinoma: a study of 93 cases. Prostate 2004;58: 164–8.
33. Curtis HJ. Formal discussion of: somatic mutations and carcinogenesis. Cancer Res 1965;25:1305–8.
34. Stewart TA, Mintz B. Successive generations of mice produced from an established culture line of euploid teratocarcinoma cells. Proc Natl Acad Sci U S A 1981;78: 6314–8.
35. Krtolica A, Campisi J. Cancer and aging: a model for the cancer promoting effects of the aging stroma. Int J Biochem Cell Biol 2002;34:1401–14.
36. Soto AM, Sonnenschein C. The somatic mutation theory of cancer: growing problems with the paradigm? BioEssays 2004;26:1097–107.
37. Opitz JM. The developmental field concept. Am J Med Genet 1985;21:1–11.
38. Rubin H. Cancer as a dynamic developmental disorder. Cancer Res 1985;45:2935–42.
39. De Robertis EM, Morita EA, Cho KW. Gradient fields and homeobox genes. Development 1991;112:669–78.
40. Dvorak HF. Tumors: wounds that do not heal. Similarities between tumor stroma generation and wound healing. N Engl J Med 1986;315:1650–9.
41. Chang HY, Sneddon JB, Alizadeh AA, et al. Gene expression signature of fibroblast serum response predicts human cancer progression: similarities between tumors and wounds. PLoS Biol 2004;2:E7.
42. Funakoshi H, Nakamura T. Hepatocyte growth factor: from diagnosis to clinical applications. Clin Chim Acta 2003;327:1–23.
43. Khoury H, Naujokas MA, Zuo D, et al. HGF converts ErbB2/Neu Epithelial morphogenesis to cell invasion. Mol Biol Cell 2004;17:17.
44. Nakashiro K, Hayashi Y, Oyasu R. Immunohistochemical expression of hepatocyte growth factor and c-Met/HGF receptor in benign and malignant human prostate tissue. Oncol Rep 2003;10:1149–53.
45. Miyazaki M, Gohda E, Kaji K, Namba M. Increased hepatocyte growth factor production by aging human fibroblasts mainly due to autocrine stimulation by interleukin-1. Biochem Biophys Res Commun 1998;246: 255–60.
46. Skrtic S, Wallenius V, Ekberg S, Brenzel A, Gressner AM, Jansson JO. Insulin-like growth factors stimulate expression of hepatocyte growth factor but not transforming growth factor β1 in cultured hepatic stellate cells. Endocrinology 1997;138:4683–9.
47. Sirotnak FM, She Y, Khokhar NZ, Hayes P, Gerald W, Scher HI. Microarray analysis of prostate cancer progression to reduced androgen dependence: studies in unique models contrasts early and late molecular events. Mol Carcinog 2004;41:150–63.
48. Nakashiro K, Okamoto M, Hayashi Y, Oyasu R. Hepatocyte growth factor secreted by prostate-derived stromal cells stimulates growth of androgen-independent human prostatic carcinoma cells. Am J Pathol 2000;157:795–803.
49. Mahtouk K, Hose D, Reme T, et al. Expression of EGF-family receptors and amphiregulin in multiple myeloma. Amphiregulin is a growth factor for myeloma cells. Oncogene 2005;28:28.
50. Bieche I, Onody P, Tozlu S, Driouch K, Vidaud M, Lidereau R. Prognostic value of ERBB family mRNA expression in breast carcinomas. Int J Cancer 2003;106: 758–65.
51. Hurbin A, Coll JL, Dubrez-Daloz L, et al. Cooperation of amphiregulin and IGF1 inhibits Bax- and Bad-mediated apoptosis via a PKC-dependent pathway in non-small cell lung cancer cells. J Biol Chem 2005;14:14.
52. Ebert M, Yokoyama M, Kobrin MS, et al. Induction and expression of amphiregulin in human pancreatic cancer. Cancer Res 1994;54:3959–62.
53. Torring N, Hansen FD, Sorensen BS, Orntoft TF, Nexo E. Increase in amphiregulin and epiregulin in prostate cancer xenograft after androgen deprivation—impact of specific HER1 inhibition. Prostate 2005; 13:13.
54. Nelson WG, De Marzo AM, Isaacs WB. Prostate cancer. N Engl J Med 2003;349:366–81.

Journal of Cellular Biochemistry 99:392–401 (2006)

Interaction of IGF Signaling and the Androgen Receptor in Prostate Cancer Progression

Jennifer D. Wu,[1] Kathy Haugk,[2] Libby Woodke,[2] Peter Nelson,[3] Ilsa Coleman,[3] and Stephen R. Plymate[1,2]*

[1]Department of Medicine, University of Washington, Seattle, Washington
[2]Geriatric Research, Education and Clinical Center, Veterans Affairs Puget Sound Health Care System, Seattle, Washington
[3]Fred Hutchinson Cancer Research Center, Seattle, Washington

Abstract The insulin-like growth factor type I receptor (IGF-IR) has been suggested to play an important role in prostate cancer progression and possibly in the progression to androgen-independent (AI) disease. The term AI may not be entirely correct, in that recent data suggest that expression of androgen receptor (AR) and androgen-regulated genes is the primary association with prostate cancer progression after hormone ablation. Therefore, signaling through other growth factors has been thought to play a role in AR-mediated prostate cancer progression to AI disease in the absence of androgen ligand. However, existing data on how IGF-IR signaling interacts with AR activation in prostate cancer are conflicting. In this Prospect article, we review some of the published data on the mechanisms of IGF-IR/AR interaction and present new evidence that IGF-IR signaling may modulate AR compartmentation and thus alter AR activity in prostate cancer cells. Inhibition of IGF-IR signaling can result in cytoplasmic AR retention and a significant change in androgen-regulated gene expression. Translocation of AR from the cytoplasm to the nucleus may be associated with IGF-induced dephosphorylation. Since fully humanized antibodies targeting the IGF-IR are now in clinical trials, the current review is intended to reveal the mechanisms of potential therapeutic effects of these antibodies on AI prostate cancers. J. Cell. Biochem. 99: 392–401, 2006.

Key words: insulin-like growth factor type I receptor (IGF-IR); androgen receptor (AR); androgen-independent (AI) prostate cancer; AR co-regulators

In the presence or possibly absence of androgen ligand, the androgen receptor (AR) translocates from the cytosol to the nucleus and functions as a transcriptional factor, which may be necessary or even crucial for the progression of prostate cancer [Scher and Sawyers, 2005]. Classically, in the absence of androgen ligand, AR remains in the cytosol and is not active. Thus, it is of particular interest that malignant prostate cancer progression occurs frequently in men who have been surgically or chemically castrated. The progression of prostate cancer after castration has been termed androgen-independent (AI) prostate cancer. More interestingly, animal studies showed that when the expression of AR was disrupted, prostate cancer ceased to progress [Taplin and Balk, 2004]. All these together posed a conundrum if the AR, rather than the androgen ligand, is a driving force in prostate cancer progression. If so, it would suggest that the AR is functioning in a non-classical manner in the absence of steroid ligand. Although non-genomic mechanisms for AR function have been proposed through an interaction with SRC–Raf–Ras–Map kinase in the cytosol rather than the nucleus, this "traditional" non-genomic mechanism also requires the presence of androgen ligand and would not explain progression of disease in a ligand-independent manner [Kousteni et al., 2001; Pandini et al., 2005].

The concept of AR functioning in AI progression was first proposed by Mohler and colleages

Grant sponsor: National Cancer Institute; Grant sponsor: Veterans Affairs Research Service; Grant sponsor: Department of Defense; Grant numbers: 1K01CA116002-01, PO1-CA85859, DOD-PC040364.

*Correspondence to: Stephen R. Plymate, MD, 325 9th Avenue, Box 359625, Seattle, WA 98104.
E-mail: splymate@u.washington.edu

Received 15 February 2006; Accepted 27 February 2006
DOI 10.1002/jcb.20929

[Gregory et al., 1998; Mohler et al., 2004]. In relevant studies, tumor biopsies were taken from prostate cancer patients who had been androgen ablated and presented with progression of the cancer [Gregory et al., 1998; Mohler et al., 2004] In these samples, the AR primarily resided in a nuclear location, contrary to what had been expected in a castrated environment. This may in part due to residual levels of androgen in the prostate tissue. When tissue levels of androgen, testosterone, and dihydrotestosterone (DHT), were measured, although lower than in non-castrated men, they were still detected in the nanomolar range in many of the castrated men [Titus et al., 2005a]. This subtle level of tissue androgen may account for the nuclear localization of the AR and signal to activate an AR transcriptional program. The failure of castration to completely abolish intraprostatic androgens has also been evidenced in the study where normal men were placed on a GnRH antagonist for 4 weeks and in whom serum levels of testosterone (T) and DHT were clearly in the castrate range (Page and Bremner, personal communication). The source of the androgens in these castrate men has yet to be determined; however, the most likely source would be conversion from adrenal androgens. The prostate has active 5α-reductase systems for both isoforms I and II ensuring that circulating T can be readily converted to DHT in the prostate [Titus et al., 2005b]. In addition, recent microarray data has shown that the prostate contains mRNAs for the enzymes necessary for the conversion of cholesterol precursor into DHT; however this conversion has not been demonstrated in the prostate. Anti-androgen drugs, such as biclutamide, have not been shown to alter the translocation of the AR to the nucleus in prostate specimens from men treated with combined androgen blockade [Mohler et al., 2004]. Therefore, it is not clear whether it is the low levels of androgens driving prostate cancer progression in castrated men. Until a total androgen ablation mechanism in men is developed, the importance of residual androgens in tumor progression cannot be determined.

Castration studies on prostate cancer xenograft and transgenic mouse models support the speculation that residual androgen production following castration is only the partial driving force for tumor progression. Since mice do not produce adrenal androgens to any significant degree, castration in a mouse results in "complete androgen ablation" [Van Weerden et al., 1992]. In these models, tumors progress from androgen-dependent (AD) to AI following castration in spite of the fact that prostate specific androgen levels decrease to nearly undetectable levels, suggesting that residual androgens are unlikely to play a part in post-castration tumor progression [Thalmann et al., 2000; Corey et al., 2003]. We and others have shown that, in these models, the majority of tumor nuclei still contain AR after castration although some of the AR moves from the nucleus to the cytoplasm (Fig. 1). Furthermore, androgen-regulated genes continue to be expressed in "AI" disease [Corey et al., 2003]. Together, these data suggest that other mechanisms beyond the traditional ligand-receptor interaction of AR signaling are responsible for AD to AI prostate cancer progression.

Alterations in co-regulators of the AR, which may enhance ligand-independent AR translocation to the nucleus and binding to DNA, have been suggested as one of the mechanisms for ligand-independent AR signaling [Gregory et al., 1998; Fujimoto et al., 1999; Kang et al., 1999; Sadar, 1999; Sadar and Gleave, 2000; Mohler et al., 2004]. It has been suggested that some peptide growth factors can act directly at the androgen-binding domain of the AR or indirectly through modifying the phosphoryla-

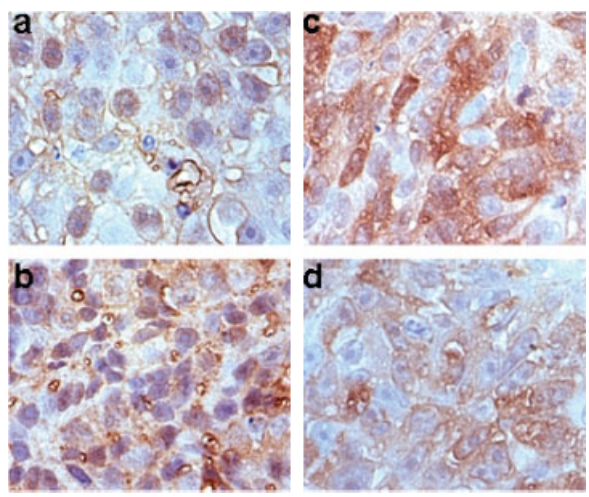

Fig. 1. IGF-IR signaling-induced translocation of AR into the nucleus in xenograft human prostate tumors. **a**: AR compartmentalization in the nucleus in intact animals. **b**: Blocking IGF-IR signaling with antibody A12 caused cytoplasmic retention of AR in intact animals. **c**: AR in the nucleus in castrated animals. **d**: A12 induced marked AR retention in the plasma in castrated animals.

tion status of the AR or its co-regulators to initiate AR signaling [Culig et al., 1994, 1995; Sadar, 1999; Sadar and Gleave, 2000; Lin et al., 2001]. In this "Prospectus" we examined the interactions between AR function and the activation of type 1 insulin-like growth factor receptor (IGF-IR). Among peptide growth factor-induced cell signaling, IGF activated IGF-IR signaling is a potential driving force for the growth of AI prostate cancer for several reasons as listed in Table I. In the following sections, we will examine the evidence for each of these components of potential interaction between the IGF-IR and AR.

IGF-IR IS NECESSARY FOR CELL TRANSFORMATION

Fibroblasts from IGF-IR knock out mice R^- do not transform spontaneously when compared to R^{wt} control cells. When the IGF-IR is re-expressed in these fibroblasts, transformation takes place. In SV40T immortalized prostate epithelial cells, inhibition of IGF-IR expression with an antisense construct significantly decreases colony formation in soft agar, a marker of transformation. In studies when growth hormone and IGF deficient LID mice were crossed with the transgenic prostate cancer (TRAMP) mouse, tumor development was significantly delayed Majeed et al., 2005). All these studies suggest an essential role of IGF-IR in cellular transformation. Hongo et al. [1998] have identified specific tyrosine residues on the β-subunit of the IGF-IR that are crucial for the transforming actions of the IGF-IR [O'connor et al., 1997; Liu et al., 1998].

TABLE I. Evidence for Interaction of the IGF-IR and AR in Prostate Cancer

1.	The IGF-IR is necessary for cell transformation
2.	Clinical data, although somewhat controversial suggests that higher levels of IGF-I in the serum of men predicts men at risk for developing clinical prostate cancer
3.	Androgens increase IGF-IR levels in prostate epithelial cells
4.	IGF-IR signaling alters AR phosphorylation
5.	IGF-IR signaling alters the AR transcriptional profile
6.	IGF-IR signaling effects translocation of the AR to the nucleus
7.	IGF-IR ligands increase in the progression of prostate cancer and are particularly abundant in bone where prostate cancer metastases are most abundant
8.	Xenograft models of prostate cancer respond differently to IGF-IR inhibition depending on the presence or absence of androgens
9.	IGF binding proteins (IGFBP) that enhance signaling of IGF ligands through the IGF-IR are increased in the period immediately after castration
10.	Inhibition of the IGF-IR in conjunction with castration
11.	Transcription factors that stimulate the IGF-IR promoter are also regulated by androgens

Since prostate cancer rarely develops in the absence of androgens, it is suspected that androgens are at least permissive in the transformation process of prostate epithelial cells. However, it should be noted that expression of the AR is necessary for normal luminal prostate epithelium to develop. It is suggested that maintaining certain levels of IGF-IR expression in the prostate may be necessary in normal prostate differentiation, increased levels of IGF-IR expression may be required for the prostate epithelia transformation process, and decreased IGF-IR expression may be required for prostate cancer malignant progression. This is consistent with the clinical findings that the levels of IGF-IR decrease following the initial transformation of the epithelium [Tennant et al., 1996]. This concept has been corroborated by the decrease in tumor metastases and increase in apoptosis associated with the re-expression IGF-IR in prostate cancer xenograft cell lines [Plymate et al., 1997a,b].

It should be pointed out that not all studies have shown an increase in IGF-IR expression during early prostate epithelia transformation or a decrease in IGF-IR expression in the progression to malignant prostate epithelia [Hellawell et al., 2002]. This may due to discrepancies in the choice of antibodies or technique in immunohistochemistry studies. The IGF-IR is a tyrosine kinase receptor that is only activated when located on the cell surface; although rapidly internalized upon activation, it is also rapidly processed through the golgi to be re-expressed on the cell surface.

CLINICAL DATA SUGGESTS THAT MEN IN THE HIGHER QUARTILES OF SERUM IGF-I LEVELS ARE AT A GREATER RISK FOR DEVELOPING PROSTATE CANCER

Large scale epidemiologic studies, such as the Physician's Health Study, have suggested that men with higher serum levels of IGF-1 as well as androgens may be at increased risk of developing prostate cancer in the following 6–9 years [Chan et al., 1998; Pollak, 2000; Pollak et al., 2004]. Also, in these studies serum levels of IGFBP-3 were inversely correlated with the risk of developing prostate cancer [Chan et al., 1998]. Of further note, the risk of cancer developing was more attributable to serum

IGF-I or IGFBP-3 than to serum testosterone. However, other studies have not shown an association of risk for prostate cancer with serum levels of IGF-I [Harman et al., 2000; Chen et al., 2005]. One should be aware that the risk of developing prostate cancer was not the primary end point of any of these studies nor did the results of the epidemiologic studies indicate a direct link between the IGF system and the risk of cancer.

ANDROGENS INCREASE IGF-IR EXPRESSION IN PROSTATE EPITHELIAL CELLS

We had initially detected an increase in IGF-IR expression at protein and mRNA levels in androgen-responsive prostate epithelial cell lines [Plymate et al., 2004]. This observation was subsequently confirmed by other investigators [Pandini et al., 2005]. The mechanism by which androgens increase the IGF-IR expression has been a topic of controversy. Pandini et al. [2005] have shown in their models that the increase in IGF-IR protein induced by androgens does not require nuclear translocation of the AR and is only partially blocked by bicluta-mide. On the other hand, this effect of AR on IGF-IR expression was completely inhibited by the ERK1/2 inhibitor PD980259 [Pandini et al., 2005]. These data suggested a "non-genomic" effect of androgen. This group further confirmed their findings using a mutated AR that will not translocate to the nucleus and demonstrated that the mutanted AR can activate the cytoplasmic Src–Raf–Ras–Map kinase pathway and enhance the transcriptional activity of IGF-IR promoter [Pandini et al., 2005]. Other investigators have not found that activation of this pathway is necessary for androgen-induced increases in IGF-IR expression [Plymate et al., 2004]. Other mechanisms including an increase in KFL6 (Kruppel factor like 6) in response to androgens have been suggested from the study in LnCaP lines (Levine-personal communication). We have shown that KFL6 increases IGF-IR expression by binding to the IGF-IR promoter [Rubinstein et al., 2004]. We have also shown in prostate cell lines that androgens can increase IGF-IR protein expression without an increase in its mRNA expression level, suggesting a post-transcriptional modification of IGF-IR expression, such as mRNA stability [Plymate et al., 2004]. Despite the existing controversials on the mechanisms, all the studies have consistently showed that androgens signaling through the AR result in increased IGF-IR protein expression in prostate epithelium, which is associated with increased phosphorylation of IGF-IR and increased cell proliferation in response to IGF ligands. However, it is not understood whether the induction of increased IGF-IR is part of the differentiation process of prostate epithelium or part of the mechanism for tumor progression. Since both IGF and androgens are necessary for epithelial differentiation, induction of increase in IGF-IR expression as part of the differentiating function of androgens may appear reasonable. On the other hand, increasing IGF-IR expression would be a mechanism by which androgens could enhance transformation and progression of prostate cancer.

IGF-IR ACTIVATION ALTERS AR PHOSPHORYLATION

One mechanism by which IGF-IR signaling could directly affect the function of the AR would be to alter AR phosphorylation. Studies by Lin et al. [2001] first suggested a role of IGF signaling in AR function. They observed that androgen induced apoptosis in AR transiently transfected DU-145 cells and treatment with IGF-1 decreased the transcriptional activity of the AR and inhibited apoptosis. We subsequently found that the effects on IGF-IR signaling on AR activity depended on whether the cells were from an orthotopic or a metastatic lesion [Plymate et al., 2004]. If the tumor was in the orthotopic site, IGF-IR activation inhibited AR transcription under a probasin promoter (AAR3) [Plymate et al., 2004]. In contrast, when the tumor was in the metastatic site, IGF-IR activation enhanced AR transcriptional activity on the AAR3 promoter. Interestingly, the effect of IGF-IR activation on the AR transcriptional activity in both primary and metastatic tumors appears to be mediated through the PI3K/AKT pathway [Plymate et al., 2004]. Lin et al. subsequently demonstrated that the effects of IGF on AR activity occurred in a biphasic manner in LnCaP cells: suppressing AR transcriptional activity at low passage numbers but enhancing AR transcriptional activity at high passage numbers [Lin et al., 2001]. Whether the effect is due to IGF-initiated phosphorylation of AR is rather controversial. Lin et al described that IGF-I phosphorylates AR at serines 210

and 790 [Lin et al., 2001], whereas Gioeli et al. [2002] failed to find any sites on the AR that were phosphorylated by IGF through a peptide terminal degeneration technique. We examined the effect of IGF-IR activation on AR phosphorylation in AR-transfected M12 (M12AR) cells. We showed that AR phosphorylation was decreased in the presence of IGF-I and that this effect was blocked by an inhibitory IGF-IR antibody A12 (Fig. 2a). Our newest study indicated that serine 16 on the AR is a potential site of dephosphorylation whereas serine 81 on the AR is a potential site of phosphorylation by IGF (Fig. 2b). The reasons for discrepancies between studies are not entirely clear. One possible reason for differences in phosphorylation would be differential expression of PP2A in different cell types.

IGF-IR SIGNALING EFFECTS TRANSLOCATION OF THE AR TO THE NUCLEUS

Phosphorylation of the AR may result in several changes that could alter the AR transcriptional functions. One of these effects could be translocation of the AR to the nucleus. Whereas AR phosphorylation was thought to be necessary for nuclear translocation, recent data has shown that phosphorylation of AR at serine 650, which takes place after the AR is in the nucleus and bound to DNA, results in the export of AR from the nucleus [Gioeli et al., 2006]. Thus, the process of dephosphorylation of specific serines on the AR may account for retention of AR in the nucleus and accentuated signaling. As we have shown in Figure 2, IGF decreases phosphorylation of the AR in our M12AR cells. We also have evidence that IGF can enhance AR nuclear translocation in the absence of androgens and that this effect can be inhibited by an IGF-IR inhibitory antibody (Fig. 3a). We have also demonstrated the changes in AR compartmentalization in nuclear and cytoplasmic fractions in response to IGF using Western blot analyses (Fig. 3b). Using the AAR3 probasin reporter assay, we show a significant transactivation of the AR in the absence of androgen and enhanced AR activation in the presence of androgen by IGF-I in M12AR cells. The AR transactivation response to IGF can be blocked by the IGF-IR antibody A12. These data indicate that even in the absence of androgen, IGF can induce transactivation of the AR. Whether this is attributed to changes in phosphorylation of the AR as we have discussed or to the recruitment of AR co-

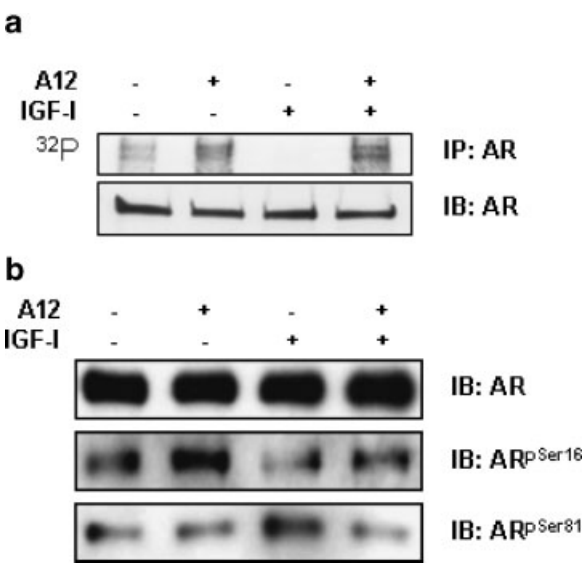

Fig. 2. IGF-I induces AR dephosphorylation. **a**: M12AR cells were labeled with ortho-^{32}P. Cell lysates were immunoprecipitated (IP) with AR-specific antibody. IB, western blotting. **b**: M12AR cells were IB with serine-specific anti-AR antibody.

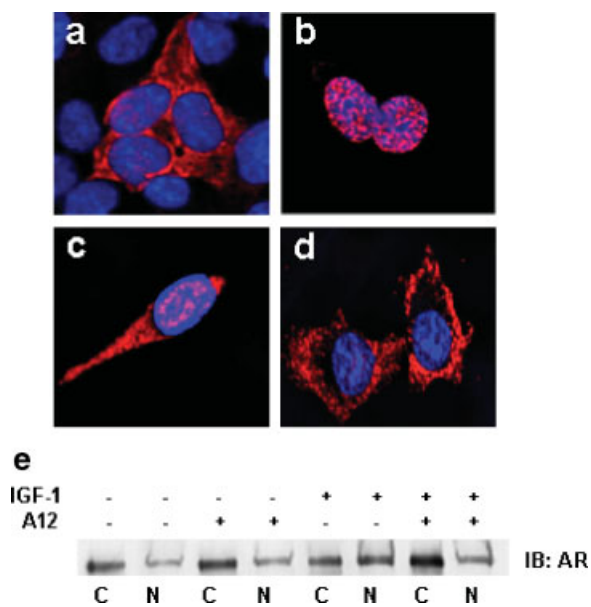

Fig. 3. Confocal image and cell fractionation showing IGF-I-induced AR translocation into the nucleus in M12AR cell lines. **a**: M12AR cells in IGF-I, DHT free medium. **b**: M12AR cells in medium containing 10^{-8}M of DHT. **c**: M12AR cells in medium containing 10 ng/ml of IGF-I. **d**: Medium containing 10 ng/ml of IGF-I and 10 μg/ml of anti-IGF-IR antibody A12. **e**: AR in cytosol and nuclear fractions of M12AR cells under various culture conditions. Red fluorescence. AR, androgen receptor. IGF-I, insulin-like growth factor I. DHT, dihydrotestosterone.

factors, or to both has yet to be determined. Regardless, these studies suggest that, in castrated patients, the increase in AR expression coupled with intact IGF-IR signaling can lead to AR-mediated AI prostate cancer progression. This marks the IGF-IR a potential therapeutic target in post-castrated prostate cancer.

XENOGRAFT MODELS OF PROSTATE CANCER RESPOND DIFFERENTLY TO IGF-IR INHIBITION DEPENDING ON THE PRESENCE OR ABSENCE OF ANDROGENS

We have reported in prostate cancer human xenograft models that inhibition of the IGF-IR with A12 results in a decreased rate of tumor growth in AD and AI tumors [Wu et al., 2005]. However, when we examined the mechanisms by which A12 caused decrease in growth rate, we noted marked differences depending on whether the tumors were AD or AI. In the AD tumors we found that A12 treatment resulted in a combination of apoptosis and G1 cell cycle arrest, whereas in the AI tumors we found that tumor cells arrested in G2 with no occurrence of apoptosis [Wu et al., 2005]. The question arose as to whether these differences in responses were due to a change in the character of the tumor or the absence of androgen. In order to address this issue, we implanted the AI tumor into intact animals. As predicted, tumor growth was inhibited in the A12 treated animals compared to vehicle treated controls. Interestingly, a majority of these tumors displayed an apoptotic response and G1 cell cycle arrest as opposed to the lack of apoptosis when implanted in the castrated animals. To determine potential mechanisms for this effect of androgen on the tumors, we performed cDNA microarray analyses of A12-treated AI tumors from castrated and intact animals and found marked differences in the gene expression profiles (Fig. 4). Some genes such as PP2A and TSC-22 were regulated in opposite direction with A12 treatment, depending on the presence or absence of androgens. It is of interest that TSC-22 has been shown to be androgen-regulated and its expression decreases from benign prostate luminal epithelium to cancer. Another interesting gene differentiated expressed is IGFBP-5, which has been demonstrated to increase post-castration and is associated with recovery from castration-induced apoptosis [Miyake et al., 2000a].

IGF BINDING PROTEINS (IGFBP) THAT ENHANCE SIGNALING OF IGF LIGANDS THROUGH THE IGF-IR ARE INCREASED IN THE PERIOD IMMEDIATELY AFTER CASTRATION

Following castration, IGFBP-2 and IGFBP-5 have been shown to increase significantly in both human prostate and mouse models of prostate cancer. Both of these IGFBPs can increase IGF-ligand signaling through the IGF-IR and enhance recovery from castration induced apoptosis and cell cycle arrest. These two IGFBPs accomplish this task by binding to extracelluar matrix and maintaining a higher concentration of IGF ligand in the proximity of the IGF-IR [Jones et al., 1995; Russo et al., 1997; Kiyama et al., 2003]. The functional importance of these changes has been demonstrated by the studies of Miyake et al. [2000b] in which over-expression of these IGFBPs in LnCaP cells markedly enhances cell growth following androgen withdraw. Using antisense oligonucleotides to IGFBP-2 or IGFBP-5, this group was able to demonstrate the stimulatory effects of the IGFBPs on tumor growth [Kiyama et al., 2003].

INHIBITION OF THE IGF-IR IN CONJUNCTION WITH CASTRATION THERAPY FOR PROSTATE CANCER

These studies suggest that blocking IGF-IR signaling at the time of castration would enhance the effects of androgen withdraw. Preliminary studies in our laboratory using mouse xenograft models have shown a marked enhancement of the castration effect on prostate tumor growth with the inhibitory IGF-IR antibody A12. Potential mechanisms of the augmented effect of A12 on androgen withdraw may include suppression of Survivin, a member of the Inhibitor of Apoptosis (IAP) family of proteins that has been shown to play a role in the recovery process of anti-androgen therapy [Zhang et al., 2005].

IGF-IR ACTIVATION CAN STIMULATE AR CO-FACTORS THAT ENHANCE AR SIGNALING

Insulin-like growth factor may also influence AR signaling by increasing the expression of AR

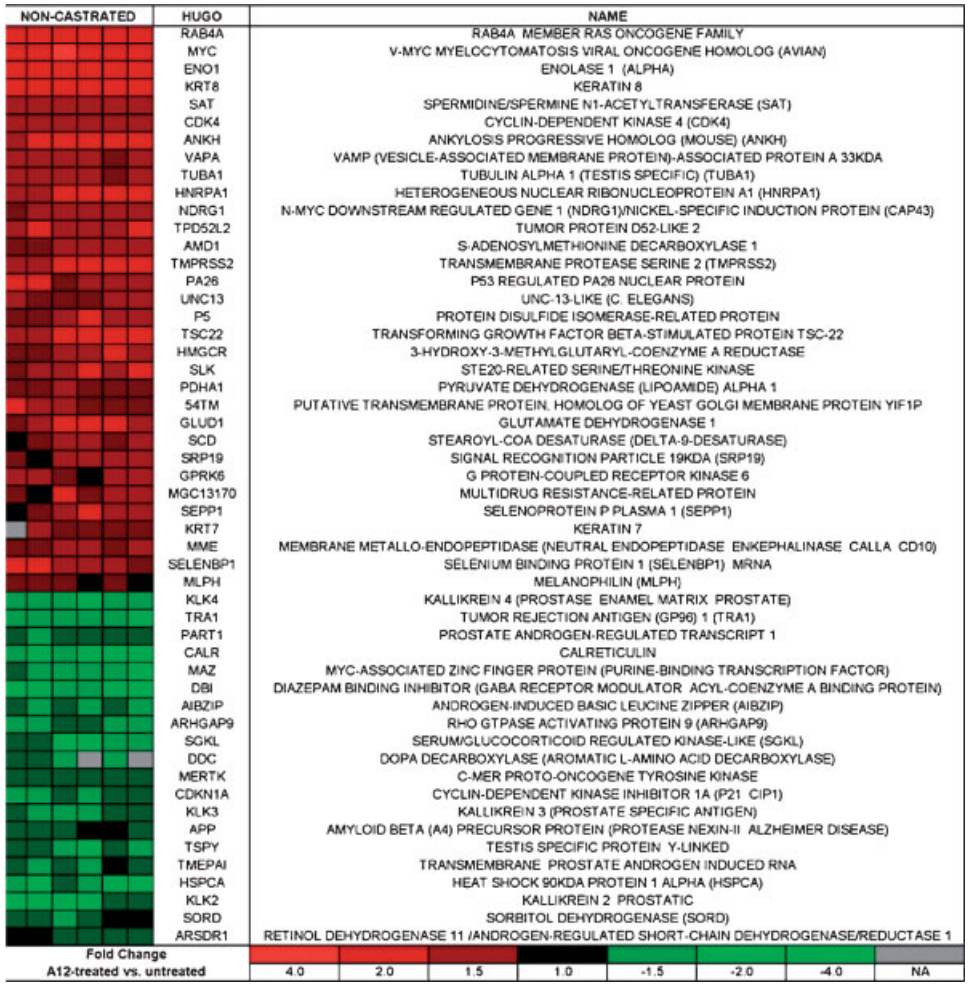

Fig. 4. cDNA microarray expression values of androgen-regulated genes differentially expressed in LuCaP 35V tumors from A12-treated relative to untreated non-castrated mice. There were 82 unique genes known to be androgen-regulated which had significantly consistent gene expression across all samples as compared to no change by a one-sample *t*-test in SAM (<1% FDR significance cut-off used). The scale represents fold-change in A12-treated relative to untreated tumors.

co-stimulatory factors. Given the known 100 or more AR co-regulatory factors, it is not surprising that IGF-IR activation would enhance the expression or activation of one or more co-regulators of the AR. Amongst them, TIF-2 (GRIP-1) and insulin degrading enzyme (IDE) are of particular interest. Studies in a series of human prostate specimens from men with prostate cancer, Mohler and Wilson have demonstrated an increased expression of TIF-2 in most of the recurrent AI prostate cancers that also have a high levels of AR in the nucleus [Gregory et al., 2001]. The same group has also shown the coincidence of increased TIF-2 expression with the recurrence of AI human prostate cancer in xenograft models. Mohler has also demonstrated that overexpression of TIF-2 in vitro can increase AR transcriptional activity in the presence of the physiological concentrations of adrenal androgen. Studies have shown that IDE is a potent co-stimulator of AR transcriptional activity and the ability of IDE to bind to the AR can be regulated by insulin and IGF ligands [Kupfer et al., 1994]. In addition, as the name implies, IDE can degrade insulin, IGF-I and IGF-II [Udrisar et al., 2005].

CONCLUSION

In this review, we have summarized our current understandings of the interactions between the IGF system and the AR (Fig. 5).

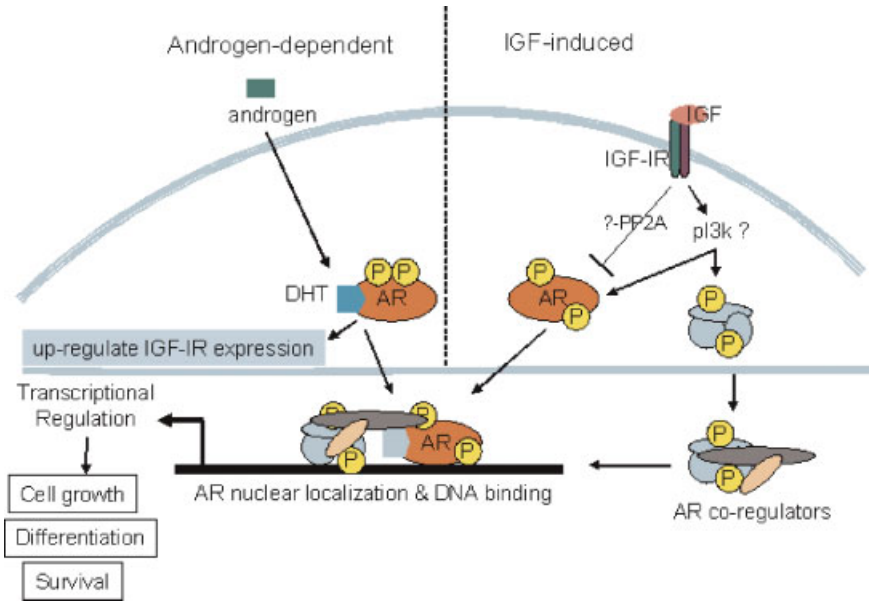

Fig. 5. Interactions of the IGF system with AR signaling. pI3k, phosphoinositide 3-kinase. PP2A, protein phosphotase 2A. [Color figure can be viewed in the online issue, which is available at www.interscience.wiley.com.]

The ability of IGF signaling to potentiate the transcriptional activity of the AR in the face of low to no androgen makes the IGF system, especially the IGF-IR, a strong candidate that leads progression of AI prostate cancer through AR signaling.

ACKNOWLEDGMENTS

Supported by NIH Temin Award 1K01CA116002-01 (J.D.W.), NIH grant PO1-CA85859, Veterans Affairs Research Service, and DOD Prostate Cancer Research grant PC040364 (S.R.P.). We thank our collaborators G.S. Yang and B.M. Paschal at the University of Virginia for donating Figure 2b.

REFERENCES

Chan JM, Stampfer MJ, Giovannucci E, Gann PH, Ma J, Wilkinson P, Hennekens CH, Pollak M. 1998. Plasma insulin-like growth factor-I and prostate cancer risk: A prospective study. Science 279:563–566.

Chen C, Lewis SK, Voigt L, Fitzpatrick A, Plymate SR, Weiss NS. 2005. Prostate carcinoma incidence in relation to prediagnostic circulating levels of insulin-like growth factor I, insulin-like growth factor binding protein 3, and insulin. Cancer 103:76–84.

Corey E, Quinn JE, Buhler KR, Nelson PS, Macoska JA, True LD, Vessella RL. 2003. LuCaP 35: A new model of prostate cancer progression to androgen independence. Prostate 55:239–246.

Culig Z, Hobisch A, Cronauer MV, Radmayr C, Trapman J, Hittmair A, Bartsch G, Klocker H. 1994. Androgen receptor activation in prostatic tumor cell lines by insulin-like growth factor-I, keratinocyte growth factor, and epidermal growth factor. Cancer Res 54:5474–5478.

Culig Z, Hobisch A, Cronauer MV, Hittmair A, Radmayr C, Bartsch G, Klocker H. 1995. Activation of the androgen receptor by polypeptide growth factors and cellular regulators. World J Urol 13:285–289.

Fujimoto N, Yeh S, Kang HY, Inui S, Chang HC, Mizokami A, Chang C. 1999. Cloning and characterization of androgen receptor coactivator, ARA55, in human prostate. J Biol Chem 274:8316–8321.

Gioeli D, Ficarro SB, Kwiek JJ, Aaronson D, Hancock M, Catling AD, White FM, Christian RE, Settlage RE, Shabanowitz J, Hunt DF, Weber MJ. 2002. Androgen receptor phosphorylation. Regulation and identification of the phosphorylation sites. J Biol Chem 277:29304–29314.

Gioeli D, Black BE, Gordon V, Spencer A, Kesler CT, Eblen ST, Paschal BM, Weber MJ. 2006. Stress kinase signaling regulates androgen receptor phosphorylation, transcription, and localization. Mol Endocrinol 20:503–515.

Gregory CW, Hamil KG, Kim D, Hall SH, Pretlow TG, Mohler JL, French FS. 1998. Androgen receptor expression in androgen-independent prostate cancer is associated with increased expression of androgen-regulated genes. Cancer Res 58:5718–5724.

Gregory CW, He B, Johnson RT, Ford OH, Mohler JL, French FS, Wilson EM. 2001. A mechanism for androgen receptor-mediated prostate cancer recurrence after androgen deprivation therapy. Cancer Res 61:4315–4319.

Harman SM, Metter EJ, Blackman MR, Landis PK, Carter HB. 2000. Serum levels of insulin-like growth factor I

(IGF-I), IGF-II, IGF-binding protein-3, and prostate-specific antigen as predictors of clinical prostate cancer. J Clin Endocrinol Metab 85:4258–4265.

Hellawell GO, Turner GD, Davies DR, Poulsom R, Brewster SF, Macaulay VM. 2002. Expression of the type 1 insulin-like growth factor receptor is up-regulated in primary prostate cancer and commonly persists in metastatic disease. Cancer Res 62:2942–2950.

Hongo A, Yumet G, Resnicoff M, Romano G, O'Connor R, Baserga R. 1998. Inhibition of tumorigenesis and induction of apoptosis in human tumor cells by the stable expression of a myristylated COOH terminus of the insulin-like growth factor I receptor. Cancer Res 58: 2477–2484.

Jones JI, Clemmons DR. 1995. Insulin-like growth factors and their binding proteins: Biological actions. Endocrinol Rev 16:3–34.

Kang HY, Yeh S, Fujimoto N, Chang C. 1999. Cloning and characterization of human prostate coactivator ARA54, a novel protein that associates with the androgen receptor. J Biol Chem 274:8570–8576.

Kiyama S, Morrison K, Zellweger T, Akbari M, Cox M, Yu D, Miyake H, Gleave ME. 2003. Castration-induced increases in insulin-like growth factor-binding protein 2 promotes proliferation of androgen-independent human prostate LNCaP tumors. Cancer Res 63:3575–3584.

Kousteni S, Bellido T, Plotkin LI, O'Brien CA, Bodenner DL, Han L, Han K, DiGregorio GB, Katzenellenbogen JA, Katzenellenbogen BS, Roberson PK, Weinstein RS, Jilka RL, Manolagas SC. 2001. Nongenotropic, sex-nonspecific signaling through the estrogen or androgen receptors: Dissociation from transcriptional activity. Cell 104:719–730.

Kupfer SR, Wilson EM, French FS. 1994. Androgen and glucocorticoid receptors interact with insulin degrading enzyme. J Biol Chem 269:20622–20628.

Lin HK, Yeh S, Kang HY, Chang C. 2001. Akt suppresses androgen-induced apoptosis by phosphorylating and inhibiting androgen receptor. Proc Natl Acad Sci USA 98:7200–7205.

Liu Y, Lehar S, Corvi C, Payne G, O'Connor R. 1998. Expression of the insulin-like growth factor I receptor C terminus as a myristylated protein leads to induction of apoptosis in tumor cells. Cancer Res 58:570–576.

Majeed N, Blouin MJ, Kaplan-Lefko PJ, Barry-Shaw J, Greenberg NM, Gaudreau P, Bismar TA, Pollak M. 2005. A germ line mutation that delays prostate cancer progression and prolongs survival in a murine prostate cancer model. Oncogene 24:4736–4740.

Miyake H, Nelson C, Rennie PS, Gleave ME. 2000a. Overexpression of insulin-like growth factor binding protein-5 helps accelerate progression to androgen-independence in the human prostate LNCaP tumor model through activation of phosphatidylinositol 3′-kinase pathway. Endocrinology 141:2257–2265.

Miyake H, Pollak M, Gleave ME. 2000b. Castration-induced up-regulation of insulin-like growth factor binding protein-5 potentiates insulin-like growth factor-I activity and accelerates progression to androgen independence in prostate cancer models. Cancer Res 60:3058–3064.

Mohler JL, Gregory CW, Ford OH III, Kim D, Weaver CM, Petrusz P, Wilson EM, French FS. 2004. The androgen axis in recurrent prostate cancer. Clin Cancer Res 10: 440–448.

O'Connor R, Kauffmann-Zeh A, Liu Y, Lehar S, Evan GI, Baserga R, Blattler WA. 1997. Identification of domains of the insulin-like growth factor I receptor that are required for protection from apoptosis. Mol Cell Biol 17: 427–435.

Pandini G, Mineo R, Frasca F, Roberts CT, Jr., Marcelli M, Vigneri R, Belfiore A. 2005. Androgens up-regulate the insulin-like growth factor-I receptor in prostate cancer cells. Cancer Res 65:1849–1857.

Plymate SR, Bae VL, Maddison L, Quinn LS, Ware JL. 1997a. Reexpression of the type 1 insulin-like growth factor receptor inhibits the malignant phenotype of simian virus 40 T antigen immortalized human prostate epithelial cells. Endocrinology 138:1728–1735.

Plymate SR, Bae VL, Maddison L, Quinn LS, Ware JL. 1997b. Type-1 insulin-like growth factor receptor reexpression in the malignant phenotype of SV40-T-immortalized human prostate epithelial cells enhances apoptosis. Endocrine 7:119–124.

Plymate SR, Tennant MK, Culp SH, Woodke L, Marcelli M, Colman I, Nelson PS, Carroll JM, Roberts CT, Jr., Ware JL. 2004. Androgen receptor (AR) expression in AR-negative prostate cancer cells results in differential effects of DHT and IGF-I on proliferation and AR activity between localized and metastatic tumors. Prostate 61: 276–290.

Pollak M. 2000. Insulin-like growth factor physiology and cancer risk. Eur J Cancer 36:1224–1228.

Pollak MN, Schernhammer ES, Hankinson SE. 2004. Insulin-like growth factors and neoplasia. Nat Rev Cancer 4:505–518.

Rubinstein M, Idelman G, Plymate SR, Narla G, Friedman SL, Werner H. 2004. Transcriptional activation of the insulin-like growth factor I receptor gene by the Kruppel-like factor 6 (KLF6) tumor suppressor protein: Potential interactions between KLF6 and p53. Endocrinology 145: 3769–3777.

Russo VC, Bach LA, Fosang AJ, Baker NL, Werther GA. 1997. Insulin-like growth factor binding protein-2 binds to cell surface proteoglycans in the rat brain olfactory bulb. Endocrinology 138:4858–4867.

Sadar MD. 1999. Androgen-independent induction of prostate-specific antigen gene expression via cross-talk between the androgen receptor and protein kinase A signal transduction pathways. J Biol Chem 274:7777–7783.

Sadar MD, Gleave ME. 2000. Ligand-independent activation of the androgen receptor by the differentiation agent butyrate in human prostate cancer cells. Cancer Res 60: 5825–5831.

Scher HI, Sawyers CL. 2005. Biology of progressive, castration-resistant prostate cancer: Directed therapies targeting the androgen-receptor signaling axis. J Clin Oncol 23:8253–8261.

Taplin ME, Balk SP. 2004. Androgen receptor: A key molecule in the progression of prostate cancer to hormone independence. J Cell Biochem 91:483–490.

Tennant MK, Thrasher JB, Twomey PA, Drivdahl RH, Birnbaum RS, Plymate SR. 1996. Protein and messenger ribonucleic acid (mRNA) for the type 1 insulin-like growth factor (IGF) receptor is decreased and IGF-II mRNA is increased in human prostate carcinoma

compared to benign prostate epithelium. J Clin Endocrinol Metab 81:3774–3782.

Thalmann GN, Sikes RA, Wu TT, Degeorges A, Chang SM, Ozen M, Pathak S, Chung LW. 2000. LNCaP progression model of human prostate cancer: Androgen-independence and osseous metastasis. Prostate 44 (2):91–103.

Titus MA, Gregory CW, Ford OH III, Schell MJ, Maygarden SJ, Mohler JL. 2005a. Steroid 5alpha-reductase isozymes I and II in recurrent prostate cancer. Clin Cancer Res 11:4365–4371.

Titus MA, Schell MJ, Lih FB, Tomer KB, Mohler JL. 2005b. Testosterone and dihydrotestosterone tissue levels in recurrent prostate cancer. Clin Cancer Res 11:4653–4657.

Udrisar DP, Wanderley MI, Porto RC, Cardoso CL, Barbosa MC, Camberos MC, Cresto JC. 2005. Androgen- and estrogen-dependent regulation of insulin-degrading enzyme in subcellular fractions of rat prostate and uterus. Exp Biol Med (Maywood) 230:479–486.

van Weerden WM, Bierings HG, van Steenbrugge GJ, de Jong FH, Schroder FH. 1992. Adrenal glands of mouse and rat do not synthesize androgens. Life Sci 50:857–861.

Wu JD, Odman A, Higgins LM, Haugk K, Vessella R, Ludwig DL, Plymate SR. 2005. In vivo effects of the human type I insulin-like growth factor receptor antibody A12 on androgen-dependent and androgen-independent xenograft human prostate tumors. Clin Cancer Res 11:3065–3074.

Zhang M, Latham DE, Delaney MA, Chakravarti A. 2005. Survivin mediates resistance to antiandrogen therapy in prostate cancer. Oncogene 24:2474–2482.